

SYSTEMATICS AND HISTORICAL
BIOGEOGRAPHY OF *Phyllotis xanthopygus*
(RODENTIA: SIGMODONTINAE)

Tesis entregada a la
Pontificia Universidad Católica de Chile
en cumplimiento parcial de los requisitos para optar al
Grado de Doctor en Ciencias con mención en Ecología

Por
BRIAN JAVIER LATORRE REYES

Director
R. Eduardo Palma

Co-Director
Ulyses J. F. Pardiñas

Diciembre, 2020

ACKNOWLEDGEMENTS

I Thank the curators at the Centro Nacional Patagónico (CNP), Puerto Madryn, Argentina; Museum of Southwestern Biology (MSB), University of New Mexico, USA; Colección de Flora y Fauna Patricio Sánchez Reyes (SSUC), Pontificia Universidad Católica de Chile (PUC); Museo de Historia Natural, Universidad Nacional Mayor de San Marcos, Lima, Peru (MUSM); Museum of Vertebrate Zoology of University of California (MVZ), Berkeley, USA. Also, Lydia Smith at Berkeley for ddRADseq protocol, Simon Yung Wa Sin at Harvard and Katterinne Mendez at Universidad Andrés Bello ddRADseq for their help with the double digest random sequencing protocol and data analysis. Furthermore, to Patricio Pliscoff at PUC for provide his knowledge and layers in niche modeling analysis. Additionally, to the Committee for their feedback. Similarly, to my advisor and co-advisor for their support and advise during this thesis.

TABLE OF CONTENTS

Acknowledgements	Page 2
Index of Figures	Page 5
Index of Tables	Page 8
Index of Abbreviations	Page 10
Resumen	Page 12
Abstract	Page 15
Introduction	Page 18
Chapter 1: Phylogenetic relationships, biogeographical history and molecular dating of the <i>xanthopygus</i> complex (Rodentia, Cricetidae)	Page 24
1.1 Introduction	Page 24
1.2 Materials and Methods	Page 26
1.2.1 Sampling and DNA isolation	
1.2.2 Markers	
1.2.3 DNA analyses	
1.2.4 Phylogenetic analyses	
1.2.5 Molecular clock analyses	
1.2.6 Biogeographic analyses	
	Page 28
1.3 Results	
1.3.1 Phylogenetic relationships	
1.3.2 Molecular clock dating	
1.3.3 Ancestral area reconstruction	
	Page 29
1.4 Discussion	
Chapter 2: Cranial morphometric variation in <i>Phyllotis xanthopygus</i>, <i>Phyllotis limatus</i> and <i>Phyllotis bonariensis</i>	Page 33
2.1 Introduction	Page 33
2.2 Materials and Methods	Page 35
2.2.1 Specimens examined	
2.2.2 Linear morphometric analysis	
2.2.3 Geometric morphometric analysis	

2.3	Results	Page 37
2.3.1	Lineal measurements	
2.3.2	Geometric measurements	Page 40
2.4	Discussion	
Chapter 3: Intraspecific phylogeography of <i>Phyllotis xanthopygus</i> (Rodentia, Sigmodontine) in Patagonia, during the Last Glacial Maximum		Page 42
3.1	Introduction	Page 42
3.2	Materials and Methods	Page 44
3.2.1	Double digest RAD sequencing (ddRADseq)	
3.2.2	Niche modeling analysis	
3.3	Results	Page 46
3.3.1	Population genomics	
3.3.2	Distribution modelling	
3.4	Discussion	Page 48
Conclusions		Page 51
Figures and Tables		Page 53
Appendices		Page 87
Appendix A: Description of cranial landmarks		
Appendix B: Percentage of variance contributed by each shape component (PC), and cumulative variance for females and males.		
Appendix C: Percent of variance contributed by each shape component (PC), and cumulative variance obtained after applying Procrustes analysis to the landmark coordinates data.		
Appendix D: Percent of variance contributed by each shape component (CV), and cumulative variance obtained after applying Procrustes analysis to the landmark coordinates data.		
Appendix E: Procrustes distances between pairwise groups (upper diagonal) and its respective <i>p</i> -values after permutation test with 10,000 permutation rounds (bottom diagonal).		
References		Page 99

INDEX OF FIGURES

<p>Figure 1 Map of species sampled: <i>P. darwini</i> (pink), <i>P. bonariensis</i> (red), <i>P. limatus</i> (green), <i>P. xanthopygus</i> (yellow).</p>	Page 54
<p>Figure 2 Maximum Likelihood and Bayesian inference phylogram of Cytochrome B and β Fgb-I7 sequences. Number above branches are bootstrap proportions and Bayesian posterior probabilities.</p>	Page 55
<p>Figure 3 Chronogram illustrating the diversification of the xanthopygus complex obtained from Bayesian analysis of a matrix combining Cytochrome B and β Fgb-I7 sequences. Number above branches are Bayesian posterior probabilities and the bar below represents time.</p>	Page 56
<p>Figure 4 Historical biogeographic analysis of the <i>xanthopygus</i> complex. Ancestral distributions were reconstructed with Dispersal vicariance Analisis (S-DIVA) in RASP using the maximum clade credibility tree recovered with BEAST. Node color represents probability of ancestral area. A. Andean Pacific Desert Region; B. Pacific Desert Coast Region; C. Andean Altiplano Region; D. Puna Region; E. Mediterranean Andean Region; F. Chacoan Region; G. Patagonian Region; H. Central Chile Region.</p>	Page 57
<p>Figure 5 Dimensions superimposed to a skull of a generalized phyllotine (after Hershkovitz, 1962: figs. 23 to 25). See Appendix C for reference numbers. For the reference of the numbers, see Appendix C.</p>	Page 60
<p>Figure 6 Landmark location on <i>P. x. xanthopygus</i> skull. (A) Dorsal, (B) Ventral, (C) Lateral, (D) Mandible in external view.</p>	Page 61
<p>Figure 7 PC1 sexual dimorphism variation. Groups not connected by the same mark are significantly different.</p>	Page 62
<p>Figure 8 PC1 phylogenetic variation. (A) Male; (B) Female. Groups not connected by the same mark are significantly different</p>	Page 65

Figure 9

PC1 taxonomic variation. Groups not connected by the same letter are significantly different. (A) Male (B) Female.

Page 67

Figure 10

PCA of lineal variables. Male (A, B), Female (C, D). phylogenetic groups (Left): Green South, Orange North. Taxonomical groups (Right), Blue *P. bonariensis*, Red *P. x. chilensis*, Green *P. limatus*, Magenta *P. x. posticalis*, Orange *P. x. ricardulus*, Cyan *P. x. rupestris*, Purple *P. x. vaccarum*, Yellow *P. x. xanthopygus*.

Page 69

Figure 11

Discriminant Function of lineal variables. Male (A, B), Female (C, D). phylogenetic groups (Left): Green South, Orange North. Taxonomical groups (Right), Blue *P. bonariensis*, Red *P. x. chilensis*, Green *P. limatus*, Magenta *P. x. posticalis*, Orange *P. x. ricardulus*, Cyan *P. x. rupestris*, Purple *P. x. vaccarum*, Yellow *P. x. xanthopygus*.

Page 70

Figure 12

Centroid size variation among taxonomic groups. Groups not connected by the same letter are significantly different. (A) Dorsal, (B) Ventral, (C) Lateral Male, (D) Lateral Female, (E) Mandible Male, (F) Mandible Female.

Page 73

Figure 13

Centroid size variation among taxonomic groups. Groups not connected by the same letter are significantly different. (A) Dorsal, (B) Ventral, (C) Lateral Male, (D) Lateral Female, (E) Mandible Male, (F) Mandible Female.

Page 75

Figure 14

Scatter plots, wireframes of each view indicate the relative landmarks displacement. Consensus shape (gray line), Target shape (black line). Phylogeographic grouping; Puna (left), North (center), South (right). Dorsal (A,B,C); Ventral (D,E,F); Lateral Male (G,H,I); Lateral Female (J,K,L); Mandible Male (M,N,O); Mandible Female (P,Q,R).

Page 78

Figure 15

Allometric analysis of the shape components showing *r*-Pearson values. (A) Dorsal, $r^2 = 0.292731$, $p < .0001$; (B) Ventral, $r^2 = 0.02103696$, $p < .0001$; (C) Lateral Male, $r^2 = 0.060101$, $p < .0001$; (D) Lateral Female, $r^2 = 0.012196$, $p = 0.0401$; (E) Mandible Male, $r^2 = 0.000082$, $p = 0.8598$; (F) Mandible Female, $r^2 = 0.061829$, $p < .0001$. Phylogenetic grouping, green South, orange North, black Puna.

Page 79

Figure 16

PCA of cranial shape variables. phylogenetic grouping (Left), green South, orange North. Taxonomical grouping (Right), Blue *P. bonariensis*, Red *P. x. chilensis*, Green *P. limatus*, Magenta *P. x. posticalis*, Orange *P. x. ricardulus*, Cyan *P. x. rupestris*, Purple *P. x. vaccarum*, Yellow *P. x. xanthopygus*. (A,B) Dorsal; (C,D) Ventral; (E,F) Lateral Male; (G,H) Lateral Female; (I,J) Mandible Male; (K,L) Mandible Female.

Page 80

Figure 17

CVA of cranial shape variables. phylogenetic grouping (Left), green South, orange North. Taxonomical grouping (Right), Blue *P. bonariensis*, Red *P. x. chilensis*, Green *P. limatus*, Magenta *P. x. posticalis*, Orange *P. x. ricardulus*, Cyan *P. x. rupestris*, Purple *P. x. vaccarum*, Yellow *P. x. xanthopygus*. (A, B) Dorsal; (C, D) Ventral; (E, F) Lateral Male; (G, H) Lateral Female; (I, J) Mandible Male; (K, L) Mandible Female.

Page 81

Figure 18

Location of samples obtained, including *P. xanthopygus* (yellow) and *P. bonariensis* (red)

Page 82

Figure 19

Graphical representation of population structure according to genetic differences, numbers relating to localities described in Table 11

Page 84

Figure 20

Location of samples obtained according to lineage; purple (high altitude, northern lineage), blue (low altitude northern lineage) and orange (southern lineage)

Page 85

Figure 21

Niche modeling distribution map. (A) 0 Kya Complete Distribution; (B) 12 Kya Complete Distribution; (C) 21 Kya Complete Distribution; (D) 0 Kya Blue Lineage; (E) 12 Kya Blue Lineage; (F) 21 Kya Blue Lineage; (G) 0 Kya Orange Lineage; (H) 12 Kya Orange Lineage; (I) 21 Kya Orange Lineage; (J) 0 Kya Purple Lineage; (K) 12 Kya Purple Lineage; (L) 21 Kya Purple Lineage.

Page 86

INDEX OF TABLES

<p>Table 1 Species sampled according to locality and región; UP (Ulyses Pardiñas), EP (Eduardo Palma), CG (Carlos Gilliari), NK (New Mexico Krio voucher), ROB (Rosario Robles), PNG (Patagonian National Geographic), PPA (Proyecto Patagonia Argentina).</p>	Page 53
<p>Table 2 Group and sex differentiation of lineal variables. TT (Traditional taxonomy), PC (Phylogenetic clades).</p>	Page 58
<p>Table 3 Group and sex differentiation of skull views. Female (F), Male (M) TT (Traditional taxonomy), PC (Phylogenetic clades).</p>	Page 59
<p>Table 4 ANOVA sexual dimorphism variation. Degree of Freedom (DF), Sum of Square (SS), Mean Square (MS).</p>	Page 63
<p>Table 5 PC1 phylogenetic variation. Sample size of group (N), Standard Deviation (SD), Confidence Interval (CI). Tukey HSD represents differences between pairs of group means. Groups not connected by the same letter are significantly different.</p>	Page 64
<p>Table 6 PC1 taxonomic variation. Sample size of taxonomic group (N), Standard Deviation (SD), Confidence Interval (CI). Tukey HSD represents differences between pairs of group means. Groups not connected by the same letter are significantly different.</p>	Page 66
<p>Table 7 Loading matrix of PCA of lineal variables</p>	Page 68
<p>Table 8 Procrustes distances between pairwise phylogenetic groups and sexual dimorphism. Respective p-values after permutation test with 10,000 permutation rounds.</p>	Page 71
<p>Table 9 Variation in centroid size. Sample size of phylogenetic group (N), standard deviation (SD) and confidence interval (CI). Tukey HSD represents differences between pairs of group means. Groups not connected by the same letter are significantly different.</p>	Page 72

Table 10

Variation in centroid size. Sample size of taxonomical group (N), standard deviation (SD) and confidence interval (CI). Tukey HSD represents differences between pairs of group means. Groups not connected by the same letter are significantly different.

Page 74

Table 11

List of localities where analyzed tissue samples of *P. xanthopygus* and *P. bonariensis* were obtained

Page 83

INDEX OF ABBREVIATIONS

Term	Abbreviation
Akaike Information Criterion	AIC
Altitude	AT
Analysis of Variance	ANOVA
Annual Average Precipitation	AAP
Annual Average Temperature	AAT
Area Under the Curve	AUC
Bayesian Inference	BA
Canonical Variate Analysis	CVA
Canonical Vector 1	CV1
Canonical Vector 2	CV2
Carlos Galliari	CG
Centro Nacional Patagónico	CNP
Colección de Flora y Fauna Patricio Sánchez Reyes	SSUC
Confidence Interval	CI
Cytochrome B	CytB
Degree of Freedom	DF
Discriminant Analysis	DA
Driest Month	DM
Double digest RAD sequencing	ddRADseq
Eduardo Palma	EP
Effective Sample Size	ESS
Escherichia coli RY13 Type I	EcoRI
Generalized Time Reversible	GTR
Highest Probability Density	HPD
Highest Temperature Month	HTM
Honestly Significant Difference	HSD
Last Glacial Maximum	LGM
Lowest Temperature Month	LTM
Maximum Clade Credibility	MCC
Markov Chain Monte Carlo	MCMC
Maximum Likelihood	ML
Mean Square	MS
Million Years Ago	Mya
Mitochondrial Deoxyribonucleic Acid	mtDNA
Moraxella species Type I	MspI
Museo de Historia Natural, Universidad Nacional Mayor de San Marcos	MUSM
Museum of Southwestern Biology	MSB
Museum of Vertebrate Zoology	MVZ
Nested Clade Analysis	NCA
New Mexico Krio voucher	NK

Nuclear Deoxyribonucleic Acid	nDNA
Phylogenetic Clade	PC
Principal Component 1	PC1
Principal Component 2	PC2
Principal Component Analysis	PCA
Patagonia National Geographic	PNG
Pontificia Universidad Católica de Chile	PUC
Quantum Geographic Information System	QGIS
Reconstruct Ancestral State in Phylogenies	RASP
Rosario Robles	ROB
Seventh Intron of Beta Fibrinogen	β Fgb-I7
Standard Deviation	SD
Statistical Dispersal-Vicariance Analysis	S-DIVA
Sum of Square	SS
Traditional Taxonomy	TT
Uncorrelated Log Normally Distributed	UCLD
Ulyses Pardiñas	UP
Wettest Month	WM

RESUMEN

Phyllotis xanthopygus es una especie ampliamente distribuida que habita en regiones de Perú, Bolivia, Chile y Argentina. Esta vasta distribución geográfica se complementa con un extenso gradiente altitudinal, que ocupa áreas desde el nivel del mar hasta los 5570m en la porción central de la Cordillera de los Andes. Esta extensa área incluye una amplia gama de ambientes, desde exuberantes matorrales hasta escasos desiertos rocosos. Tradicionalmente, se han reconocido seis subespecies en *P. xanthopygus*, descritas sobre la base de características morfológicas, principalmente diferencias en la pigmentación del pelaje. La subespecie distribuida más al norte es *P. x. posticalis*, que se encuentra aproximadamente desde los 11 hasta los 16° S. Más al sur y habitando las tierras altas de Bolivia se reconoce a *P. x. chilensis* y *P. x. rupestris*, para lo cual se ha reportado una extensa zona de contacto en las áreas de Arequipa, Moquegua y Tacna en Perú. Más al sur se reconoce a *P. x. vaccarum* y *P. x. ricardulus*, esta última endémica al noroeste de Argentina. Ocupando la distribución más austral, la subespecie nominotípica, *P. x. xanthopygus* habita en regiones desde aproximadamente los 38 hasta los 50° S. Adicionalmente, se considera que *P. limatus* y *P. bonariensis* están incluidas dentro de *P. xanthopygus* constituyendo un "complejo de especies" junto con, formando un grupo polifilético, aunque las relaciones taxonómicas específicas no están aún claras. *Phyllotis limatus*, una vez reconocida como subespecie de *P. xanthopygus*, actualmente se considera una especie diferente y cuya divergencia data durante el Último Máximo Glacial determinado mediante análisis de paleo-madrigueras y estudios de relación filogenética. Igualmente, *P. bonariensis*, se ha diferenciado de *P. xanthopygus* en base a caracteres morfológicos sutiles y aislamiento geográfico en la Sierra de la Ventana, Buenos Aires, aunque se sugirió investigación adicional. Teniendo en cuenta los eventos climáticos y

la limitada de evidencia fósil en la Patagonia, se requiere la reconstrucción de la paleodistribución del complejo *xanthopygus*. Para resolver estos problemas taxonómicos y poblacionales, este estudio evaluó las relaciones filogenéticas dentro del complejo *xanthopygus* para validar la taxonomía actual, incluyendo *P. bonariensis* y *P. limatus* mediante un enfoque filogenético. Además, se develó la historia biogeográfica de estos taxa mediante la reconstrucción de áreas de distribución ancestral; igualmente se estimaron los límites de especies usando un enfoque morfométrico lineal y geométrico para poner a prueba la congruencia con los datos moleculares, incluidos *P. limatus* y *P. bonariensis*. Finalmente, se evaluó la estructura poblacional de *Phyllotis* en la Patagonia del complejo *xanthopygus*, incluyendo *P. x. vaccarum*, *P. x. xanthopygus* y *P. bonariensis*, utilizando un enfoque genómico. Con estos resultados poblacionales se develaron posibles refugios durante los períodos glaciales y rutas de recolonización desde el Último Máximo Glacial a través de modelamiento de nicho. En cuanto a los resultados filogenéticos, dos grupos distintos componen el clado sur, *P. x. xanthopygus* forma el primer grupo, mientras que *P. bonariensis* y la distribución oriental más alejada de *P. vaccarum* el segundo. Del mismo modo, dos grupos distintivos se incluyeron en el clado norte, el primero formado por *P. limatus* y la distribución norte de *P. x. posticalis*. Se observó una divergencia en el segundo grupo del clado norte, que consiste en las muestras de *P. x. posticalis*, *P. x. chilensis*, *P. x. rupestris* y el rango de distribución norte de *P. x. vaccarum*. Asimismo, la región ancestral del complejo *xanthopygus* fue ubicada en la Región de la Puna hace aproximadamente 1.925 millones de años atrás. Morfológicamente, las especies que forman el complejo *xanthopygus* presentaron dimorfismo sexual, pero no se observó diferenciación entre los grupos taxonómicos (subespecies y especies). Sin embargo, se encontró que las muestras de ambos sexos estaban agrupadas

basadas en los grupos filogenéticos principalmente en el eje del Componente Principal 2 y el Vector Canónico 1. El análisis filogeográfico reveló dos grupos geográficamente diferenciados; norte (morado y azul) y sur (naranja). Posteriormente, el grupo norte se dividió en dos grupos, diferenciados por altitud; alto (púrpura) y bajo (azul). También, refugios del Plio-Pleistoceno fueron ubicados en zonas similares para cada linaje en la Patagonia de la distribución actual de *P. xanthopygus*. Este estudio resolvió algunos de problemas taxonómicos que rodean al complejo de especies, correcta representación de la taxonomía del grupo considera que *P. limatus* es una subespecie de *P. xanthopygus* situada en el clado norte. Agrupado dentro del clado sur, *P. bonariensis* también puede considerarse una subespecie de *P. xanthopygus* e invita a el numero de subespecies dentro de *P. xanthopygus* de seis a tres, con el fin que cada subespecie se vea reflejada en los clados filogenéticos encontrados en este estudio. El clado basal identificado por análisis genético también se demostraron en la variación del tamaño del cráneo, donde se observó un menor tamaño del cráneo en muestras que ocupaban zonas de alta montaña en la Puna. Por último, el impacto de los ciclos glaciales habría generado dos barreras; una barrera geográfica formada por el ambiente relativamente libre de rocas que rodea el Río Negro, un hábitat poco asociado con la distribución de *P. xanthopygus* y una barrera fisiológica, caracterizada por la altitud. Una compleja dinámica poblacional y de refugios compartidos durante los períodos glaciales ha amplificado la conexión entre linajes patagónicos, incluyendo las poblaciones de *P. bonariensis*, ahora consideradas parte de *P. xanthopygus* que corroboran los hallazgos filogenéticos y morfológicos de este estudio

ABSTRACT

Phyllotis xanthopygus is currently understood to be a widespread species, inhabiting regions of Peru, Bolivia, Chile and Argentina. This vast geographic distribution is complemented by an extensive altitudinal gradient, occupying areas at sea level up to 5570m in the central Andes cordillera. This extensive colonization area includes a broad array of environments, from lush bushland through to sparse rocky deserts. Traditionally six subspecies have been recognized in *P. xanthopygus*, described on the basis of morphological features, primarily differences in coat pigmentation. The northernmost distributed subspecies being *P. x. posticalis*, found at approximately 11 to 16° S. Further south and concentrated in the Bolivian highlands are *P. x. chilensis* and *P. x. rupestris*, for which an extensive contact zone has been reported in the Arequipa, Moquegua and Tacna areas of Peru. Relative to these subspecies, *P. x. vaccarum* and *P. x. ricardulus* are recognized further south, the latter endemic to the north-west of Argentina. Occupying the southernmost distribution, the nominotypical subspecies, *P. x. xanthopygus* inhabits regions at approximately 38 to 50° S. Once recognized as a subspecies of *P. xanthopygus*, it was thought that divergence of *P. limatus*, occurred during the last glaciation, as ascertained by paleoburrow analysis and phylogenetic relationship studies. Presently considered a different species, *P. bonariensis* has been differentiated from *P. xanthopygus* based on subtle morphological characters and geographical isolation to the Sierra de la Ventana, Buenos Aires, although further research was suggested. Currently, it is understood that *P. limatus* and *P. bonariensis* are included in a complex with *P. xanthopygus*, forming a paraphyletic group, although specific taxonomical relationships are not clear. Considering the climactic events and the limited prevalence of widespread direct (fossil) evidence in Patagonia,

paleodistribution reconstruction of the *xanthopygus* complex was needed, including spatial geographical aspects. To attempt to solve these taxonomical and population issues, this study evaluated current phylogenetic relationships within the *xanthopygus* complex and tested the validity of the current taxonomical arrangement, placing emphasis on the species *P. bonariensis* and *P. limatus*. In order to unveil the biogeographic history of this taxa, ancestral distribution areas were reconstructed. Species limits were estimated through use of a lineal and a geometric morphometric approach, to test congruency based on molecular results with morphological data across the entire distribution range of the *xanthopygus* complex, including *P. limatus* and *P. bonariensis*. In order to ascertain potential refugia during glacial periods and recolonization routes since the Last Glacial Maximum, niche modelling was conducted. Using a genomic approach, the population structure of individuals from the *xanthopygus* complex in southern Patagonia was discovered, including *P. x. vaccarum*, *P. x. xanthopygus* and *P. bonariensis*. Phylogenetic results showed the southern clade to be composed of two distinct groups; *P. x. xanthopygus* forming the first group, and *P. bonariensis*, alongside the furthest eastern distribution of *P. vaccarum* forming the second. Similarly, two distinctive groups were included in the northern clade. The northern clade contained the group formed by *P. limatus* and the northern distribution of *P. x. posticalis*. A divergence was observed in the second northern clade group, consisting of the samples *P. x. posticalis*, *P. x. chilensis*, *P. x. rupestris* and the northern distribution range of *P. x. vaccarum*. Furthermore, the ancestral region of the *xanthopygus* complex was determined to be located in the Puna Region, at an estimated crown age of 1.925 million years ago. Morphologically, the species forming the *xanthopygus* complex presented sexual dimorphism, but no differentiation was noted between taxonomical groups (subspecies and species). However according to phylogenetic groups, samples of both sexes were found to

be clustered primarily on the Principal Component 2 and Canonical Vector 1 axis. The phylogeographic analysis revealed two geographically differentiated clusters; north (purple and blue) and south (orange). Subsequently, the northern cluster was divided into two groups, differentiated by altitude; high (purple) and low (blue). Plio-pleistocene refugia were located in similar areas for each lineage, occupying the Patagonian distribution of *P. xanthopygus*. This study resolved some previous taxonomic issues surrounding the species complex, suggesting the inclusion of *P. limatus* as a subspecies of *P. xanthopygus* and situated in the northern clade. Grouped within the southern clade, *P. bonariensis* can also be considered a subspecies of *P. xanthopygus*. Therefore, this study calls for the number of subspecies within *P. xanthopygus* to be reduced to three, accurately reflecting the phylogenetic clades. The basal clade identified by genetic analysis were also demonstrated in skull size variation, where smaller skull size was observed in samples occupying the relatively higher area in Puna. Lastly, the impact of the glacial cycles extends to the genesis of two barriers; a geographical barrier formed by the relatively rock-free environment surrounding the Río Negro, a habitat less associated with *P. xanthopygus* distribution and a physiological barrier, characterized by altitude. Population genetics shows a complex population dynamic and shared refugia during glacial periods. This has amplified the connection between Patagonian lineages and, corroborated phylogenetic and morphological findings, to consider *P. bonariensis* populations as part of *P. xanthopygus*.

INTRODUCTION

Phylogenetic systematics provides a window into the historical context of a species, through testing ancestry-descent hypothesis and the construction of phylogenetic trees (Hennig, 1965). The study of these relationship patterns provides a base for the division of species into taxa, constructed from shared derived characters. Similarly, phylogeography is the study of historical processes that govern the geographical distribution of genealogical lineages, mainly those between, and within closely related species (Avice, 2000). The resulting phylogeographic structure reflects the interaction between both demographic and genealogical processes, and the dynamics of geological and climatic processes (Avice *et al.*, 1987).

The results of phylogeographic studies alongside other approaches traditionally used in systematics, such as morphology and ethology, assist in establishing boundaries between species (Domínguez-Domínguez and Vásquez-Domínguez, 2009). More recently, ecological niche modeling studies have been incorporated to phylogeography (Alvarado-Serrano and Lacey, 2014). This new approach is centered on exploring the individual response of species to their abiotic environment, combining concepts of ecology and life story. These niche models can be applied in order to predict species distribution in new and unexplored geographical domains, or during climate change events (or ‘under climate change conditions’) (Soberón and Peterson, 2005). Biogeographic patterns can be used to evaluate these extrapolated environments, as derived from the niche model analysis. Biogeographic patterns are established by: the presence of specific geographical barriers, dispersion limits imposed by non-suitable biotic or abiotic conditions including species adaptability to new conditions (Kirkpatrick and Barton, 1997; Gaston, 2009) and, ability to migrate to environments similar to the predecessor (Weins *et al.*, 2010). In this way biogeographic factors cannot be viewed independently (Wiens, 2011) and as such were considered alongside niche modeling in this study.

Recently, numerous studies have been carried out using combined phylogeography and niche modeling, both with plants (Viruel *et al.*, 2014; Moussalli *et al.*, 2009) and animals (Homburg *et al.*, 2013; Zhao, 2012; Gutiérrez-Tapia y Palma 2016). The integrated use of these two

approaches clarifies the evolutionary history, dispersion and demography during the numerous climatic changes in the Quaternary, at the species and subspecies level (Graham, 2004; Jakob *et al.*, 2007; Rissler and Apodaca, 2007; Zink, 2015). This blended approach proved ideal when solving intraspecific taxonomic problems, especially when modeling lineages separately in a species with wide geographical distribution, such as the sigmodontine rodent *Phyllotis xanthopygus*. The application of niche modeling with combined lineages includes unoccupied area, also called false positive area (Raxworthy *et al.*, 2007). For this reason, both the entire distribution range and separate lineages were modeled in this study, to ensure accurate results. In addition, the combination of phylogeography and lineage specific niche modeling was a useful tool to unveil glacial refugia (Peterson *et al.*, 2004) and possible postglacial recolonization routes, where there was no direct (fossil) evidence of past distribution.

Phyllotis xanthopygus is currently understood to be a widespread species, inhabiting regions of Peru, Bolivia, Chile and Argentina (Pardiñas and Ruelas, 2017). This vast geographic distribution is complemented by an extensive altitudinal gradient, occupying areas at sea level up to 5570 m in the central Andes Mountain Range. This extensive colonization area includes a broad array of environments, from lush bushland through sparse rocky deserts (Kramer *et al.*, 1999). Traditionally six subspecies have been recognized in *P. xanthopygus*, described on the basis of morphological features, primarily differences in coat pigmentation (Hershkovitz, 1962; Stepan, 1993; Thomas, 1912; 1919; Pearson, 1958). The northernmost distributed subspecies is *P. x. posticalis*, found between 11 to 16° S approximately. Further south and concentrated in the Bolivian highlands are *P. x. chilensis* and *P. x. rupestris*, for which an extensive contact zone has been reported in the Arequipa, Moquegua and Tacna areas of Peru (Pearson, 1958). Relative to these subspecies, *P. x. vaccarum* and *P. x. ricardulus* are recognized further south, the latter endemic to the north-west of Argentina. Occupying the southernmost distribution, the nominotypical subspecies, *P. x. xanthopygus* inhabits regions between 38 to 50° S approximately (Pardiñas and Ruelas, 2017).

However, other two phyllotine taxa are recognized within *P. xanthopygus*, and for this reason some authors named it, the "*xanthopygus* complex". This complex is formed by *P. xanthopygus*,

P. limatus and *P. bonariensis* due to its phylogenetic arrangement (Steppan, *et al.* 2017). Once recognized as a subspecies of *P. xanthopygus*, it was thought that divergence of *P. limatus* Thomas, 1912, occurred during the Last Glaciation, as ascertained by paleoburrow analysis (Kuch *et al.*, 2002) and phylogenetic studies (Steppan *et al.*, 2007). Presently considered a different species, *P. bonariensis* Crespo, 1964, has been differentiated from *P. xanthopygus* based on subtle morphological characters and geographical isolation to the Sierra de la Ventana, Buenos Aires (Reig, 1978; Galliari *et al.*, 1996), although further research was suggested (Musser and Carleton, 2005). Currently, it is understood that *P. limatus* and *P. bonariensis* are included in a complex with *P. xanthopygus*, forming a paraphyletic group (Steppan *et al.*, 2007), although specific taxonomical relationships are not clear.

It is postulated that the *xanthopygus* complex is characterized by deep divergences and high genetic diversity among populations, considering both mtDNA and nDNA (Kim *et al.*, 1998; Lessa *et al.*, 2010; Steppan *et al.*, 2007). In light of these divergences, additional research was required to verify the subspecies proposed across the geographical range (Steppan *et al.*, 2007). Morphological and molecular studies (cytochrome b) of the genus *Phyllotis*, have suggested phylogenetic patterns consistent with successful colonization of the western Andes by *P. xanthopygus* (Steppan, 1998). These patterns may be the result of expansion and contraction of species distribution, within a short period of time, relative to the age of the clade (Albright, 2004; Riverón, 2011).

Using various approaches, systematic studies to distinguish *P. xanthopygus* from *Phyllotis darwini* have included electrophoretic, morphometric (Spotorno and Walker, 1983) and karyotype analyses (Walker *et al.*, 1984). These two *Phyllotis* species have parapatric distribution in central Chile: *P. darwini* inhabits the Pacific Coast, the Central Valley and areas of the Andes cordillera below 2000 m (Pardiñas and Ruedas, 2017), whilst *P. xanthopygus* is distributed from 1800 to 4000 m in the same mountain range. In this line, absence of gene flow has been reported between these two taxa *P. d. darwini* and *P. x. vaccarum* (previously known as *P. d. vaccarum*; Walker *et al.*, 1984) due mainly on morphological differences at the molar level, and differences in their karyotypes, particularly in C banding pattern (Walker *et al.*,

1984).. In addition, *P. xanthopygus* was found to have larger C bands in all chromosomes, contrasting with other species of the genus, and intraspecific differentiation was detected at the X chromosome between *P. x. xanthopygus* compared with *P. x. rupestris* and *P. x. vaccarum* (Walker *et al.*, 1991). Proposed as an adaptive character, the large genomic size of *P. xanthopygus* would enable the colonization of different environments (Walker *et al.*, 1991).

Phylogeographic studies applying Nested Clade Analysis (NCA) based on cytochrome B sequencing analysis of *P. xanthopygus* have distinguished two clades, the Altiplano clade and the North-South clade (Albright, 2004). The Altiplano clade is comprised of Peru, Bolivia and northern Chile, and the North-South clade Argentina and the remaining regions of southern Chile. This two-clade arrangement was in disagreement with the subspecies traditionally proposed by morphology. Due to the low number of individuals sampled by Albright (2004) and criticism of the methodology used in that work (NCA; Petit, 2008), it is questionable if accurate phylogeographic inferences were possible based on this kind of methodologies. Similarly, Riverón (2011) also using cytochrome b mitochondrial sequences to perform phylogeographic studies and applying Refugia Theory at the Last Glacial Maximum (LGM) in Argentinian Patagonia found a reduced genetic diversity of *P. xanthopygus* in southern regions, probably due to the recent recolonization of this ecoregion. The study by Riverón (2011) suggested that Patagonian *xanthopygus* consisted of a northern and a southern haplogroups, thus comprising the subspecies *P. x. vaccarum* and *P. x. xanthopygus*. These haplogroups would be geographically divided by the Río Negro (40°S), however, due to the phylogenetic polytomy recovered among the individuals of the southern group, the latter river was unable to be considered as a phylogeographic break (Riverón, 2011). The latter result is similar to the distribution patterns found in other sympatric taxa to *P. xanthopygus* such as the sigmodontines *Oligoryzomys longicaudatus* and *Abrothrix longipilis*; Kim *et al.*, 1998; Lessa *et al.*, 2010), and some liolaemid lizards (Morando *et al.*, 2007; Victoriano *et al.*, 2008).

Multiple phylogeographic breaks have been recorded in Patagonia and subsequently classified according to geographic position (Sérsic *et al.*, 2011, Lessa *et al.*, 2012). Andean breaks are associated with pre-Quaternary and Quaternary processes such as Andean orogenesis and

paleo-basins. Whilst other transient breaks located in the Pampas region of Argentina are likely the result of Quaternary events such as glaciations, which generated changes in the dynamics of river basins and the coastline (Pardiñas *et al.*, 2011).

Despite previous studies, phylogenetic relationships within *Phyllotis xanthopygus* remained unclear. Therefore, a combined molecular systematic and morphological study was required in order to clarify the evolutionary history of this species, and evaluate the validity of subspecies traditionally recognized within the geographical range of *P. xanthopygus*. Additionally, in Patagonia, the South American region that was affected by the Plio-Pleistocene glacial cycles to a substantial degree (i.e., the Andes and the piedmont), the population structure of the *xanthopygus* complex was still unknown, thus unable to be explained under a exclusive biogeographic scenario (Riverón, 2011). Therefore, a phylogeographic study of *P. xanthopygus* in the Patagonian region, using high temporal resolution and a genomic approach was required to evaluate the phylogeographic breaks between 35 and 45° S.

Climate oscillations in the Pleistocene had a profound impact on the distribution of many species, leading to different diversification patterns and timing among isolated populations (Avise, 2000). It is well understood that *P. xanthopygus* inhabits high mountain areas, similar to those previously covered by the ice sheet during the LGM in the Andes cordillera, which may have acted as a temporary geographical barrier (Rabassa, 2008). Considering this climatic event and the limited prevalence of widespread direct (fossil) evidence in Patagonia (Tammone *et al.*, 2014), paleodistribution reconstruction of the *xanthopygus* complex was needed, including spatial geographical aspects (Hugall *et al.*, 2002). This detailed reconstruction assisted in identifying possible glacial refugia and postglacial recolonization routes, based on the phylogeographic lineages of the species complex. Therefore, an integrated approach of morphologic and molecular analysis was considered in this thesis to correctly approach taxonomic problems within *Phyllotis xanthopygus*, as this approach can successfully recognize and define subspecies (Patton and Conroy, 2017). In view of the wide distribution of the focal species of this study, the intra and interspecific taxonomic issues and deep divergences among populations found in previous studies; in this study a combined methodology between

molecular systematics, morphology and population genetics was used to clarify the phylogenetic and biogeographic history of the *xanthopygus* complex. Thus, the main objective of this thesis was to evaluate the evolutionary history of *Phyllotis xanthopygus* across its distributional range, from a phylogenetic, morphometric and biogeographical perspective.

In line with this objective, it is hypothesized in a molecular and morphological base, that *Phyllotis xanthopygus* will be constituted for what it is currently known as the *xanthopygus* complex, including *P. limatus* and *P. bonariensis*, divided into subspecies within the distributional range, forming a monophyletic group. Among those subspecies, the populations of the southern part of the distribution have been the most impacted during the LGM changing their distributional range to find optimal environmental conditions.

CHAPTER 1: PHYLOGENETIC RELATIONSHIPS, BIOGEOGRAPHAL HISTORY AND MOLECULAR DATING OF THE *xanthopygus* COMPLEX (Rodentia, Cricetidae).

1.1 INTRODUCTION

The sigmodontine rodent *Phyllotis xanthopygus* is currently understood to be a widespread species, inhabiting an extensive altitudinal gradient, occupying areas from sea level up to 5570 m in the central Andes of Peru, Bolivia, Chile and Argentina (Pardiñas and Ruelas, 2017). This extensive colonization area includes a broad array of environments, from lush bushland through sparse rocky deserts (Kramer et al., 1999). Traditionally six subspecies have been recognized in *P. xanthopygus* based on morphological features, primarily differences in coat pigmentation (Hershkovitz, 1962; Steppan, 1993; Thomas, 1912; 1919; Pearson, 1958). The subspecies with the northernmost distribution is *P. x. posticalis*, found between 11 and 16° S. Further south and concentrated in the Bolivian highlands are *P. x. chilensis* and *P. x. rupestris*, for which an extensive contact zone has been reported surrounding the Peruvian towns of Arequipa, Moquegua and Tacna. (Pearson, 1958). Relative to these subspecies, *P. x. vaccarum* and *P. x. ricardulus* are recognized further south, the latter endemic to the north-west of Argentina. Occupying the southernmost distribution is the nominotypical subspecies, *P. x. xanthopygus* which inhabits regions between 38 and 50° S (Pardiñas and Ruelas, 2017).

Contrary to the traditional taxonomic recognition of six subspecies within *P. xanthopygus*, two other species are included within the same clade, forming the "*xanthopygus* complex". In fact, it is currently understood that *Phyllotis limatus*, *P. bonariensis* and *P. xanthopygus* form a polyphyletic group (Steppan et al. 2007) (hereafter referred as the *xanthopygus* complex). Nonetheless, specific taxonomical relationships within this taxonomic complex are not clear. Once recognized as a subspecies of *P. xanthopygus*, it was thought that divergence of *P. limatus* Thomas, 1912 occurred during the last glaciation, based on paleoburrow (Kuch et al., 2002) and phylogenetic studies (Steppan et al., 2007). Furthermore, considered as a different species, *P. bonariensis* Crespo, 1964, has been differentiated from *P. xanthopygus* based on subtle

morphological characters and geographical isolation in Sierra de la Ventana, Buenos Aires province (Reig, 1978; Galliari et al., 1996). However, further research to explore the latter issue has been suggested (Musser and Carleton, 2005).

It has been postulated that the *xanthopygus* complex is characterized by deep divergences and high genetic diversity among populations, considering both mtDNA and nDNA (Kim et al. 1998; Lessa et al., 2010; Steppan et al., 2007). In light of these divergences, additional research was required to verify the subspecies proposed across the geographical range (Steppan et al., 2007). Previously, morphological and molecular studies (cytochrome b) of the genus *Phyllotis*, suggested a phylogeny consistent with successful colonization of the western Andes cordillera by *P. xanthopygus* (Steppan, 1998). This pattern may be the result of expansion and contraction of species distribution, within a short period of time relative to the age of the clade (Albright, 2004; Riverón, 2011).

Phyllotis darwini, an endemic phyllotine from the Mediterranean ecoregion of Chile, is considered a sister clade of the *xanthopygus* complex (Steppan et al., 2007). It is often mistaken with *P. xanthopygus*, due to its parapatric distribution in central Chile: *P. darwini* inhabits the Pacific coast, the central valley and areas of the Andes cordillera, below altitudes of 2000m (Pardiñas and Ruedas, 2017). Within the same mountain range, *P. x. vaccarum* (previously known as *P. d. vaccarum*; Walker et al., 1984) is distributed from 1800m to 4000 m. Systematic studies to distinguish these two *Phyllotis* species have included electrophoretic, morphometric (Spotorno and Walker, 1983) and karyotype analyses (Walker et al., 1984). Between *P. d. darwini* and *P. x. vaccarum* an absence of gene flow has been reported, as well as differences at the morphology and the karyotype level, particularly through molar and C banding pattern, respectively. In addition, *P. xanthopygus* was found to have larger C bands in all chromosomes, contrasting with other species within the genus. Additionally, intraspecific differentiation was detected in the X chromosomes between *P. x. xanthopygus* when compared with *P. x. rupestris* and *P. x. vaccarum* (Walker et al., 1991). Proposed as an adaptive feature, the large genome size of *P. xanthopygus* would have enabled the colonization of a wide variety of environments, such as those currently occupied by this species (Walker et al., 1991).

Giving the former scenario, the major aims of this study were: i) to evaluate the phylogenetic relationships within the *xanthopygus* complex using a combination of mitochondrial and nuclear sequences; ii) to test the validity of the traditional taxonomical arrangement, with emphasis on the species *P. bonariensis* and *P. limatus* using a phylogenetic approach; iii) unveil the biogeographic history of these taxa by reconstructing ancestral distribution areas.

1.2 MATERIALS AND METHODS

1.2.1. Sampling and DNA Isolation. - Tissue samples were obtained from 33 individuals (Table 1; Figure 1) identified as *P. xanthopygus*, *P. limatus* and *P. bonariensis*, from the entire geographic distribution of the species. The species *Phyllotis darwini*, currently considered the sister clade of the *xanthopygus* complex (Steppan *et al.*, 2007), was used as outgroup. Of the 33 samples obtained, 17 were from Centro Nacional Patagónico (CNP), Puerto Madryn, Argentina (CG, ROB, PNG, UP); 5 from the Museum of Southwestern Biology (MSB), University of New Mexico, USA; 6 from Colección de Flora y Fauna Patricio Sánchez Reyes (SSUC), Pontifical Catholic University of Chile (PUC) (NK, EP), and 5 from the Museo de Historia Natural, Universidad Nacional Mayor de San Marcos, Lima, Peru (MUSM).

1.2.2. Markers. – Both genes have been previously used within *P. xanthopygus* (Storz *et al.*, 2020) or with closely related species (Palma *et al.*, 2010; Steppan *et al.*, 2007). Historically, cytochrome B has been frequently used in phylogeny reconstruction showing good resolution due to its high mutation rate in mammals (Nabholz *et al.*, 2009), this align with the results displaying in this study (Appendix A); on the other hand, β -Fibrinogen Intron 7 evolves 2.8 times slower than cytochrome B (Prychitko and Moore, 2000) and its been exhibited in this study (Appendix B) showing more polytomies in the tips of the phylogenetic tree but solving the base nodes in the phylogeny.

1.2.3. DNA Analyses. - The DNA isolation was performed using a phenol-chloroform method, modified from Sambrook *et al.* (1989). For each individual (n=33) a mitochondrial and a nuclear

gene were analyzed. All samples were amplified in a Veriti thermal Cyclor 96 at PUC in a volume of 36- μ l reactions; consisting of 4.5 μ l of 10x PCR Buffer, 4.5 μ l of MgCl₂, 4.5 μ l of dNTP's, 1 μ l of each primer and 0.6 μ l of Platinum® Taq DNA polymerase. The following genes, primers and thermal protocols were used: (a) Cytochrome B (CytB): primers MVZ 05 – MVZ 16 (Smith *et al.*, 1992) an initial denaturation (95°C, 3 minutes), 30 cycles of denaturation (95°C, 30 seconds), annealing (46°C, 30 seconds) and extension (72°C, 1 minute), and a final extension (72°C, 5 minutes); (b) Seventh Intron of Beta Fibrinogen (β Fgb-I7): MAMML – MAMMU (Matocq *et al.*, 2007), initial denaturation (94°C, 5 minutes), 35 cycles of denaturation (94°C, 1 minute), annealing (54°C, 30 seconds) and extension (72°C, 40 seconds), and a final extension (72°C, 4 minutes). Sequencing of purified PCR products were performed in both directions at MacroGen Incorporated or at the PUC sequencing facility. The chromatograms were analyzed and edited in Geneious 11.0.3 (Kearse *et al.*, 2012).

1.2.4. Phylogenetic Analyses. - Sequence alignment was carried out using MUSCLE (Edgar, 2004). A total of 872 bp were used, of which 603 bp corresponded to Cyt B gene, and 269 bp to the β Fgb-I7 gene. Phylogenetic trees were constructed through maximum likelihood (ML) and Bayesian inference (BA) methods, using the programs PAUP v4.0 (Swofford, 2002) and MrBayes (Huelsenbeck and Ronquist, 2001) respectively. The trees were rooted with the outgroup criterion, using sequences of *P. darwini*. The best-fit models of nucleotide substitution were selected using the Akaike Information Criterion (AIC) in the software PAUP. A 1000-replicate bootstrap analysis was performed for maximum likelihood using PAUP. BA included two chain runs of 2×10^6 Markov chain Monte Carlo (MCMC) with generations sampled every 100 generations reaching a standard deviation below 0.05.

1.2.5. Molecular Clock Analyses. - To estimate divergence times, the program BEAST v1.8.3 (Drummond *et al.*, 2012) was used. This included the use of a partitioned data set that simultaneously estimated substitution model parameters, and dates for cladogenetic events for all genes (henceforth referred to as “combined dataset”). A speciation Yule Process with a GTR model was established and the *ucl.d.mean* parameter was set up using basal split range as established by Steppan *et al.* (2007). Calibrations were implemented in the form of normal

distribution, with standard deviations of 0.2. Runs were performed under an uncorrelated lognormal relaxed clock model; one independent run of 6.0×10^7 conducted with generations sampled every 5000 generations. Convergence to stable values was confirmed with Tracer v1.7.1 (Rambaut and Drummond, 2013) and an effective sample size (ESS) greater than 200 for all parameters was obtained. Following this, trees were compiled into a maximum clade credibility (MCC) tree through use of TreeAnnotator v1.8.3 (Rambaut and Drummond, 2016), in order to display mean aged nodes and highest probability density (HPD) intervals of 95% (upper and lower) for each node.

1.1.6. Biogeographic Analyses. - Ancestral distributions were reconstructed using BioGeoBears package in the program Reconstruct Ancestral State in Phylogenies (RASP) v2.1 alpha (Yu *et al.*, 2015). Eight broad ecogeographic distributional areas or ecoregions were recognized following (citation here): (A) Andean Pacific Desert Region, (B) Pacific Desert Coast Region, (C) Andean Altiplano Region, (D) Puna Region, (E) Mediterranean Andes Region, (F) Chacoan Region, (G) Patagonian Region, and (H) Central Chilean Region. To account for uncertainties in the phylogenies, all post-burnin trees obtained with BEAST for the combined dataset were used. The possible ancestral ranges at each node on the MCMC Bayesian tree were recovered. Ten MCMC chains were run simultaneously for 5×10^5 generations. The state was sampled every 1000 generations and the temperature of heating the chains was 0.1. A model with all biogeographic events equally likely, similar to a fixed Jukes-Cantor model, was used along with a wide root distribution, this model was chosen based on Parada *et al.* (2013) using the Sigmodontinae subfamily, which contains *P. xanthopygus* and species with similar vagility.

1.3. RESULTS

1.3.1 Phylogenetic Relationships. – The combined phylogeny of the mtDNA and nDNA genes analyzed with ML and BA produced a single topology (Figure 2). Samples of the northeast distribution of *P. x. rupestris* were recovered as the basal subspecies of *P. xanthopygus*, this clade is closely related to a sister group composed by two major internal clades. These two clades major internal clades were formed geographically, the first and southern clade composed of *P. x. xanthopygus* (ML = 99, BA = 1), consisting of the southernmost clade within the

xanthopygus phylogeny (Figure 2). This clade is closely related to *P. bonariensis* and the furthest eastern distribution of *P. vaccarum* (BA = 0.89). The northern clade is divided in two clades. The first northern clade (ML = 100, BA = 1) contained the group formed by *P. limatus* and the northern distribution of *P. x. posticalis*. The second northern clade recovered in the phylogeny (ML = 98, BA = 1), consisted of *P. x. posticalis*, *P. x. chilensis*, *P. x. rupestris* and the northern distribution range of *P. x. vaccarum* (ML = 85, BA = 1). Remarkably from this topology, *P. limatus* and *P. bonariensis* are included in these two geographic clades, the northern and southern distribution of *P. xanthopygus* respectively.

1.3.2 Molecular Clock Dating. – Through the use of molecular clock dating, the estimated crown age of the *xanthopygus* complex was found to be 1.925 Ma. (HPD 1.64 – 2.22) (Figure 3), following this, the split of the two geographic clades is dated at 1.1168 Ma. (HPD 0.453 – 1.5762) and the remainder of the northern group at 0.9015 Ma. (HPD 0.3193 – 1.3652).

1.3.3 Ancestral Area Reconstruction. - Results based on the ancestral area reconstruction using S-DIVA ('maximum area' option set as 2) ascertained that the most recent common ancestor of *xanthopygus* complex originated in the Puna ecoregion (Figure 4). The most likely areas where the divergence between the northern and southern clades occurred were a combination of 50% Puna ecoregion and an equal percentage for Mediterranean Andes, Chacoan and Patagonian ecoregions. The most recent ancestor of the southern clade is inferred to have originated from a combination of 50% Patagonia ecoregion with an equal percentage for the Chacoan and Mediterranean Andes ecoregions. The Northern clade presented a congruent mix between the Pacific Desert Coast and the Puna ecoregions.

1.4 DISCUSSION

Phyllotis xanthopygus has been divided into subspecies according to fur coloration, cranial morphometrics, and subtle morphological traits (Osgood 1943, Cabrera 1961, Mann 1978). It is found to inhabit a wide variety of environments, over a large geographic range in the central Andes. Samples previously identified as *P. limatus*, *P. x. vaccarum*, *P. x. rupestris* and *P. x. posticalis* were found to be polyphyletic in the phylogenetic tree. The sample MUSM 35468,

incorrectly labeled as *P. x. posticalis*, is located in a separate clade to the remaining *P. x. posticalis* samples. This may be due to an extensive contact zone, which is shared with *P. x. rupestris* and *P. x. chilensis*.

In the northern geographic clade, *P. x. vaccarum* appears in a polytomy with *P. x. rupestris*, and as a sister clade to *P. x. chilensis*. In the southern geographic clade, *P. x. vaccarum* can be considered a sister to *P. bonariensis*. This is supported by the close relation of *P. bonariensis* to the southern geographic clade sample CG109 of *P. x. vaccarum*, located in the eastern disjunct range. This finding aligns with previous studies, based on shared parasites (Robles *et al.*, 2014) and phylogenetic analyses (Albright, 2004; Riverón, 2011). Forming part of the northern clade, the Andean distribution range of this subspecies is considered a sister clade to the south-west Bolivian distribution of *P. x. rupestris*. According to the taxonomy proposed by Cabrera (1961), all samples currently classified as *P. x. vaccarum* in this study, should be categorized as *P. x. ricardulus*, demonstrating taxonomical problems in identifying these subspecies. Therefore, the traditional subspecies recognized in the molecular phylogeny are far from being a monophyletic group, according to what has been previously proposed, based on morphologic traits (Steppan, 1998).

The polyphyly between *P. xanthopygus*, *P. limatus* and *P. bonariensis* has systematic and taxonomical implications. Individuals currently recognized as *P. limatus* were formally classified as *P. x. limatus*, including populations from the northern Pacific coast of Chile (Kuch *et al.*, 2002a). This categorization was based on morphological and molecular (mtDNA) data (Steppan, 1998). Similarly, the evidence supporting the taxonomic rise of *P. bonariensis* as a species is attributed to the disjunct distribution from *P. xanthopygus*. These findings are contrary to those of Albright (2004) and Steppan *et al.* (2007), who proposed that these species cannot be separated based on mitochondrial and nuclear data, respectively. Corroborating these hypotheses, in this study mtDNA and nDNA data were used to find the *xanthopygus* complex to have a basal clade located in the Bolivian Altiplano, and two major internal clades to be founded by geographical differences with moderate to high node support. Furthermore,

morphological and population analyses have supported this grouping among the *xanthopygus* complex (chapter two and three of this thesis).

The molecular clock analysis estimated that *P. bonariensis* appeared to have an independent lineage from approximately 646 800 years ago and *P. limatus* from around 92 500 years ago. These events occurring in the late Pleistocene, suggesting that this recent divergence was probably due to distributional changes during the glacial-interglacial cycles. Because this cycle triggered recurrent movement of the populations, in order to reach suitable environments during glacial time, the gene flow between these groups was not interrupted sufficiently to accomplish significant molecular differentiation (Mayr, 1954). The basal split dates to 1.8878 Mya, and the split between the *xanthopygus* complex and *P. darwini* at 1.9656 Mya, both during early Pleistocene, which suggests these divisions cannot be explained by glacial cycles.

Biogeographical analyses proposed that basal divergence of the *xanthopygus* complex took place in the Puna Region. Following this event, the split between the northern and southern clades likely took place, in a transition area between the Puna and three other ecoregions (Chacoan, Mediterranean Andean and Patagonian Regions). This scenario suggests a dispersal movement through the eastern Andes cordillera to lower altitude and higher latitude zones. Later, the southern clade reached the Patagonian ecoregion through the Chacoan and Mediterranean Andes Region, whereas the northern clade moved to the westside of the Andes, settling in the Pacific Desert Region and recolonizing the Puna Region.

This study based on both mitochondrial and nuclear genes has clarified some of the relationships among the *xanthopygus* complex. Demonstrating polyphyly of the subspecies, these results place *P. limatus* and *P. bonariensis* within the *P. xanthopygus* clade. These key findings suggest the need for taxonomic and systematic changes within the species complex. The results propose the occurrence of three clades (Northern, Southern and Basal), each representing a subspecies of *P. xanthopygus*. It is suggested that the basal clade is comprised of the north-eastern populations of *P. x. rupestris*. The northern geographic clade is most accurately reflected by the taxonomical name *P. x. posticalis*. Included in this taxonomic

arrangement, the populations of *P. limatus* form part of *P. x. posticalis*. The southern geographic clade can be considered inclusive of *P. bonariensis*, and taxonomically recognized as *P. x. xanthopygus*.

CHAPTER 2: CRANIAL MORPHOMETRIC VARIATION IN *Phyllotis xanthopygus*, *Phyllotis limatus* AND *Phyllotis bonariensis*

2.1 INTRODUCTION

The genus *Phyllotis* Waterhouse, 1837 has been extensively studied using morphological (Pearson, 1958; Hershkovitz, 1962) and molecular (Steppan *et al.*, 2007) approaches. Contained within this genus is *P. xanthopygus*, the species with the largest distributional range (Waterhouse, 1837). This taxon was previously considered synonymous of *P. darwini* Waterhouse, 1837 (Pearson, 1958; Hershkovitz, 1962), however, Walker *et al.*, 1984 showed that both species exhibit reproductive isolation at chromosome level. It is currently understood that *P. xanthopygus* includes populations in the highlands of the Andes Mountain range and adjacent shrubland habitats, along the eastern and western Andean slopes. The species ranges from central Peru to the Magallanes and Santa Cruz provinces in Chile and Argentina, respectively, and from sea level up to 5,570 m in the Andean cordillera (Pardiñas and Ruelas, 2017).

Traditionally six subspecies have been recognized in *P. xanthopygus*, described on the basis of morphological features (Steppan, 1993; Pearson, 1958; Hershkovitz, 1962). The most northerly distributed subspecies is *P. x. posticalis*, found between 11 to 16° S, approximately. Further south and concentrated in the Bolivian highlands *P. x. chilensis* and *P. x. rupestris* occur, for which an extensive contact zone has been reported surrounding the Peruvian towns of Arequipa, Moquegua and Tacna. (Pearson, 1958). *P. x. vaccarum* is recognized to the south-west, and *P. x. ricardulus* to the south-east, the latter endemic to north-western Argentina. Occupying the southernmost distribution of the species, *P. x. xanthopygus* roughly inhabits regions between 38 and 50° S. These taxa were diagnosed by their general body size, external coloration patterns, and minor differences in skull features (Pearson, 1958).

Once recognized as a subspecies of *P. xanthopygus*, it was thought that divergence of *P. limatus* Thomas, 1912, occurred during the Last Glaciation, as ascertained by paleoburrow analysis

(Kuch *et al.*, 2002) and phylogenetic studies (Steppan *et al.*, 2007). Presently, considered a different species, *P. bonariensis* Crespo, 1964, has been differentiated from *P. xanthopygus* based on subtle morphological characters and geographical isolation to the Sierra de la Ventana, Buenos Aires (Reig, 1978; Galliari *et al.*, 1996, Teta *et al.*, 2018), although further research was suggested (Musser and Carleton, 2005). Currently, it is understood that *P. limatus* and *P. bonariensis* are included in a complex with *P. xanthopygus*, forming a paraphyletic group (Steppan *et al.* 2007), although specific taxonomical relationships are not clear.

In Patton and Conroy (2017) it is argued that the current emphasis on molecular applications alone has incorrectly limited the definition of subspecies and thus the taxa that can and should be recognized, for that reason, it decided to incorporated geometric morphometric methods. These methods are commonly used to reveal systematic and phylogenetic associations between species, or the relationships between the effects of ecological factors in morphology (Jojic *et al.*, 2012). Also, these analyses have been proved useful when determining shape variation, with results couched in the statistical analysis of landmark points (Evin *et al.*, 2008; Macholan *et al.*, 2008; Milenkovic *et al.*, 2010; Jojic *et al.*, 2012; Lu *et al.*, 2014). On the contrary, classic morphometrics can fail to distinguish groups and reflect the true organization of morphological characteristics (Zelditch *et al.*, 2004; Evin *et al.*, 2008). For this reason, geometric morphometric analyses.

Understanding that the systematics of *P. xanthopygus* is still confuse, and that the molecular phylogeny presented in chapter 1 did not completely clarify the relationships among the different subspecies of *P. xanthopygus*, the major goals of this chapter were: i) to evaluate the traditional taxonomic arrangement of the *xanthopygus* complex using a lineal and a geometric approach; ii) to test the congruency between the molecular results (Chapter 1) and morphological data across the entire distribution range of the *xanthopygus* complex, including *P. limatus* and *P. bonariensis*.

2.2 MATERIALS AND METHODS

2.2.1 Specimens Examined. - Specimens studied are kept in Colección de Mamíferos del Centro Nacional Patagónico (CNP; belonging to the Instituto de Diversidad y Evolución Austral in Puerto Madryn, Chubut, Argentina) and the Museum of Vertebrate Zoology of University of California (MVZ; Berkeley, USA). A total of 712 adult individuals were analyzed, representing the species traditionally recognized as *P. limatus*, *P. bonariensis* and *P. xanthopygus*. Samples were classified into two groups based on morphological traits (Steppan, 1998) and the phylogenetic clades recovered in the molecular phylogeny proposed in Chapter 1 (hereafter referred to simply taxonomic and phylogenetic group respectively; Table 2, Table 3). Adult individuals were categorized based on the tooth wear, occlusal surface and the eruption of the third molar with respect to the other teeth (Gould, 2001). In addition, sex was recorded during the analysis to test for potential sexual dimorphism in skull morphology.

2.2.2 Linear Morphometric Analysis.

Measurements. - A total of 17 cranial measurements (Hershkovitz, 1962) were obtained from 712 individuals (Figure 5): Greatest Length (1), Condylbasal Length (2), Palatal Length (3), Diastema Length (4), Zygomatic Breadth (5), Width of Braincase (6), Mastoid Width (7), Width of Rostrum (8), Palatal-Bridge Length (9) Bullar Length less tube (10), Incisive Foramen Length (11), Molar Row Length (12), Width of M1 (13), Least Interorbital Breadth (14), Nasal Length (15), Eye Orbit Length (16), Greatest Nasal Width (17). Measurements were taken in millimeters and employing a digital calliper to the nearest 0.01mm.

Statistical Analysis. - An analysis of variance (ANOVA) was performed to test the occurrence of sexual dimorphism on skull size, and samples were grouped according to the phylogenetic clades obtained in Chapter 1. This species complex can be divided into three clades according to geography (Puna (basal clade, chapter 1), north and south; from this point forward, it will be address as phylogenetic group; Table 2). The differences between phylogenetic groups were evaluated using ANOVA. Principal component analysis (PCA) was conducted using data from morphometric variables, alongside a discriminant analysis (DA) which grouped the individuals

based on taxonomic labels provided by the collector. The differences between taxonomic groups (Table 2) were evaluated using Tukey HSD. All analyses were performed using JMP 15 (Jones and Sall, 2011).

2.2.3 Geometric Morphometric Analysis

Measurements. - In total, four views of the skull were mapped and analyzed: ventral, dorsal, lateral and mandible in lateral external view (Appendix B). Slight variances of sample numbers between each view were due to broken structures, which interfered in locating certain landmarks (Table 3). A total of 16 ventral view landmarks (Figure 6a), 11 dorsal view landmarks (Figure 6b) and 13 lateral view landmarks (Figure 6c) were used in skull analyses; 14 landmarks were used when mapping the mandible (Figure 6d). A digital camera Nikon D3300, with a resolution of 300 pixels per inch was utilized. The software TpsDig 2.15 (Rohlf, 2008) was used for digitization of landmarks. Skull landmarks were unilaterally mapped, to avoid redundant information due to the symmetrical nature of the structure. A generalized Procrustes Superposition in MorphoJ (Klingenberg, 2011) was performed to eliminate variation unrelated to shape. Additionally, the Procrustes Superposition produced an overall average shape that was used as a reference in subsequent analyses (Zelditch *et al.*, 2004).

Statistical Analysis. - Separate analyses were performed for each individual view. Sexual dimorphism and intraspecific geographical differences in size and shape were evaluated using a canonical variate analysis (CVA). Taxonomic intraspecific differences in centroid size were analyzed using a multivariate analysis (Tukey HSD).

For each skull view, size differences across species were independently assessed using box plots of centroid size and from a skull size proxy, obtained by summing the centroid sizes of separate views, for each individual. PCA was used to reduce the dimensionality of the shape variable data set. The number of principal components analyzed were selected by measuring the correlation between the matrix of Procrustes shape distances in the full shape space, and pairwise Euclidean distance in the reduced shape space (Cardini, Jansson and Elton, 2007).

Alongside Canonical Variant Analysis (CVA), the individuals were grouped according to the taxonomic label provided by the collector.

2.3 RESULTS

2.3.1 Lineal Measurements

Sexual Dimorphism. - The species forming the *xanthopygus* complex presented sexual dimorphism using the Principal Component 1 (PC1) as variable, indicating a significant difference between both sexes (Table 4; Figure 7). For subsequent analyses, male and female samples were treated separately.

Group Differentiation. - To verify the congruency of current taxonomic labels, the difference in size between clades was significant across both sexes based on the PC1 (Table 5, Figure 8). The results are showing a bigger size in the skulls of the southern and northern rather than in the skulls of the Puna clade. The mean of the PC1 was compared between different taxonomic groups (Table 6; Figure 9), with the only notable similarity reported between *P. x. vaccarum* and *P. x. xanthopygus* across both sexes. Whilst *P. bonariensis* had the highest mean among all the groups, this difference was not statistically significant compared to the remaining groups. The unremarkable mean of *P. limatus* demonstrates that it was not separated from other groups.

Principal Component Analysis. – According to the loading matrix, the PC1 is mainly explained by the length and the width of the skull (Table 7), whereas, the PC2 is explained by the interorbit breadth and the bullar length . The PC1 explained 54.8% of the variance for females and 52.6% for males. The cumulative variance between PC1 and PC2 was 61.1% for females and 60.2% for males (Appendix D), with no differentiation between taxonomic groups. When contrasting the morphologic clusters with the phylogenetic groups, the northern and southern clades clustered on the PC2 axis for both sexes. However, the Puna clade was not recovered as a different morphologic cluster on the PCA (Figure 10).

Discriminant Function. - This analysis used taxonomical groups as the discriminant variable; although no group differences were detected. However, when the phylogenetic groups were used as a discriminant variable, the northern, southern and puna group primarily on the canonical vector 1 (CV1), differentiation was noted in both sexes (Figure 11).

2.3.2 Geometric Measurements

Sexual Dimorphism Differentiation. - An analysis was performed based on the Procrustes distances for each view. After permutation testing there was found a significant difference in the lateral and mandible views, and a non-significant difference in dorsal and ventral views (Table 8). In subsequent analyses male and female samples were treated separately for these views.

Phylogenetic Group Differentiation. - A Tukey HSD analysis using the centroid size, Puna group was differentiated from the other two groups in every view and both sexes, showing lower values in the Puna (Table 9, Figure 12).

Taxonomic Group Differentiation in Centroid. - A Tukey HSD analysis using the centroid size, differentiated *P. x. posticalis*, *P. x. rupestris* and *P. x. xanthopygus* in dorsal view of the skull. In ventral view, *P. x. rupestris* separated from the remaining taxonomic groups except *P. x. vaccarum*. In lateral view, the male subset divided *P. x. rupestris* from all of the remaining groups except *P. limatus*, *P. x. ricardulus* and *P. x. vaccarum*. Distinct from their male counterparts, the female group associated *P. x. rupestris* with *P. x. chilensis*, *P. limatus*, *P. x. ricardulus* and *P. x. vaccarum*. Furthermore, *P. bonariensis* females were distinguished from the group formed between *P. x. posticalis* and *P. x. ricardulus*. The mandible view on the male subset separated *P. x. posticalis* from the group constituted by *P. x. rupestris* and *P. x. xanthopygus*. On the contrary, this view isolated *P. x. rupestris* from the remaining groups

within the female subset (Table 10, Figure 16). No taxonomic groupings were able to be ascertained from any view, in either sex (Appendix G).

Phylogenetic Group Differentiation in Shape and Size. - The skull shape differentiated phylogenetic groups among the views (Figure 14); the Puna group is the most distinguishable among the groups; it showed longer nasals and a narrower (in width) skull in dorsal view; it also showed a wider teeth front row and the molar row was located closer to the sagittal axis in ventral view; in the mandible, the angle is flatter in both sexes and the skull is taller among females in lateral view. Compared to the other two groups, the northern group is shorter for males in lateral view. There was no correlation between the centroid size and PC1 in any view (figure 15).

Principal Component Analysis. - The amount of variance showed by the PC1 was 62.3% (dorsal), 28.2% (ventral), 27% (male lateral), 32.6% (female lateral), 16% (male mandible) and 17.3% (female mandible) (Appendix E). This resulted in the clustering of geographic groups by the mandible view across both sexes (Figure 16). Considering the PC2 variance was 13.6% (dorsal), 13.3% (ventral), 19.5% (male lateral), 16.7% (female lateral), 12.8% (male mandible) and 14% (female mandible), the northern and southern groups were formed using the mandible view for both sexes, but the puna group was not able to be differentiated. Taxonomic groups were unable to be separated or distinguished according to any view.

Canonical Variate Analysis. - The CVA used taxonomic groups as a discriminant variable; nonetheless, neither of these groups were separated by CV1 or CV2 (Figure 17). Instead, when phylogenetic groups were used as a discriminant variable, they were clustered primarily on the CV1 axis, based on phylogenetic groupings in every view and sex; although, the puna group was always placed close to the northern group. The CV1 explained 62.3% (dorsal), 67.6% (ventral), 68.6% (male lateral), 63.8% (female lateral), 56.8% (male mandible) and 56.5% (female mandible) of the total variance (Appendix F).

2.4 DISCUSSION

Variance and multivariate analyses were conducted according to the current taxonomic label for each sample, to test the morphometric differences within the *xanthopygus* complex. Despite the separation tendency between *P. x. rupestris* from the remaining subspecies, the individual scores showed a marked superposition from the taxonomic groups. Analyzing the linear and the geometric morphometric data, the grouping of the *xanthopygus* complex was contrary to current taxonomic labelling practices.

The results of this lineal morphologic study show a consistent trend in clustering and differentiating the phylogenetic groups of *P. xanthopygus* distributions, being the smaller skull sizes restricted to the Puna group. This could be explained through new competition for resources at higher elevations, previously demonstrated in other rodent (*Peromyscus maniculatus*) (Holmes *et al.*, 2016). Instead, the geometric morphometric analysis does not show size differentiation between groups, but there is shape variation between the Puna group and the rest of the distribution. These changes are located mainly in the rostrum, the molars and the mastoid bone, which suggested a group differentiation mainly in chewing structures (Spotorno and Walker, 1983); this scenario is particularly interesting among herbivorous species (HersHKovitz, 1962).

Considering the phylogenetic results of mtDNA and nDNA (Chapter 1), the *xanthopygus* complex can be divided into northern, southern and puna groups. Similar patterns in morphology have been reported in other sigmodontine species, such as the clinal variation dividing in *Euryoryzomys russatus* into two groups (Libardi and Percequillo, 2016). Furthermore, similar changes have been found in overall body size of *Abrothrix olivacea* and in the skull of *Abrothrix hirta*, across a latitudinal gradient in Argentina and Chile (Pearson and Smith, 1999; Teta and Pardiñas, 2014). This suggests that the morphological differentiation in this study would have been driven by differential selection among an ecological gradient, despite gene flow.

Currently the species known as *P. bonariensis* is geographically disjunct from *P. xanthopygus*, as detailed in the taxon diagnosis (Crespo, 1964, Pardiñas *et al.*, 2004). Recently, larger values for the breadth of incisive foramina, width of nasals and frontal length have been suggested as characters of *P. bonariensis* (Teta *et al.*, 2018). According to these authors, the morphological differentiation would be attributed to geographic segregation. Contrary to these findings, morphometric results obtained in this study were unable to separate the samples of *P. bonariensis* from the rest of the *xanthopygus* complex. This suggests that there are no morphometric differences between the two species, currently considered as independent. These results may be due to the phylogenetic proximity (Chapter 1) and cyclical movement and gene flow between the species, caused by overlapping glacial refugia (Chapter 3).

Based on morphological and molecular analysis, *P. limatus* is currently considered a different species to *P. xanthopygus* (Steppan, 1998; Kuch *et al.*, 2002b). In this study, *P. limatus* has not found to be segregated from other samples, as it grouped with the northern subspecies of *P. xanthopygus*. This is most likely attributed to the species recent divergence, geographical approximation and gene flow, particularly to *P. x. posticalis*, considered the same taxon (Chapter 1).

The morphometric results align with the phylogenetic results from chapter 1. This reaffirms the taxonomical proposal that three clades representing different subspecies constitutes *P. xanthopygus*. Morphological analyses conducted in this study supported genetic results in that *P. x. rupestris* is differentiated from other subspecies. The basal clades identified by genetic analysis were also demonstrated in skull size variation, where smaller skull size was observed in samples occupying the Puna area (Holmes *et al.*, 2016) and variation in teeth shape and positioning.

CHAPTER 3: INTRASPECIFIC PHYLOGEOGRAPHY OF *Phyllotis xanthopygus* (RODENTIA, SIGMODONTINAE) IN PATAGONIA, DURING THE LAST GLACIAL MAXIMUM

3.1 INTRODUCTION

Phylogeographic data has evolved during the past decade due to conceptual, technological, and analytical-computational developments. Among these developments there has also been a growing appreciation of the potential for incongruence within species trees. This discordancy has led to an increasingly important interface between population genetics and phylogenetics (Edwards, 2009). To clarify phylogeographic patterns in recently colonized areas, and to provide higher genetic resolution than gene-based methods (Peterson *et al.*, 2013), there has been an overwhelming shift toward datasets comprising multiple nuclear loci, such as double digest random sequencing (ddRADseq). Such technique has enhanced the relationship between population genetics and phylogenetics in studies that encompasses Last Glacial Maxima (Wagner *et al.*, 2013; Gaither *et al.*, 2015; Jeffries *et al.*, 2016; Wyngaarden *et al.*, 2016).

Climate oscillations during the Pleistocene had a profound impact on the distribution of many species, leading to different diversification patterns and timing among isolated populations (Avice, 2000). It is well understood that within the sigmodontine rodent lineages *Phyllotis xanthopygus* is among the species impacted during climate changes cycles of the Pleistocene. This species inhabits high mountain areas, similar to those previously covered by the ice sheet during the LGM in the Andes cordillera, which may have acted as a temporary geographical barrier (Rabassa, 2008). Considering this climactic event and the limited prevalence of widespread direct (fossil) evidence in Patagonia (Tammone *et al.*, 2014), paleodistribution reconstruction of the southern clade (chapter 1) of *P. x. xanthopygus* was needed, including spatial geographical aspects (Hugall *et al.*, 2002). This detailed reconstruction assisted in identifying possible glacial refugia and postglacial recolonization routes, based on the phylogeographic lineages of the species.

Despite previous studies, phylogenetic relationships within *Phyllotis xanthopygus* remained unclear. Therefore, a combined molecular systematic and morphological study was required, to clarify the evolutionary history of this species, and examine the validity of subspecies traditionally recognized within the geographical range. Additionally, *P. xanthopygus* is found to be distributed approximately from 11 to 50° South, along the Andes mountain range and the Atlantic coast in southern Patagonia considering that the Patagonian region of South America was affected by the glacial cycles of the Plio-Pleistocene to a high degree (i.e., the Andes mountains and the piedmont), the population structure of *P. x. xanthopygus* was still unknown and unable to be explained by geographical reasoning (Riverón, 2011). Therefore, a phylogeographic study of the Patagonian region, using high temporal resolution with a genomic approach was required to evaluate the phylogeographic breaks between 35° S and 45° S.

Phylogeographic studies applying nested clade analysis (NCA) in *P. xanthopygus* based on cytochrome B data have distinguished two clades, the Altiplano clade and the North-South clade (Albright, 2004). The Altiplano clade occupies areas of Peru, Bolivia and northern Chile, whereas the North-South clade covers Argentina and southern Chile. This two-clade arrangement is in disagreement with the subspecies proposed through morphologic analyses (Steppan, 1993). Due to the low number of individuals sampled by Albright (2004), and the criticisms against NCA methodology (Petit, 2008), it is questionable if accurate phylogeographic conclusions can be inferred, based on the former study. Similarly, in a phylogeographic study based on cytochrome b data (Riverón, 2011), low genetic diversity of *P. xanthopygus* in Argentinean Patagonia was found, probably due to the recent recolonization of this ecoregion since the Last Glacial Maximum (LGM). These results suggest that Patagonia consists of two haplogroups, north and south, comprising the subspecies *P. x. vaccarum* and *P. x. xanthopygus*, respectively. These haplogroups would be separated by the Río Negro in the Argentinean Patagonia (40°S). However, this phylogeographic break of the latter two haplogroups cannot be recognized, due to the polytomy present among the individuals of the southern group (Riverón, 2011). This is similar to the distribution patterns found among other sympatric sigmodontine taxa in Patagonia, such as rodents of the genera *Abrothrix*,

Eligmodontia, *Oligoryzomys* (Kim *et al.*, 1998; Lessa *et al.*, 2010), and lizards of the *Liolaemus* genus (Morando *et al.*, 2007; Victoriano *et al.*, 2008).

In Patagonia multiple phylogeographic breaks have been recorded and classified according to geographic position (Sérsic *et al.*, 2011, Lessa *et al.*, 2012). The series of phylogeographic breaks located within the Andes cordillera are considered distinct from those located within lower altitude areas of Argentina. Andean breaks are associated with pre-Quaternary and Quaternary processes such as Andean orogenesis and paleo-basins (Sérsic *et al.*, 2011). Whilst other transient breaks located in the Pampas region of Argentina are likely the result of Quaternary events, such as glaciations, which have generated changes in the dynamics of river basins and the coastline (Pardiñas *et al.*, 2011).

Considering the previously discussed paleo-biogeographic context, the aims of this study are: i) Through application of genomics, uncover the population structure of individuals from *P. x. xanthopygus* in southern Patagonia, comprised of and formally known as *P. x. vaccarum*, *P. x. xanthopygus* and *P. bonariensis*; and ii) Discover potential refugia areas during glacial periods and recolonization routes since the LGM through niche modeling.

3.2 MATERIALS AND METHODS

3.2.1 Double Digest RAD Sequencing (ddRADseq).

Sampling. - A total of 264 specimens from the collection Centro Nacional Patagónico (CNP) labelled as *Phyllotis xanthopygus* (n=245) and *Phyllotis bonariensis* (n=19), but currently known as *P. x. xanthopygus* (Chapter 1) were collected from 37 localities across the Patagonian ecoregion and central Chile (Table 11; Figure 18). The Patagonia ecoregion is defined as the region which extends from the Río Colorado (approximately 35° S to 36° S) in Argentina and the south of Valdivia (approximately 39° S) in Chile, to the southernmost point of South America (56° S) *sensu* Sérsic *et al.* (2011). Tissue samples were collected and preserved at -80° C or in 80% ethanol solution. DNA extraction was performed using the phenol-chloroform method. All DNA samples were quantified using the Qubit dsDNA HS assay kit and read on a Qubit v2.0 (Life Technologies).

Data Collection. - The libraries were prepared using the methodology outlined in Peterson *et al.* (2012) at the Evolutionary Genetics Lab, located at the University of California, Berkeley, USA. This method included the use of EcoRI and MspI as restriction enzymes. Samples were pooled into a multiplexed library and sequenced on a single-end read Illumina HiSeq 4000 with a 20X coverage.

Data Filtering. - Raw data sets were checked for quality by using the software FastQC v0.11.5 (Andrews, 2015), which provided a modular set of analyses. Data sets were further analyzed using the software pipeline Stacks v2.3b (Catchen *et al.*, 2013), to identify Single Nucleotide Polymorphisms (SNPs) within or among populations. Furthermore, the use of Stacks v2.3b filtered and clustered the data prior to enable exportation into Structure v3.2 (Pritchard *et al.*, 2000). This software performed population clustering, including seven iterations for 70000 Markov chain Monte Carlo (MCMC), with a burning of 7000.

3.2.2 Niche Modeling Analysis.

Study Area. - The area studied included the complete distributional range of *P. xanthopygus* extending from southern Peru into Bolivia, Chile and Argentina. This area is comprised of diverse biomes (from lush bushland through to sparse rocky deserts) and a wide altitudinal range (sea level up to 5570m). The study also included *P. bonariensis* located solely in the Sierra de la Ventana.

Database. - The database included 395 individuals of *P. xanthopygus* and *P. bonariensis*, taken from captures and data points available online (Global Biodiversity Information Facility, 2019). The geographical coordinates were standardized to an area of 1 km² and graphed using QGIS v2.18.9 (QGIS Development Team, 2016), coordinates were then converted to degrees using the *WGS84* global reference system.

Environmental Variables. - A spatial resolution of 1 km² was used. Employing thousand-year intervals, each climatic and geographic layer over the last 21 000 years was analysed. The variables considered within each interval were: Highest Temperature Month (HTM), Lowest Temperature Month (LTM), Annual Average Temperature (AAT), Driest Month (DM), Wettest Month (WM), Annual Average Precipitation (AAP) and Altitude (AT), as taken from Pliscoff *et al.* (2014).

Ecological Niche Modeling. - Ecological niche and potential geographic distribution, under both present-day and past environmental conditions, were modeled by the maximum entropy method (Maxent), using the DISMO package in R (R Core team, 2015). Randomly within the Patagonian continental area, two thousand background sites were created. The model performance was assessed on the area under the curve (AUC) of the receiver operating characteristic, estimated from test data (Fielding and Bell, 1997). In order to avoid false positives (Pearson *et al.*, 2007), niche modeling according to lineage was conducted.

3.3 RESULTS

3.3.1 Population Genomics. - Based on the DNA concentration, 15 pools were grouped, each containing a maximum of 20 samples. EcoRI barcodes from 1-20 (Peterson *et al.*, 2012) were assigned to each individual sample within each pool, to clearly identify and differentiate sequences. A total of two sequenced lanes were produced generating 2.93×10^8 usable reads in lane one, and 2.95×10^8 usable reads in lane two.

The *de novo* assembly of all reads produced a total of 990 unique contigs, or putative loci (hereafter referred as loci). The *ref map* assembly utilized the *Peromyscus maniculatus* genome as a reference, producing a superior quantity of total loci (n=6992), the mean heterozygosity was 0.0088 with a standard deviation of 0.00764. These data were prepared to be phylogeographically analyzed in the software Structure (Pritchard *et al.*, 2000), based on Bayesian clustering. The analysis geographically differentiated two clusters. The southern cluster (depicted in orange) was separated from the northern cluster (depicted in purple and

blue). Subsequently, the northern cluster was divided into two groups, differentiated by altitude; high (blue) and low (purple) and glacial refugia (Figure 19; Figure 20 F, L; Table 11), which resulted in ΔK for $K=3$ (Figure 19) applying the protocol described in Evano *et al.*, 2005. *Fst* values between clusters were found to be: purple/orange = 0.146, purple/blue = 0.857 and orange/blue = 0.928.

3.3.2 Distribution Modeling. – The phylogeographic clusters were modeled using 36 individuals for the orange cluster, 73 for the blue cluster and 107 for the purple cluster. Bioclimatic modeling of *P. xanthopygus* distribution, yielded an AUC score of 0.86. Heuristic estimation of relative variable contribution to the model, indicated that the most informative variables were HTM (43.1%) and AT (28.3%). The least informative variable was WM (2.6%).

The species distribution model post LGM indicated a reduction in the northern distribution range, and a separation between the northern and the southern distribution, reaching low altitude areas (Figure 21c). Following this, the southern distribution expanded in size, to reach coastal areas in the Patagonian Region (Figure 21b). The current distribution model of *P. xanthopygus* (Figure 21a) includes the high-altitude areas in the Andes cordillera like puna region as well as coastal regions in the most northern and southern distributions.

Individual population lineages were modeled to reveal possible glacial distribution and recolonization of the Patagonian Region. Consistent throughout 21Kya and the present, the blue lineage showed a high probability of distribution in the Patagonian Andes cordillera, occupying from approximately 35 to 45° S (Figure 21d, 21e, 21f). During the LGM, the orange lineage occupied the southern part of the Patagonian Region (Figure 21h, 21i). As temperatures rose in southern Patagonia, the orange lineage colonized the Atlantic coast (Figure 21g). Alternatively, the purple lineage paleodistribution spanned the northern Patagonian Andes (Figure 21K 21L). In present-day, this lineage occupies Argentinean and Chilean Patagonia (Figure 21j). The area of probability in Chacoan region have expanded throughout the last 21Ky, oscillating between 20-40%.

3.4 DISCUSSION

ddRADseq provides simple and inexpensive means to collect genome-wide sequence data from diverse non-model organisms (Arnold *et al.*, 2013). Although the amount of information extracted from this type of data depends on the method used, in this study the use of a reference genome increased the total number of Loci produced; even though the chosen genome used was not from the species studied, it did belong to the same family (*Peromyscus maniculatus*; Cricetidae). The increase in the total number of markers generated when using a reference genome, are predicted to increase statistical accuracy and power, in order to recognize special patterns (Allendorf *et al.*, 2010).

Despite the wide altitudinal and latitudinal range of the species studied, results show a significant population differentiation and structure across the Patagonian range of *P. x. xanthopygus*. According to the statistical analysis the Patagonian ecoregion can be divided in three separate lineages. From the biological perspective, the different refugia and glacial cycles, with local adaptation to different abiotic conditions such as altitude, can explain the separation of these genetic groups. Body size differs in *P. xanthopygus*, as a result of thermal acclimatization and oxygen consumption (Nespolo *et al.*, 2003); similarly, there were genetic variances attributed to altitude within the blue lineage. Found exclusively in the Patagonian portion of the Andes cordillera, at areas of high-altitude, the blue lineage was genetically distinguished from orange and purple lineages.

Genetic variance between the purple and orange lineages can be attributed to the area surrounding Río Negro in Argentina, which acts as a geographical barrier between the two groups. Historically, research on species with similar vagility to *P. xanthopygus*, suggested that rivers can act as a phylogeographic break within the Patagonian region (Sérsic *et al.*, 2011). Interestingly, populations west of the Andes cordillera, including southern Chilean Patagonia, are genetically aligned to populations of northern Argentina; although found geographically closer to the orange lineage, located in southern Argentinean Patagonia. This genetic distribution can be explained by the geographical barrier between the two lineages, formed by

the southern Andean cordillera. Furthermore, northern Argentinean populations may have recolonized southern Chilean Patagonia at the time of ice sheet retreat, due to the absence of geographic barriers. Both geographic and physiologic barriers may have impacted genetic divergence (Avise, 2000; Irwin, 2002), and can be measured by F_{st} values. Considering low F_{st} values were recorded between the orange and purple lineages, it can be established that in *P. x. xanthopygus*, genetic variances are most pronounced between groups separated by a geographic barrier.

Species distribution across the entire range has been maintained fairly consistent since LGM to present-day. At 21 Kya both the northern and southern distribution were not connected, and the Puna region had low probability of distribution. Potentially caused by low temperatures at 21Kya, the distribution pattern at the LGM could depict a forced migration of populations, in order to maintain similar environmental conditions. A notable temperature surge at 12Kya within Patagonia (Metcalf *et al.*, 2016), allowed populations to expand their distribution, reaching areas in the eastern side of the cordillera. As temperatures have continued to rise up until present-day (Pollock and Bush, 2013), populations of *P. xanthopygus* has followed the ecological corridor of the Andes, migrating to areas of higher altitudes. This recolonization of the Puna region and the high mountains of the Pacific desert region has formed the modern distribution pattern of the species.

Niche modeling of the lineages showed a southward trend during LGM. Results according to phylogeographic analysis, suggested that individual lineages occupied similar refugia, most likely in the Patagonian Andes. The orange lineage has the largest range between 40° and 54° S, in an area which at the time intersected with the blue lineage. Occupying a smaller geographical area, the blue lineage was also found to have high probability of inhabiting the Andes of northern Patagonia. This is the area in which the purple lineage had the highest probability of occurrence at this time. These paleodistributions are congruent with the F_{st} values between the lineages, providing further explanation of the genetic differences and similarities between lineages. During the last 21k years, the distribution of these lineages did not change

significantly, until present-day, when warmer temperatures allowed the recolonization of the high-altitude areas.

The population structure analysis showed that the species formerly known as *P. bonariensis* was included in the purple lineage of *P. xanthopygus*, thus not forming an exclusive lineage. The current distribution of *P. bonariensis* is located within a small Sierra surrounded by flatland, known as Sierra de la Ventana (Buenos Aires, Argentina; Locality 1). This flatland habitat is not suitable for the genus *Phyllotis* which thrives in high-altitude rocky environments (Patton *et al.*, 2015). An explanation for this disjunct distribution of *Phyllotis* could be the Patagonian recolonization pattern of the “purple” lineage, which likely took place through the Chacoan region, leaving a remnant population in this Sierra which prospered because of suitable habitat. A similar distribution pattern has been found in *Oligoryzomys longicaudatus* (Palma *et al.*, 2012), a sigmodontine with comparable vagility to *P. xanthopygus*. The high genetic connection between *P. xanthopygus* and *P. bonariensis* may be explained due to an unbroken gene flow during glacial cycles (Petit *et al.*, 1999). This would have prevented the significant genetic and morphological differentiation (Chapter 1 and Chapter 2) required to be considered as a different species.

CONCLUSIONS

Phylogenetic relationships among the subspecies of *P. xanthopygus* recovered in this study concluded that; a basal clade formed by *P. x. rupestris* located in Bolivian high-altitudinal areas, and two internal clades, differentiated by an ecological gradient. The separation of the northern and southern internal clades is presumed to have originated from a dispersal event, triggering population movements from high mountain regions to lower altitudinal areas of the northern Andes. The results of dating hypothesized that dispersal to the Patagonian ecoregion was approximately 1.12 Mya. Consequently, according to the phylogenetic results showed in chapter 1 the taxonomic classification should consider *P. limatus* as a subspecies of *P. xanthopygus* being part of the northern clade. Similarly, *P. bonariensis* should also be considered as a subspecies of *P. xanthopygus* grouped within the southern clade. Therefore, it can be proposed that *P. xanthopygus* is composed of three subspecies, *P. x. rupestris* (basal clade), *P. x. posticalis* (Northern clade) and *P. x. xanthopygus* (Southern clade). This hypothesis addresses the previously unsolved taxonomic issue surrounding the species, and calls for the number of subspecies within *P. xanthopygus* to be reduced to three including *P. limatus* and *P. bonariensis*, accurately reflecting the phylogenetic clades.

Morphological analyses conducted in this study supported genetic results in that *P. x. rupestris* is differentiated from other subspecies. The basal clade identified by genetic analysis were also demonstrated in skull size variation with lineal morphometric methods, where smaller skull size was observed in samples occupying the relatively high-altitude in the Puna area. Similar to other studies, where elevation has been related to skull size in rodents (Holmes *et al.*, 2016). According to geometric morphometric methods, size is not a factor in the differentiation of the genetic clades, but shape in the rostrum, molar and mastoid showed variation between the Puna group and the rest of the distribution.

Challenges to accurately understand the phylogeography of *P. xanthopygus* in the Patagonian region are the recency of colonization and cyclical perturbations in the area. The glacial-interglacial cycle greatly influenced the connection within species groups; most notably

molding populations from the southern regions of South America into three lineages. The impact of these cycles extends to the genesis of two barriers; a geographical barrier formed by the relatively rock-free environment surrounding the Río Negro, a habitat less associated with *P. xanthopygus* distribution (Kim *et al.*, 1998) and a physiological barrier, characterized by altitude. Corroborating previous findings, a complex population dynamic and shared refugia during glacial periods has amplified the connection between Patagonian lineages; this is inclusive of *P. bonariensis* populations, now considered part of *P. xanthopygus*.

Further genetic studies are required to clarify the exact geographical demarcation between the northern and southern internal clades, in the Mediterranean region of Chile and the Pampas region of Argentina. It is also recommended to include individuals from the northern part of the distribution and that the genome of *P. xanthopygus* be completely sequenced to improve the volume of loci in ddRADseq data and to contribute to higher temporal resolution of population structure and a complete history of the species.

FIGURES AND TABLES

Chapter 1

Table 1. Species sampled according to locality and region; UP (Ulyses Pardiñas), EP (Eduardo Palma), CG (Carlos Gilliari), NK (New Mexico Krio voucher), ROB (Rosario Robles), PNG (Patagonian National Geographic), PPA (Proyecto Patagonia Argentina).

Sample	Species or subspecies	Locality	Latitude	Longitude	Region
MUSM35476	<i>P. x. posticalis</i>	Quebrada	-15.0506	-73.6573	A
MUSM35467	<i>P. x. posticalis</i>	Cerro Parhros	-15.0718	-73.6648	A
MUSM35468	<i>P. x. posticalis</i>	Cerro Parhros	-15.0718	-73.6648	A
MUSM31521	<i>P. limatus</i>	Quiscos	-16.1896	-71.6530	A
MSB235368	<i>P. x. rupestris</i>	Cochabamba	-17.6667	-65.5833	B
MSB234915	<i>P. x. rupestris</i>	Cochabamba	-17.75	-65.0333	B
MUSM21601	<i>P. limatus</i>	Palca	-17.7738	-69.9584	A
NK96039	<i>P. x. chilensis</i>	Chungara	-18.2506	-69.1766	B
NK96033	<i>P. x. chilensis</i>	Chungara	-18.2506	-69.1766	B
MSB237237	<i>P. x. rupestris</i>	Tarabuco	-19.1729	-64.9242	B
NK96053	<i>P. x. chilensis</i>	Enquelga	-19.2205	-68.7452	B
MSB75287	<i>P. x. rupestris</i>	Potosi	-19.65	-65.3333	B
EP426	<i>P. limatus</i>	Quebrada Tarapaca	-19.9474	-69.5324	A
EP427	<i>P. limatus</i>	Quebrada Tarapaca	-19.9474	-69.5324	A
MSB232423	<i>P. x. rupestris</i>	Serranía del Sama	-21.45	-64.8667	B
UP666	<i>P. x. vaccarum</i>	Sierra de Zenta	-23.0662	-65.0626	B
CG109	<i>P. x. vaccarum</i>	Cerro los Linderos	-32.005	-64.9335	C
NK96754	<i>P. darwini</i>	Rinconada	-33.0177	-70.8170	D
ROB138	<i>P. bonariensis</i>	Abra de la Ventana	-38.069	-62.0233	C
ROB74	<i>P. bonariensis</i>	Abra de la Ventana	-38.069	-62.0233	C
ROB22	<i>P. bonariensis</i>	Abra de la Ventana	-38.069	-62.0233	C
ROB132	<i>P. bonariensis</i>	Abra de la Ventana	-38.069	-62.0233	C
ROB142	<i>P. bonariensis</i>	Abra de la Ventana	-38.069	-62.0233	C
PNG167	<i>P. x. xanthopygus</i>	Cerro Corona Grande	-41.7306	-67.1636	E
PPA894	<i>P. x. xanthopygus</i>	E. Los Manantiales	-45.4642	-69.4905	E
PPA437	<i>P. x. xanthopygus</i>	Est. La Península	-47.2684	-71.5421	F
UP3076	<i>P. x. xanthopygus</i>	Cañadón Yaten	-50.1780	-70.1480	E
		Juagen			
UP3064	<i>P. x. xanthopygus</i>	Cerro Fortaleza	-50.2237	-70.8839	E
UP3063	<i>P. x. xanthopygus</i>	Cerro Fortaleza	-50.2237	-70.8839	E
UP3071	<i>P. x. xanthopygus</i>	Balsa Helmich	-50.2172	-71.5085	E
UP3056	<i>P. x. xanthopygus</i>	Estancia Rincón Grande	-50.2911	-70.1581	E
UP3068	<i>P. x. xanthopygus</i>	Balsa Helmich	-50.2172	-71.5085	E
UP3070	<i>P. x. xanthopygus</i>	Balsa Helmich	-50.2172	-71.5085	E

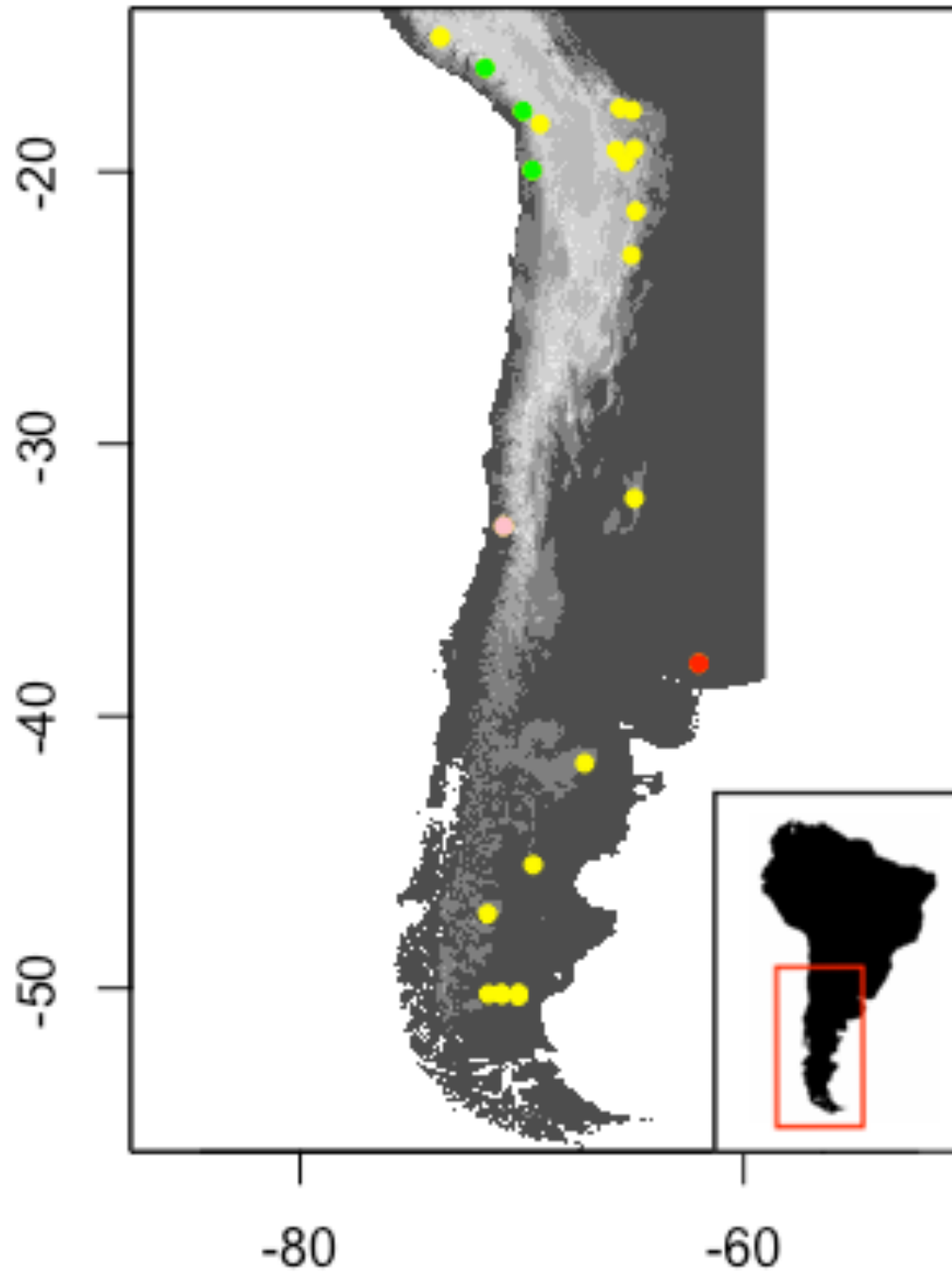


Figure 1. Map of species sampled: *P. darwini* (pink), *P. bonariensis* (red), *P. limatus* (green), *P. xanthopygus* (yellow).

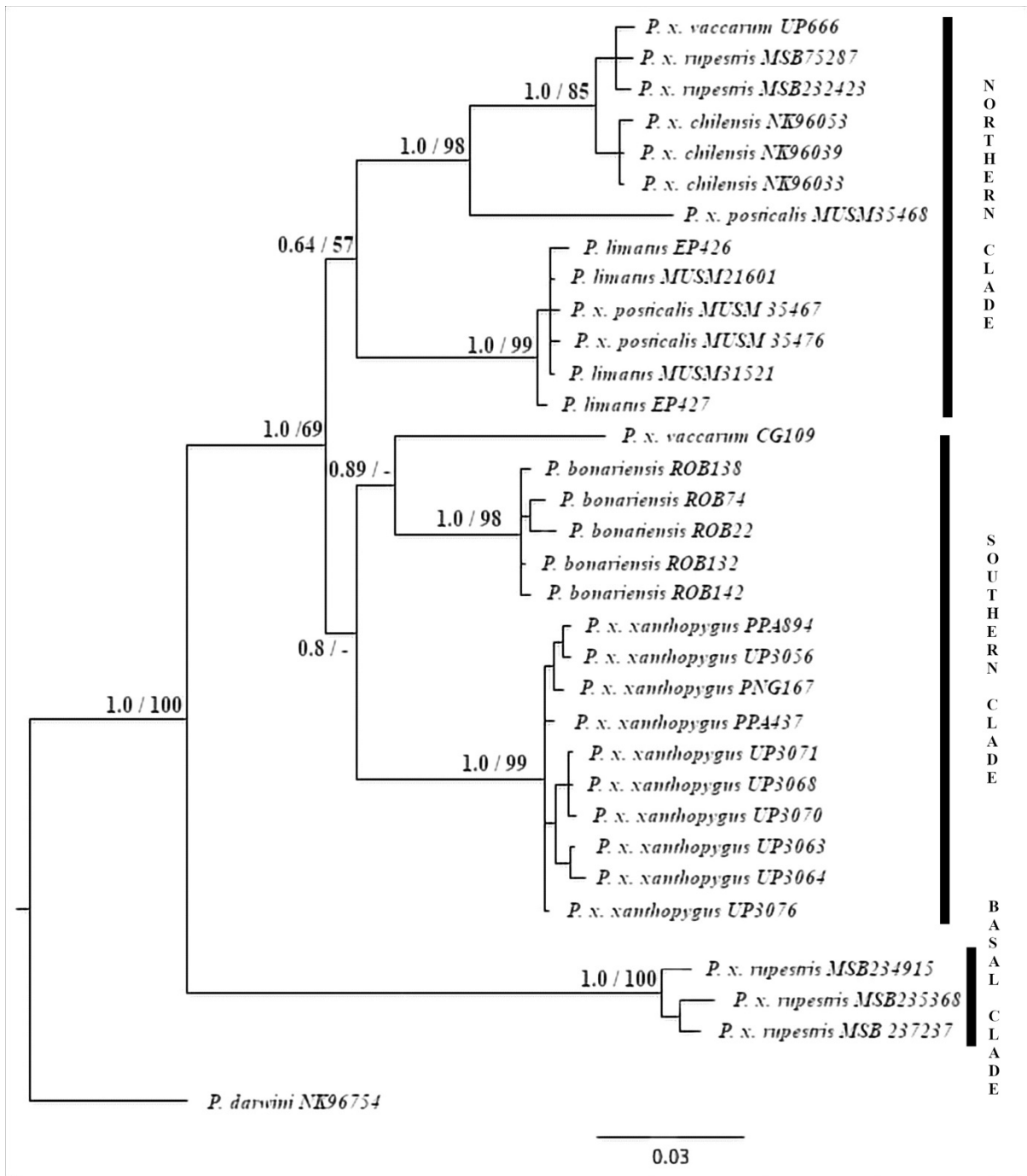


Figure 2. Maximum Likelihood and Bayesian inference phylogram of Cytochrome B and β Fgb-I7 sequences. Number above branches are bootstrap proportions and Bayesian posterior probabilities.

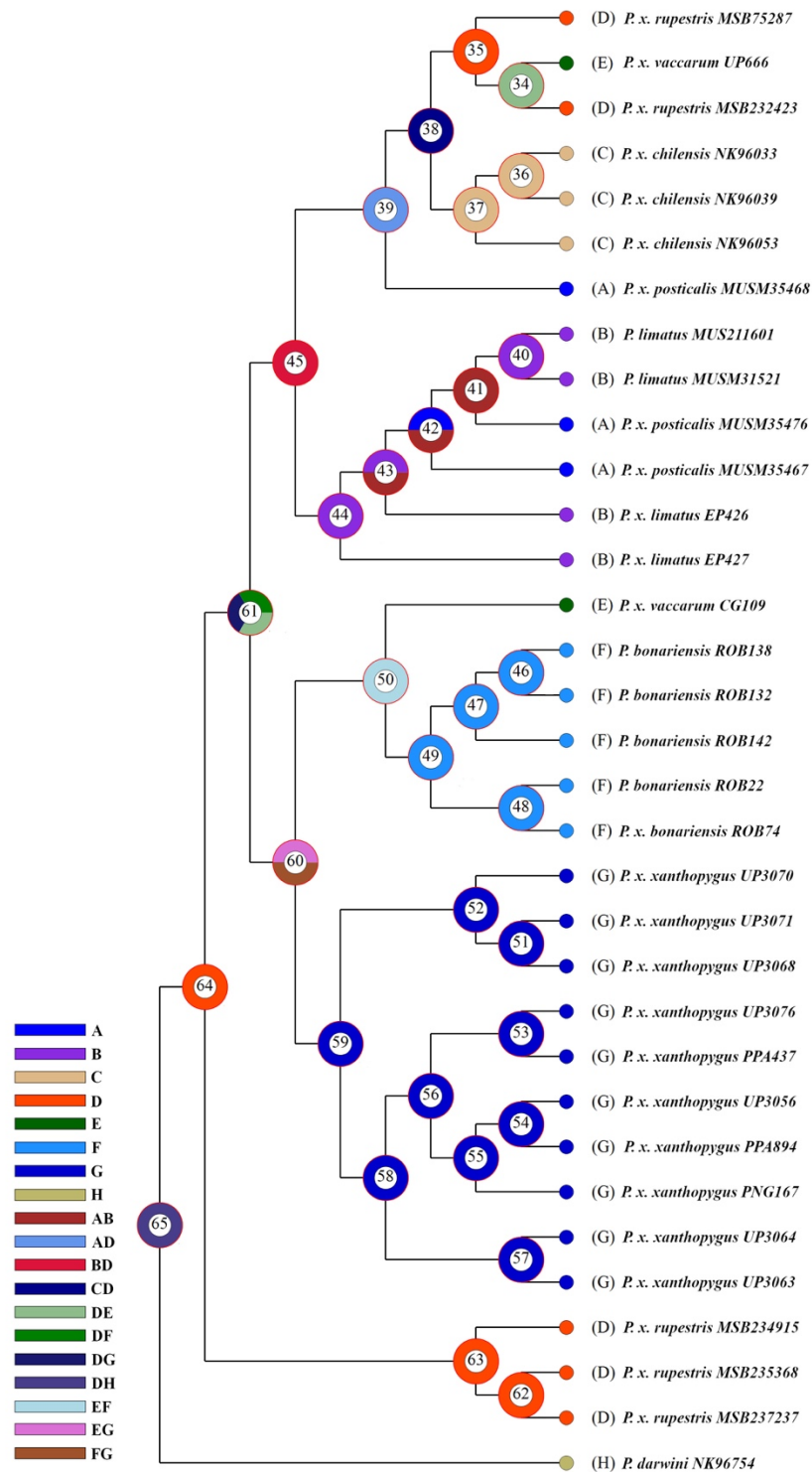


Figure 4. Historical biogeographic analysis of the *xanthopygus* complex. Ancestral distributions were reconstructed with Dispersal vicariance Analysis (S-DIVA) in RASP using the maximum clade credibility tree recovered with BEAST. Node color represents probability of ancestral area. A. Andean Pacific Desert Region; B. Pacific Desert Coast Region; C. Andean Altiplano Region; D. Puna Region; E. Mediterranean Andes Region; F. Chacoan Region; G. Patagonian Region; H. Central Chile Region.

Chapter 2

Table 2. Group and sex differentiation of lineal variables. TT (Traditional taxonomy), PC (Phylogenetic clades)

Species	Group		LINEAL	
	TT	PC	Female	Male
<i>P. bonariensis</i>	Bona	South	3	7
<i>P. limatus</i>	Lima	North	26	38
<i>P. x. chilensis</i>	Chile	North	30	40
<i>P. x. posticalis</i>	Posti	North	39	44
<i>P. x. ricardulus</i>	Ricar	North	7	4
<i>P. x. rupestris</i>	Rupes	North	31	54
<i>P. x. vaccarum</i>	Vacca	South	9	7
<i>P. x. xanthopygus</i>	Xantho	South	196	177
Subtotal			341	371
Total			712	

Table 3. Group and sex differentiation of skull views. Female (F), Male (M) TT (Traditional taxonomy), PC (Phylogenetic clades).

SPECIES	GROUP		DORSAL		VENTRAL		LATERAL		MANDIBL E	
	TT	PC	F	M	F	M	F	M	F	M
<i>P. bonariensis</i>	Bona	South	7	7	7	8	7	7	7	8
<i>P. limatus</i>	Lima	North	26	40	26	40	24	39	25	40
<i>P. x. chilensis</i>	Chile	North	39	47	39	47	37	49	39	47
<i>P. x. posticalis</i>	Posti	North	36	48	38	47	38	46	38	49
<i>P. x. ricardulus</i>	Ricar	North	6	4	6	4	6	4	5	4
<i>P. x. rupestris</i>	Rupes	North	31	52	31	52	31	53	31	51
<i>P. x. vaccarum</i>	Vacca	South	10	6	10	5	10	6	10	5
<i>P. x. xanthopygus</i>	Xantho	South	194	176	194	176	193	177	197	179
Subtotal			349	380	351	379	346	381	352	383
Total			729	730	727	735				

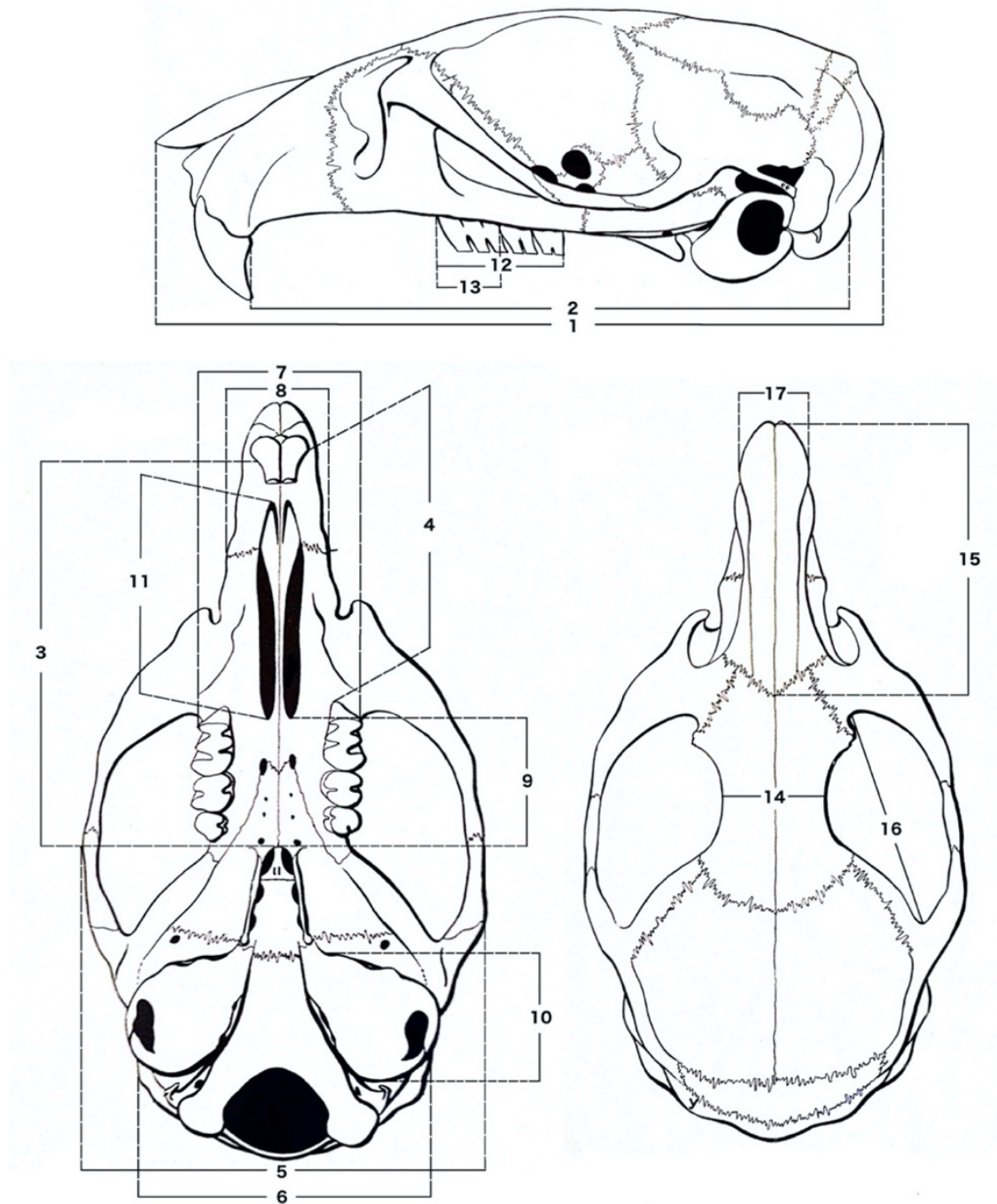


Figure 5. Dimensions superimposed to a skull of a generalized phyllotine (after Hershkovitz, 1962: figs. 23 to 25). See Appendix G for reference numbers.

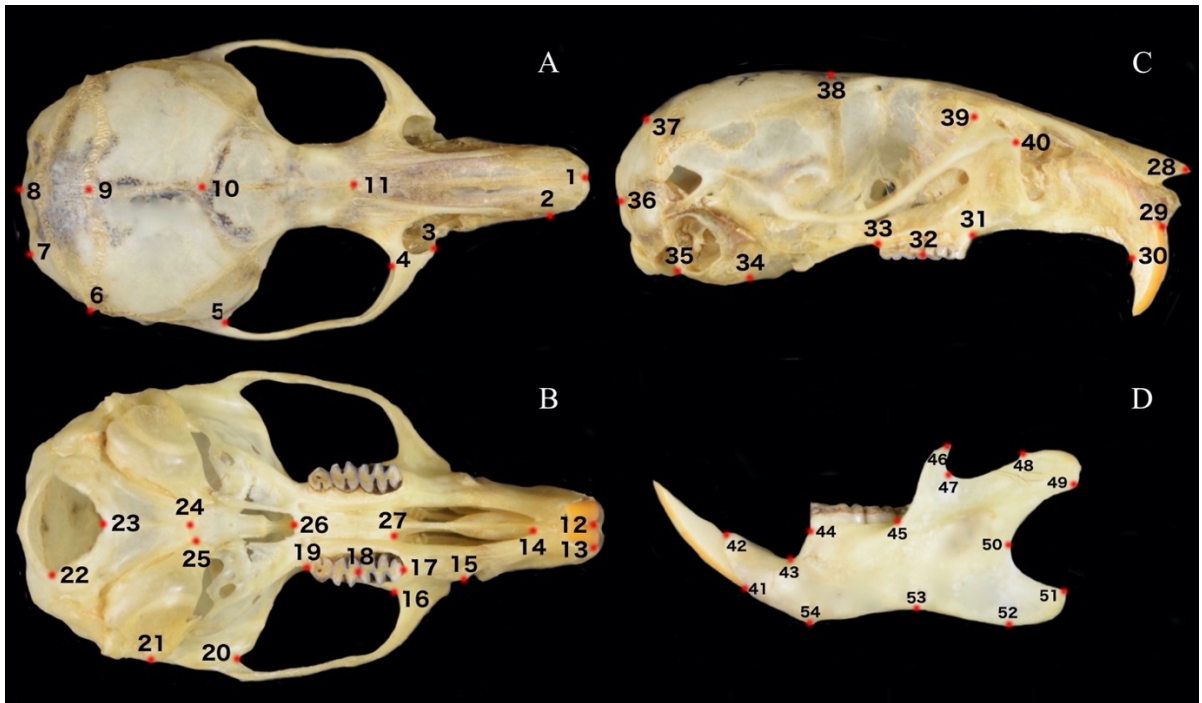


Figure 6. Landmark location on *P. x. xanthopygus* skull. (A) Dorsal, (B) Ventral, (C) Lateral, (D) Mandible in external view.

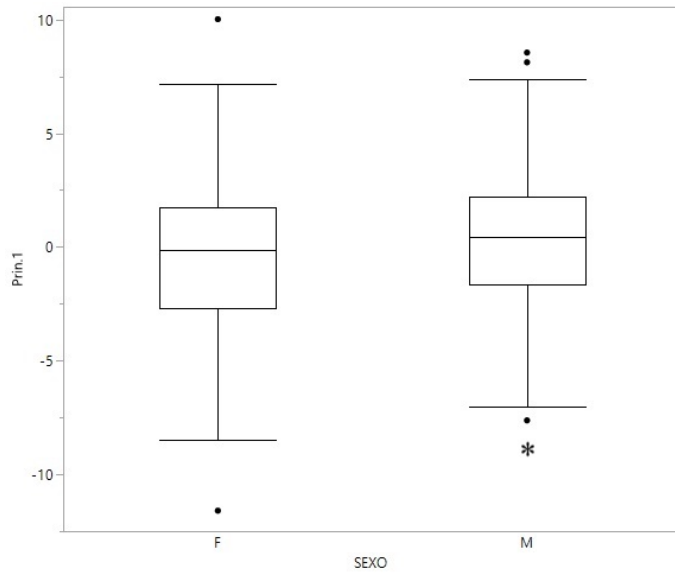


Figure 7. PC1 sexual dimorphism variation. Groups not connected by the same mark are significantly different.

Table 4. ANOVA sexual dimorphism variation. Degree of Freedom (DF), Sum of Square (SS), Mean Square (MS).

Source	DF	SS	MS	F Ratio	Prob > F
SEXO	1	124.1619	124.162	14.2264	0.0002*
Error	710	6196.5610	8.728		
C. Total	711	6320.7229			

Table 5. PC1 phylogenetic variation. Sample size of group (N), Standard Deviation (SD), Confidence Interval (CI). Tukey HSD represents differences between pairs of group means. Groups not connected by the same letter are significantly different.

Sex	Group	N	Mean	SD	95% CI		Tukey HSD
					Lower	Upper	
Male	North	155	-0.68001	2.78845	-1.12246	-0.23755	A
	Puna	25	-3.59714	1.79482	4.338	-2.85627	B
	South	191	1.02267	2.75297	0.62974	1.41559	C
Female	North	120	-1.40259	2.68665	-1.8882	-0.91695	A
	Puna	13	-3.75758	1.40494	-4.60657	-2.9086	B
	South	208	-1.04433	2.8178	0.65884	1.4292	C

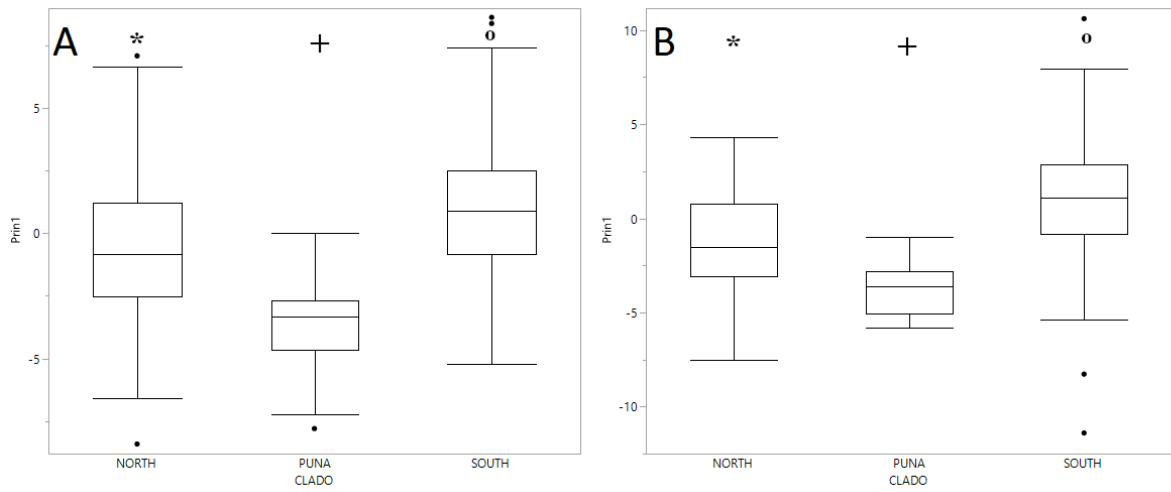


Figure 8. PC1 phylogenetic variation. (A) Male; (B) Female. Groups not connected by the same mark are significantly different.

Table 6. PC1 taxonomic variation. Sample size of taxonomic group (N), Standard Deviation (SD), Confidence Interval (CI). Tukey HSD represents differences between pairs of group means. Groups not connected by the same letter are significantly different.

Sex	Group	N	Mean	SD	95% CI		Tukey HSD
					Lower	Upper	
Male	Bona	7	3.7426	0.9762	1.823	5.662	A
	Chile	40	-0.3606	0.4084	-1.164	0.442	A B
	Lima	38	-1.7870	0.4190	-2.611	-0.963	A B C
	Posti	44	0.8712	0.3894	0.105	1.637	A B
	Ricar	4	1.4801	1.2914	-1.059	4.020	A B
	Rupes	54	-2.9120	0.3515	-3.603	-2.221	B C
	Vacca	7	1.9742	0.9762	0.055	3.894	CD
	Xantho	177	0.8775	0.1941	0.496	1.259	D
Female	Bona	3	3.3966	1.5418	0.364	6.429	A
	Chile	30	-2.2645	0.4876	-3.224	-1.305	A
	Lima	26	-1.9117	0.5237	-2.942	-0.881	A B C
	Posti	39	-0.1744	0.4276	-1.016	0.667	A B C D
	Ricar	7	0.3742	1.0093	-1.611	2.360	A B
	Rupes	31	-3.0754	0.4796	-4.019	-2.132	B C D
	Vacca	9	-0.0236	0.8901	-1.775	1.727	C D
	Xantho	196	1.0570	0.1907	0.682	1.432	D

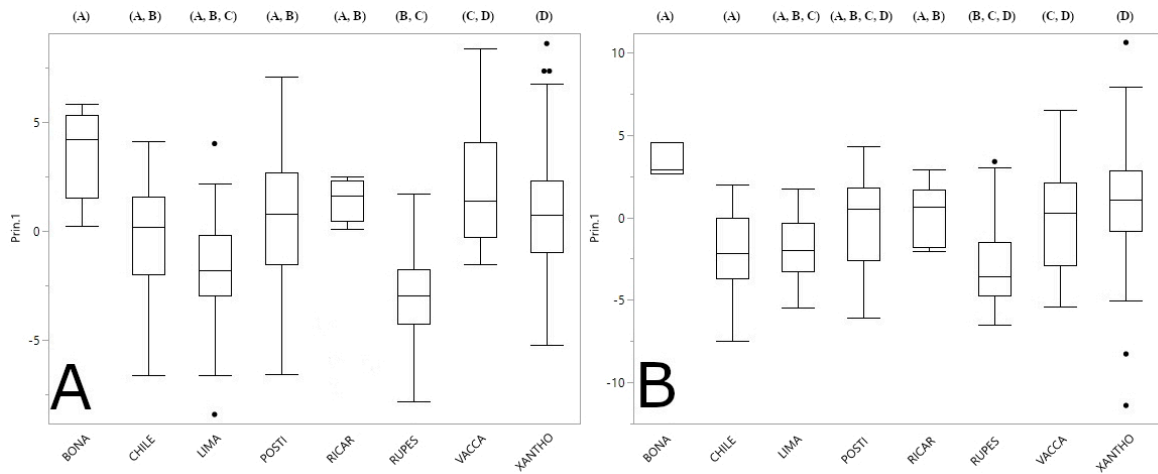


Figure 9. PC1 taxonomic variation. Groups not connected by the same letter are significantly different. (A) Male (B) Female.

Table 7. Loading matrix of PCA of lineal variables.

Variable	Male		Female	
	PC1	PC2	PC1	PC2
Greatest Length	0.96521	-0.00254	0.95884	-0.03490
Condylbasal Length	0.95499	-0.08781	0.95743	-0.05358
Palatal Length	0.93346	-0.21247	0.88446	-0.13615
Diastema Length	0.85500	-0.20064	0.89236	-0.10349
Zygomatic Breadth	0.92590	0.05054	0.67257	-0.05849
Mastoid Width	0.76535	0.37383	0.80893	0.21418
Width of Braincase	0.58782	0.02308	0.60918	0.07066
Width of Rostrum	0.44286	0.14530	0.32651	-0.01713
Palatal-Bridge Length	0.58152	-0.16764	0.51894	-0.32149
Bullar Length less tube	0.54948	0.53809	0.49908	0.46649
Incisive Foramen Length	0.85964	-0.26563	0.89466	-0.15254
Molar Row Length	0.66368	0.22696	0.75298	0.20040
Width of M1	0.25473	0.31545	0.63357	0.39400
Least Interorbital Breadth	0.01594	0.66048	-0.06973	0.60743
Nasal Length	0.76659	-0.25216	0.75870	-0.22805
Greatest Nasal Width	0.50587	-0.04782	0.78963	-0.00464
Orbit Length	0.88657	0.05811	0.91698	0.01660

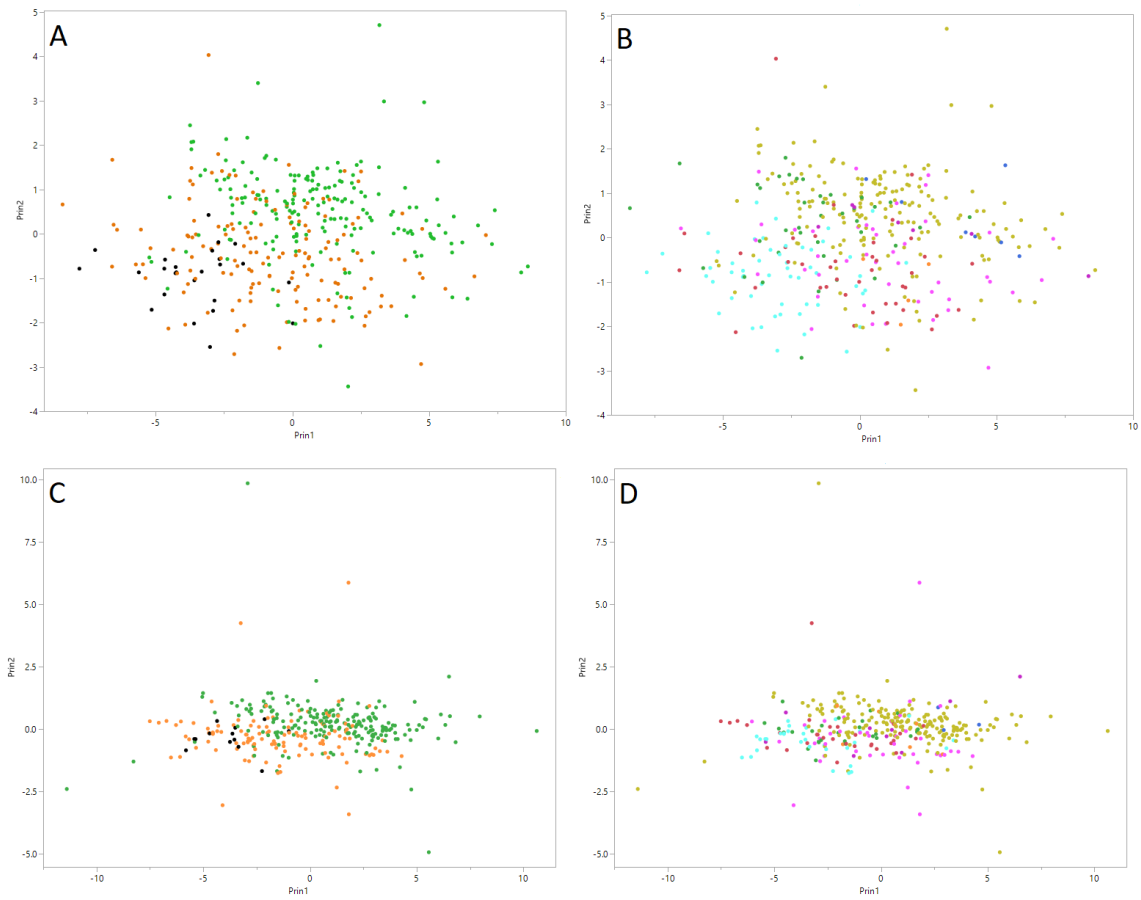


Figure 10. PCA of lineal variables. Male (A, B), Female (C, D). phylogenetic groups (Left): Green South, Orange North. Taxonomical groups (Right), Blue *P. bonariensis*, Red *P. x. chilensis*, Green *P. limatus*, Magenta *P. x. postalis*, Orange *P. x. ricardulus*, Cyan *P. x. rupestris*, Purple *P. x. vaccarum*, Yellow *P. x. xanthopygus*.

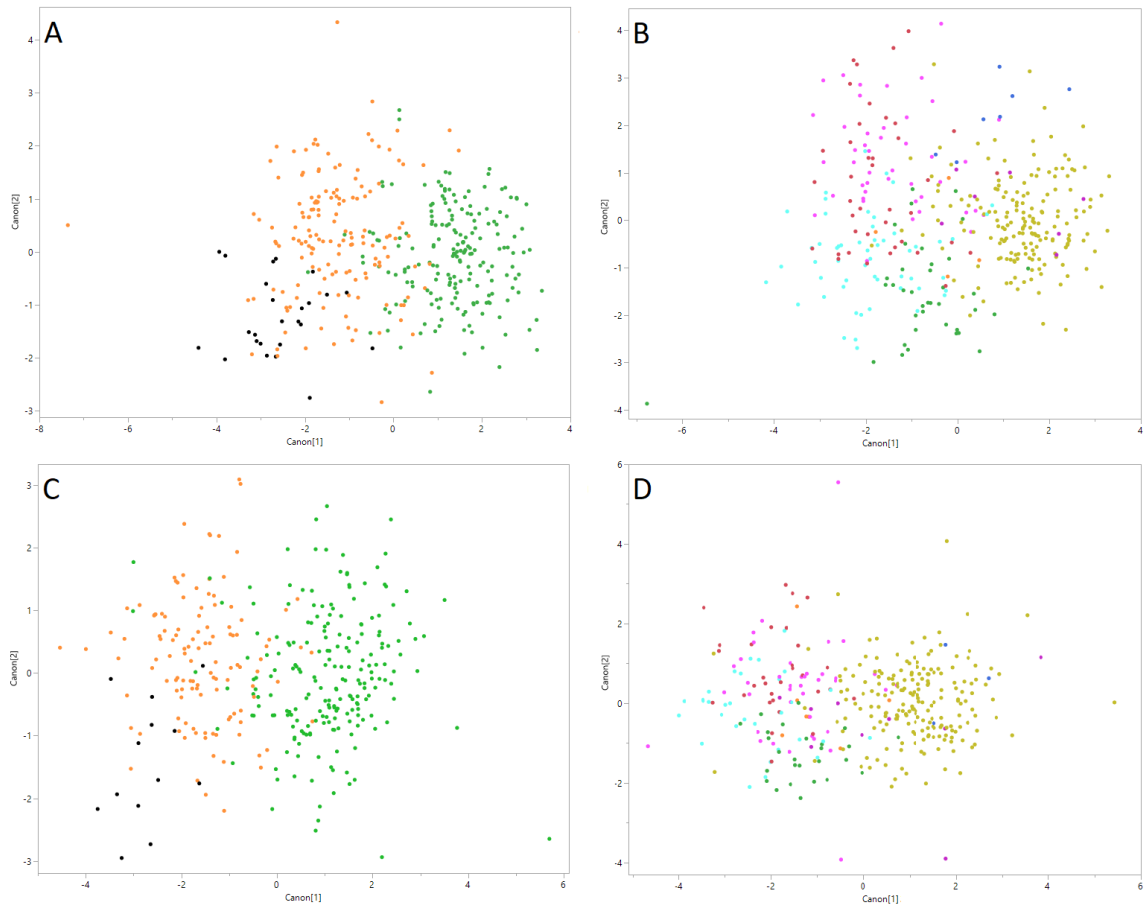


Figure 11. Discriminant Function of lineal variables. Male (A, B), Female (C, D). phylogenetic groups (Left): Green South, Orange North. Taxonomical groups (Right), Blue *P. bonariensis*, Red *P. x. chilensis*, Green *P. limatus*, Magenta *P. x. posticalis*, Orange *P. x. ricardulus*, Cyan *P. x. rupestris*, Purple *P. x. vaccarum*, Yellow *P. x. xanthopygus*.

Table 8. Procrustes distances between pairwise sexual dimorphism. Respective p-values after permutation test with 10,000 permutation rounds.

View	Procrustes distance	P-value
Dorsal	0.0031	0.1456
Ventral	0.0032	0.1050
Lateral	0.0059	0.0052*
Mandible	0.0061	0.0185*

Table 9. Variation in centroid size. Sample size of phylogenetic group (N), standard deviation (SD) and confidence interval (CI). Tukey HSD represents differences between pairs of group means. Groups not connected by the same letter are significantly different.

View	Group	N	Mean	SD	95% CI		Tukey HSD
					Lower	Upper	
Dorsal	North	291	3.69692	0.19943	3.6739	3.7199	A
	Puna	38	3.48467	0.11327	3.4474	3.5219	B
	South	400	3.66832	0.20392	3.6483	3.6884	A
Ventral	North	291	3.70444	0.25392	3.6751	3.7337	A
	Puna	37	3.47607	0.1354	3.4309	3.5212	B
	South	402	3.69619	0.23513	3.6731	3.7192	A
Lateral Male	North	166	3.95939	0.21399	3.9266	3.9922	A
	Puna	25	3.67747	0.11839	3.6286	3.7263	B
	South	190	3.95543	0.2345	3.9219	3.989	A
Lateral Female	North	124	3.84881	0.20805	3.8118	3.8858	A
	Puna	12	3.57699	0.10745	3.5087	3.6452	B
	South	210	3.88914	0.23076	3.8577	3.9205	A
Mandible Male	North	166	2.29011	0.14134	2.2684	2.3118	A
	Puna	25	2.12403	0.0854	2.0888	2.1593	B
	South	192	2.26237	0.15451	2.2404	2.2844	A
Mandible Female	North	126	2.25842	0.14795	2.2323	2.2845	A
	Puna	12	2.05767	0.08745	2.0021	2.0021	B
	South	214	2.24483	0.15861	2.2235	2.2662	A

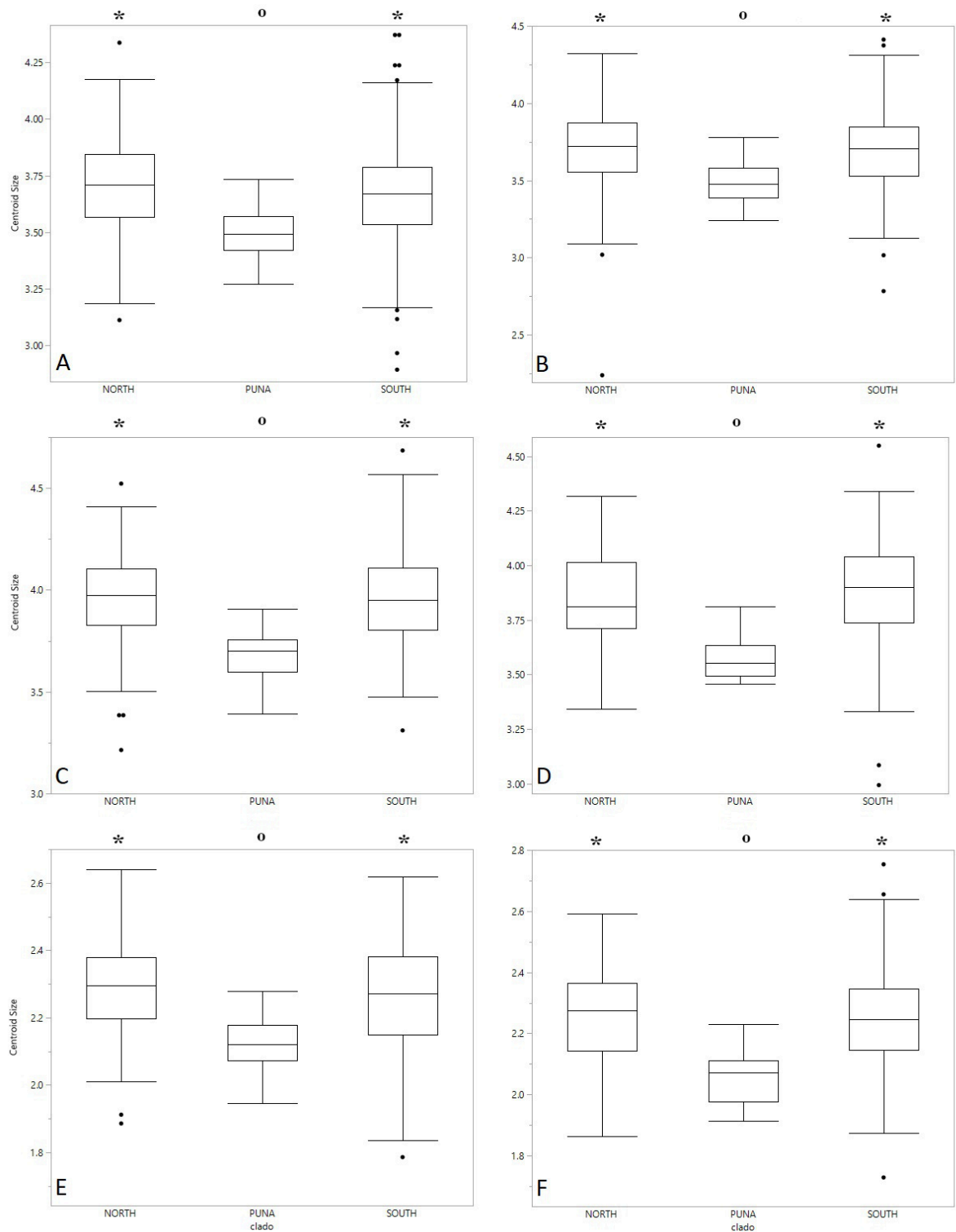


Figure 12. Centroid size variation among phylogenetic groups. Groups not connected by the same mark are significantly different. (A) Dorsal, (B) Ventral, (C) Lateral Male, (D) Lateral Female, (E) Mandible Male, (F) Mandible Female.

Table 10. Variation in centroid size. Sample size of taxonomical group (N), standard deviation (SD) and confidence interval (CI). Tukey HSD represents differences between pairs of group means. Groups not connected by the same letter are significantly different.

View	Group	N	Mean	SD	95% CI		Tukey HSD
					Lower	Upper	
Dorsal	Bona	14	3.81516	0.05285	3.7114	3.9189	A B
	Chile	85	3.67243	0.02145	3.6303	3.7145	A B
	Lima	65	3.70478	0.02453	3.6566	3.7529	A B
	Posti	85	3.74503	0.02145	3.7029	3.7871	A
	Ricar	10	3.76246	0.06253	3.6397	3.8852	A B C
	Rupes	84	3.56312	0.02158	3.5208	3.6055	C
	Vacca	16	3.64441	0.04944	3.5474	3.7415	A B C
	Xantho	370	3.66380	0.01028	3.6436	3.6840	B
Ventral	Bona	15	3.84006	0.06173	3.7189	3.9613	A
	Chile	86	3.68662	0.02578	3.6360	3.7372	A
	Lima	66	3.69634	0.02943	3.6386	3.7541	A
	Posti	85	3.74888	0.02593	3.6980	3.7998	A
	Ricar	10	3.83170	0.07560	3.6833	3.9801	A
	Rupes	82	3.57022	0.02640	3.5184	3.6221	B
	Vacca	15	3.65850	0.06173	3.5373	3.7797	A B
	Xantho	371	3.69073	0.01241	3.6664	3.7151	A
Lateral Male	Bona	7	4.11139	0.08382	3.9466	4.2762	A
	Chile	49	3.96396	0.03168	3.9017	4.0263	A
	Lima	39	3.92731	0.03551	3.8575	3.9971	A B
	Posti	46	4.01149	0.03270	3.9472	4.0758	A

	Ricar	4	4.08353	0.11089	3.8655	4.3016	A B
	Rupes	53	3.79122	0.03046	3.7313	3.8511	B
	Vacca	6	4.01036	0.09054	3.8323	4.1884	A B
	Xantho	177	3.94740	0.01667	3.9146	3.9802	A
Lateral Female	Bona	7	4.15494	0.08166	3.9943	4.3156	A
	Chile	37	3.80827	0.03552	3.7384	3.8781	B C
	Lima	24	3.83202	0.04410	3.7453	3.9188	B C
	Posti	38	3.93140	0.03505	3.8625	4.0003	A B
	Ricar	6	3.91912	0.08821	3.7456	4.0926	A B C
	Rupes	31	3.69012	0.03881	3.6138	3.7664	C
	Vacca	10	3.81868	0.06833	3.6843	3.9531	B C
	Xantho	193	3.88315	0.01555	3.8526	3.9137	B
Mandible Male	Bona	8	2.36548	0.05176	2.2637	2.4673	A B
	Chile	47	2.26826	0.02136	2.2263	2.3103	A B
	Lima	40	2.25992	0.02315	2.2144	2.3054	A B
	Posti	49	2.33535	0.02092	2.2942	2.3765	A
	Ricar	4	2.38350	0.07321	2.2396	2.5274	A B
	Rupes	51	2.20172	0.02050	2.1614	2.2420	B
	Vacca	5	2.27066	0.06548	2.1419	2.3994	A B
	Xantho	179	2.25753	0.01094	2.2360	2.2790	B
Mandible Female	Bona	7	2.37408	0.05734	2.2613	2.4869	A
	Chile	39	2.23588	0.02429	2.2837	2.2837	A B
	Lima	25	2.25856	0.03034	2.3182	2.3182	A B

Posti	38	2.29648	0.02461	2.3449	2.3449	A
Ricar	5	2.39193	0.06785	2.5254	2.5254	A
Rupes	31	2.14078	0.02725	2.1944	2.1944	B
Vacca	10	2.29448	0.04798	2.3888	2.3888	A B
Xantho	197	2.23772	0.01081	2.2590	2.2590	A

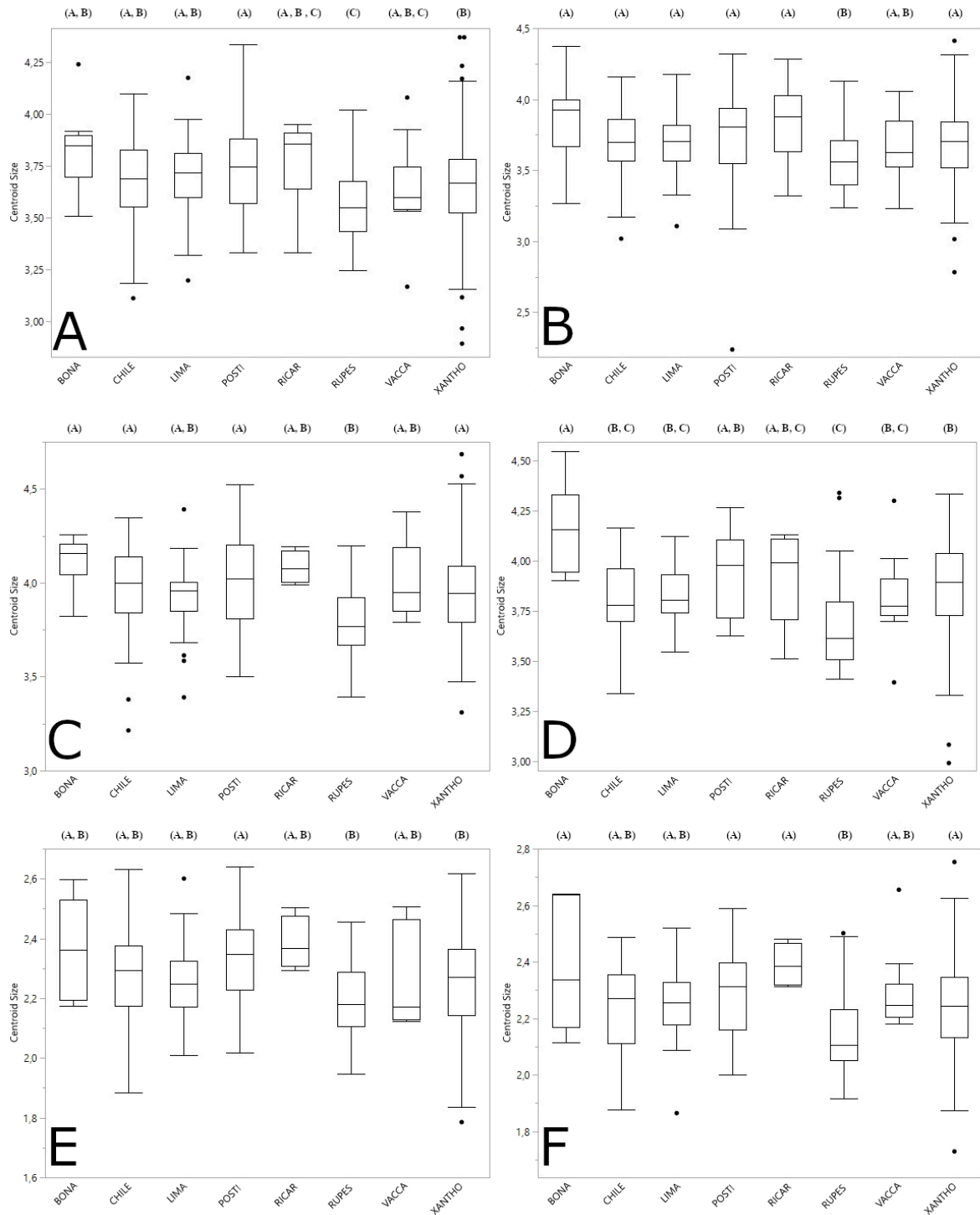


Figure 13. Centroid size variation among taxonomic groups. Groups not connected by the same letter are significantly different. (A) Dorsal, (B) Ventral, (C) Lateral Male, (D) Lateral Female, (E) Mandible Male, (F) Mandible Female.

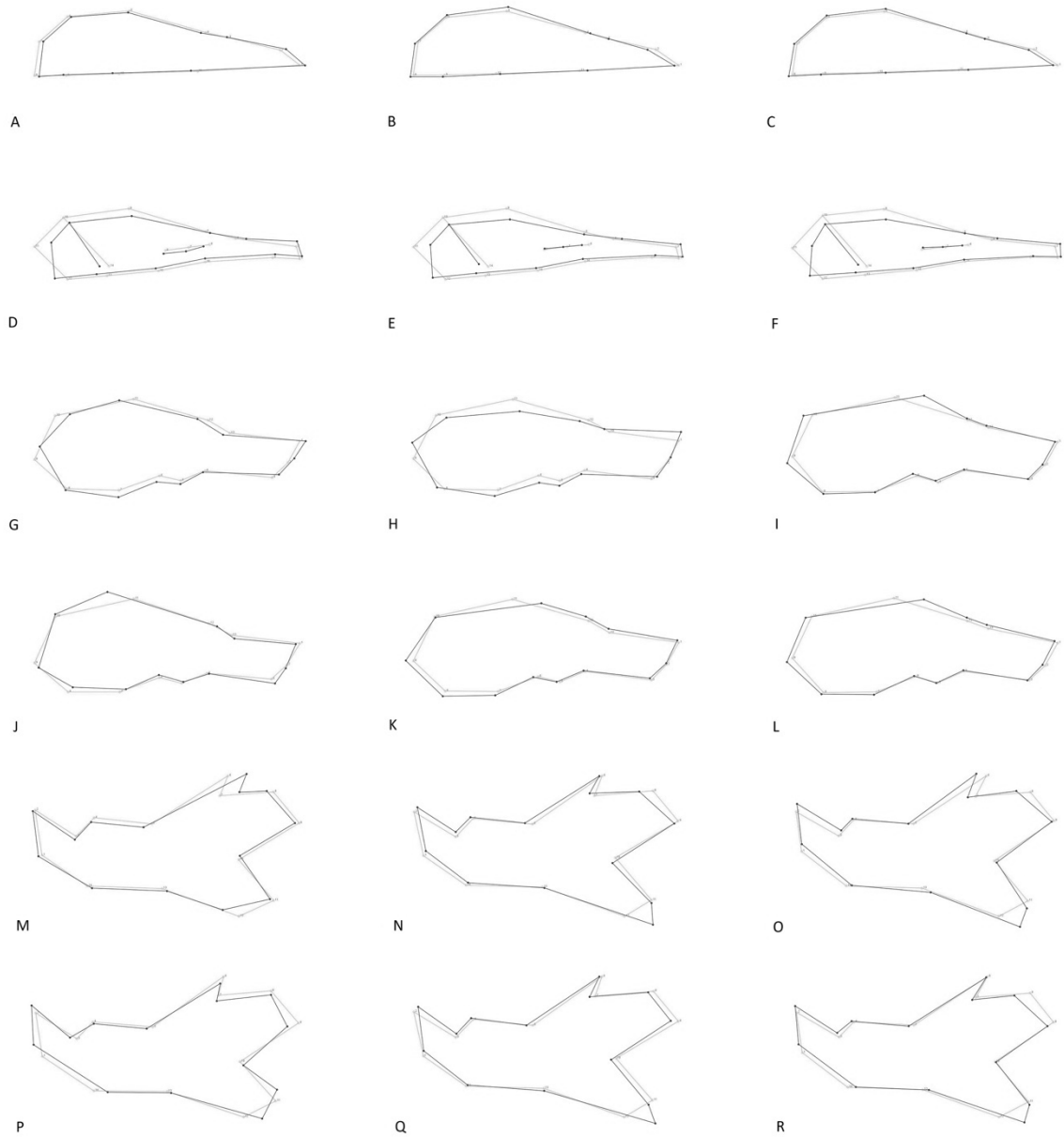


Figure 14. Scatter plots, wireframes of each view indicate the relative landmarks displacement. Consensus shape (gray line), Target shape (black line). Phylogeographic grouping; Puna (left), North (center), South (right). Dorsal (A,B,C); Ventral (D,E,F); Lateral Male (G,H,I); Lateral Female (J,K,L); Mandible Male (M,N,O); Mandible Female (P,Q,R).

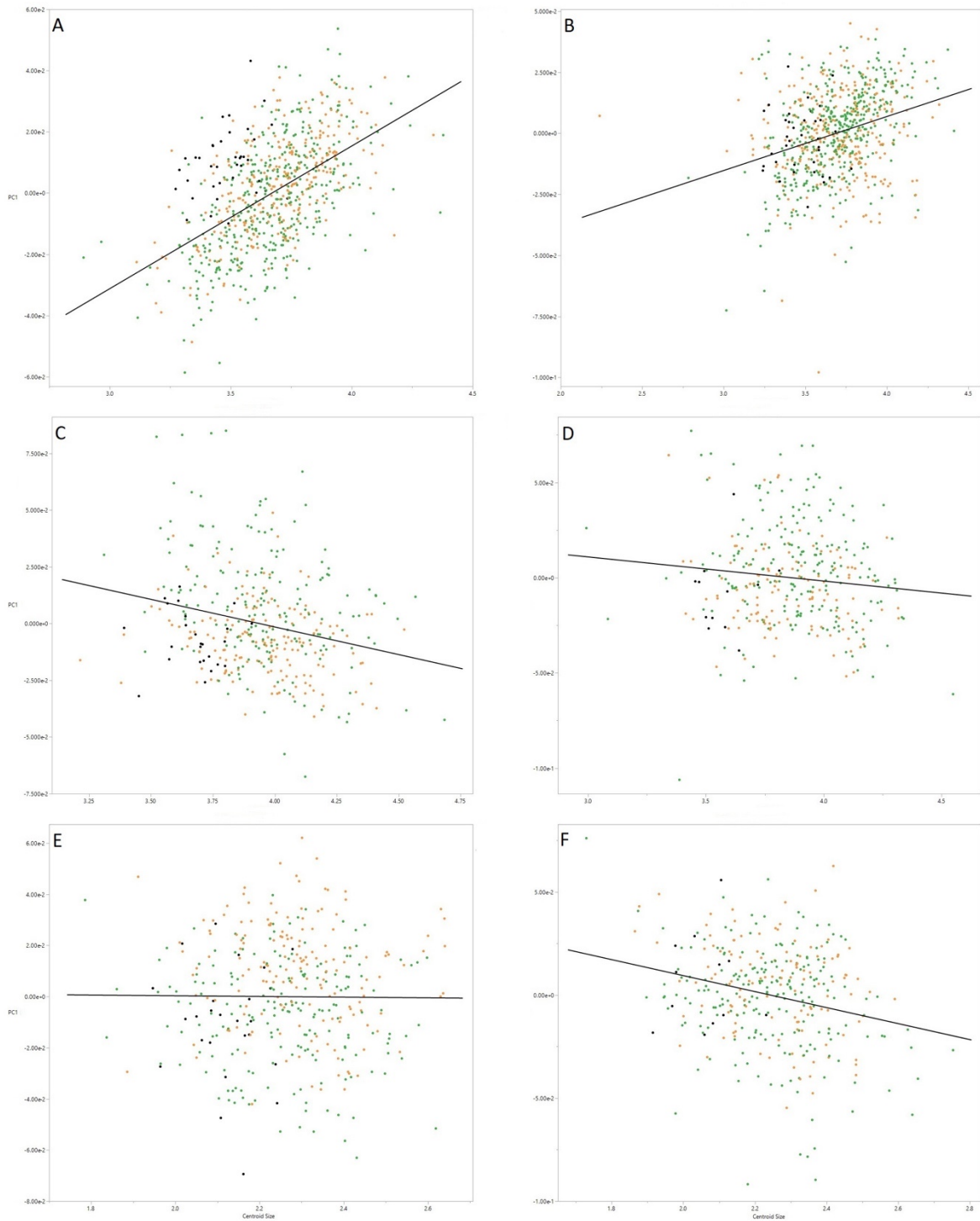


Figure 15. Allometric analysis of the shape components showing r -Pearson values. (A) Dorsal, $r^2 = 0.292731$, $p < .0001$; (B) Ventral, $r^2 = 0.02103696$, $p < .0001$; (C) Lateral Male, $r^2 = 0.060101$, $p < .0001$; (D) Lateral Female, $r^2 = 0.012196$, $p = 0.0401$; (E) Mandible Male, $r^2 = 0.000082$, $p = 0.8598$; (F) Mandible Female, $r^2 = 0.061829$, $p < .0001$. Phylogenetic grouping, green South, orange North, black Puna.

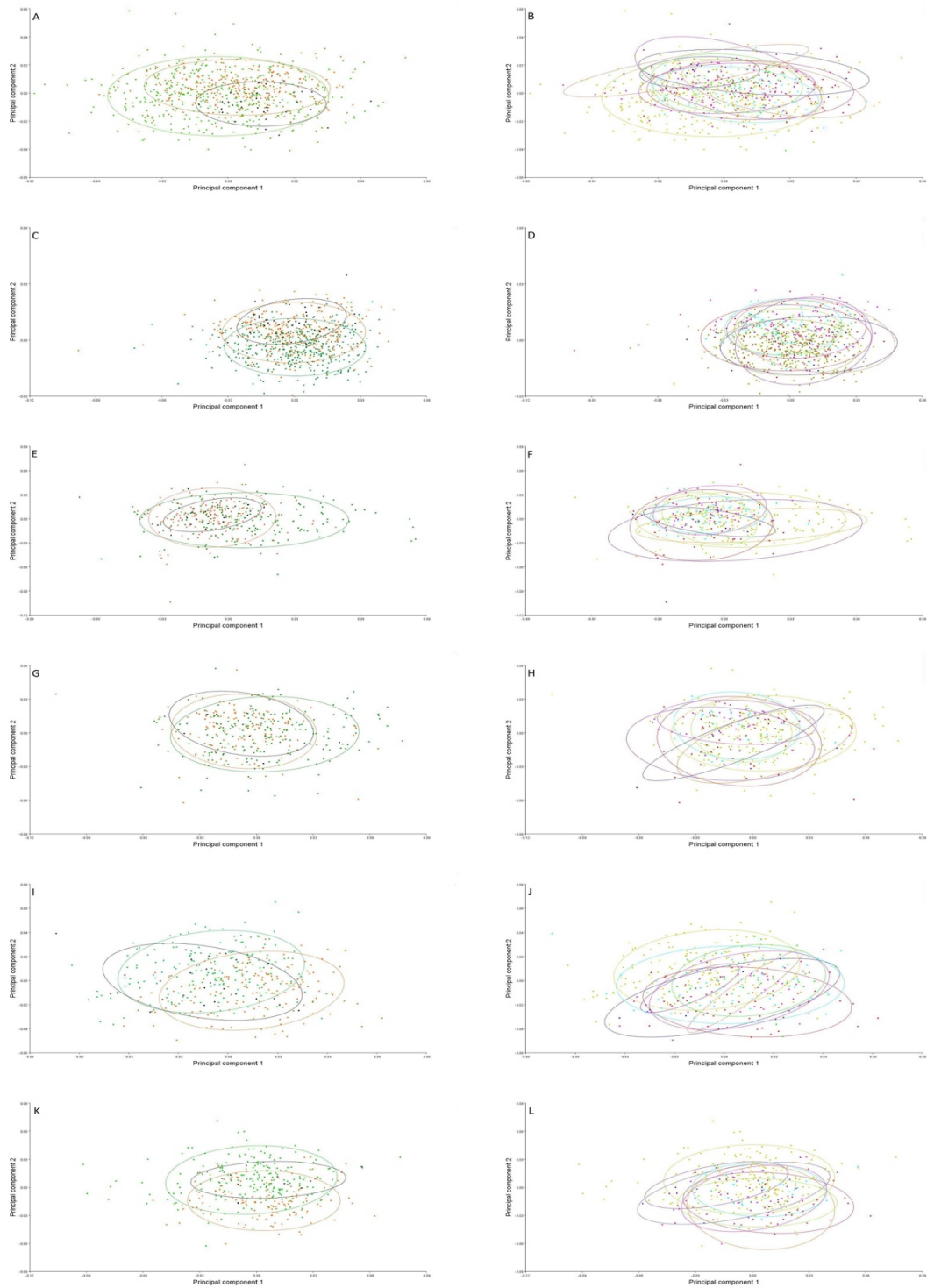


Figure 16. PCA of cranial shape variables. Confidence ellipses were drawn with a probability of 0.8. Phylogenetic grouping (left), green South, orange North, black Puna. Taxonomical grouping (right), Blue *P. bonariensis*, Red *P. x. chilensis*, Green *P. limatus*, Magenta *P. x. posticalis*, Orange *P. x. ricardulus*, Cyan *P. x. rupestris*, Purple *P. x. vaccharum*, Yellow *P. x. xanthopygus*. (A,B) Dorsal; (C,D) Ventral; (E,F) Lateral Male; (G,H) Lateral Female; (I,J) Mandible Male; (K,L) Mandible Female.

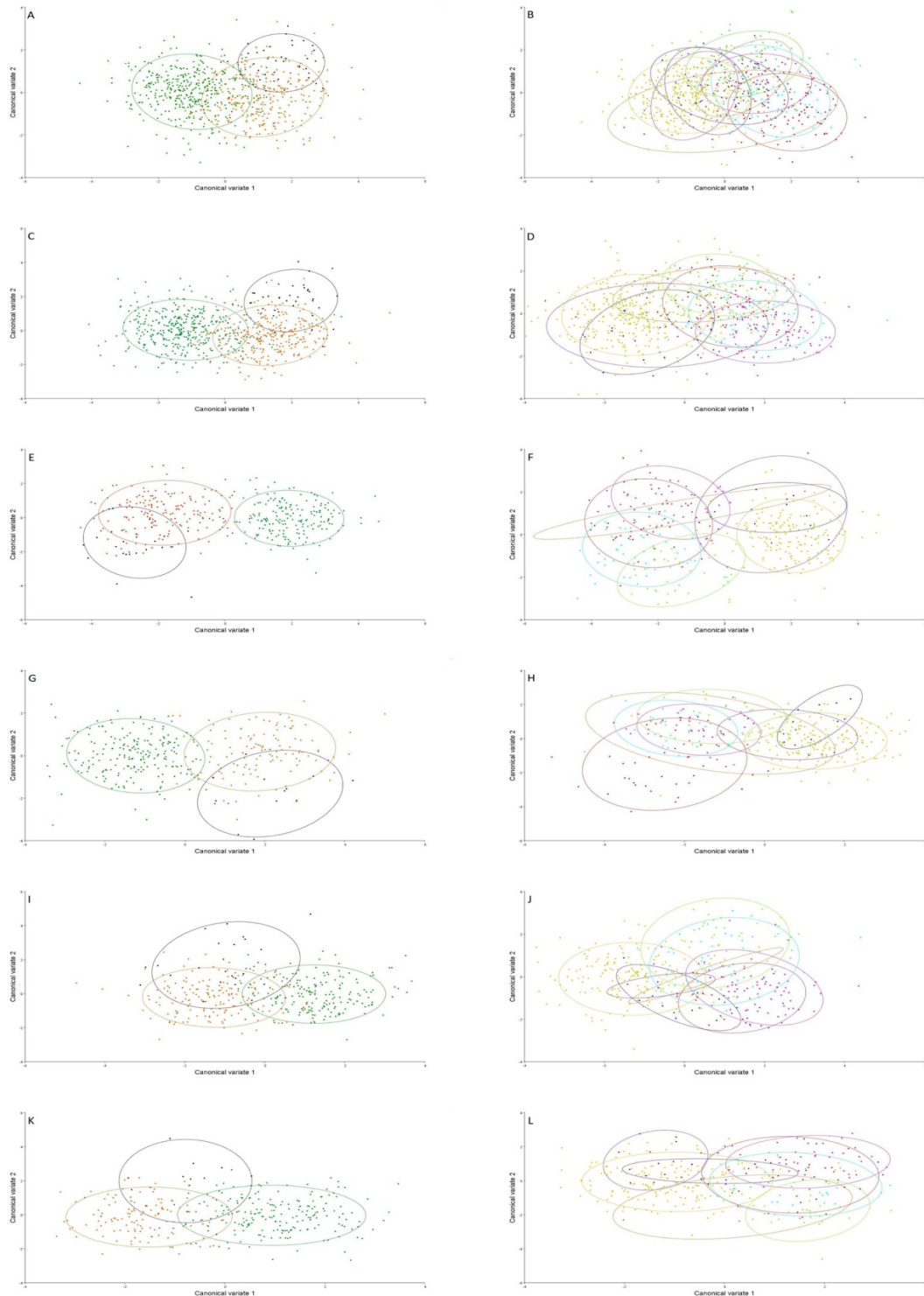


Figure 17. CVA of cranial shape variables. Confidence eclipses were draw with a probability of 0.8. Phylogenetic grouping (left), green South, orange North, black Puna. Taxonomical grouping (right), Blue *P. bonariensis*, Red *P. x. chilensis*, Green *P. limatus*, Magenta *P. x. postcalis*, Orange *P. x. ricardulus*, Cyan *P. x. rupestris*, Purple *P. x. vaccarum*, Yellow *P. x. xanthopygus*. (A, B) Dorsal; (C, D) Ventral; (E, F) Lateral Male; (G, H) Lateral Female; (I, J) Mandible Male; (K, L) Mandible Female.

Chapter 3

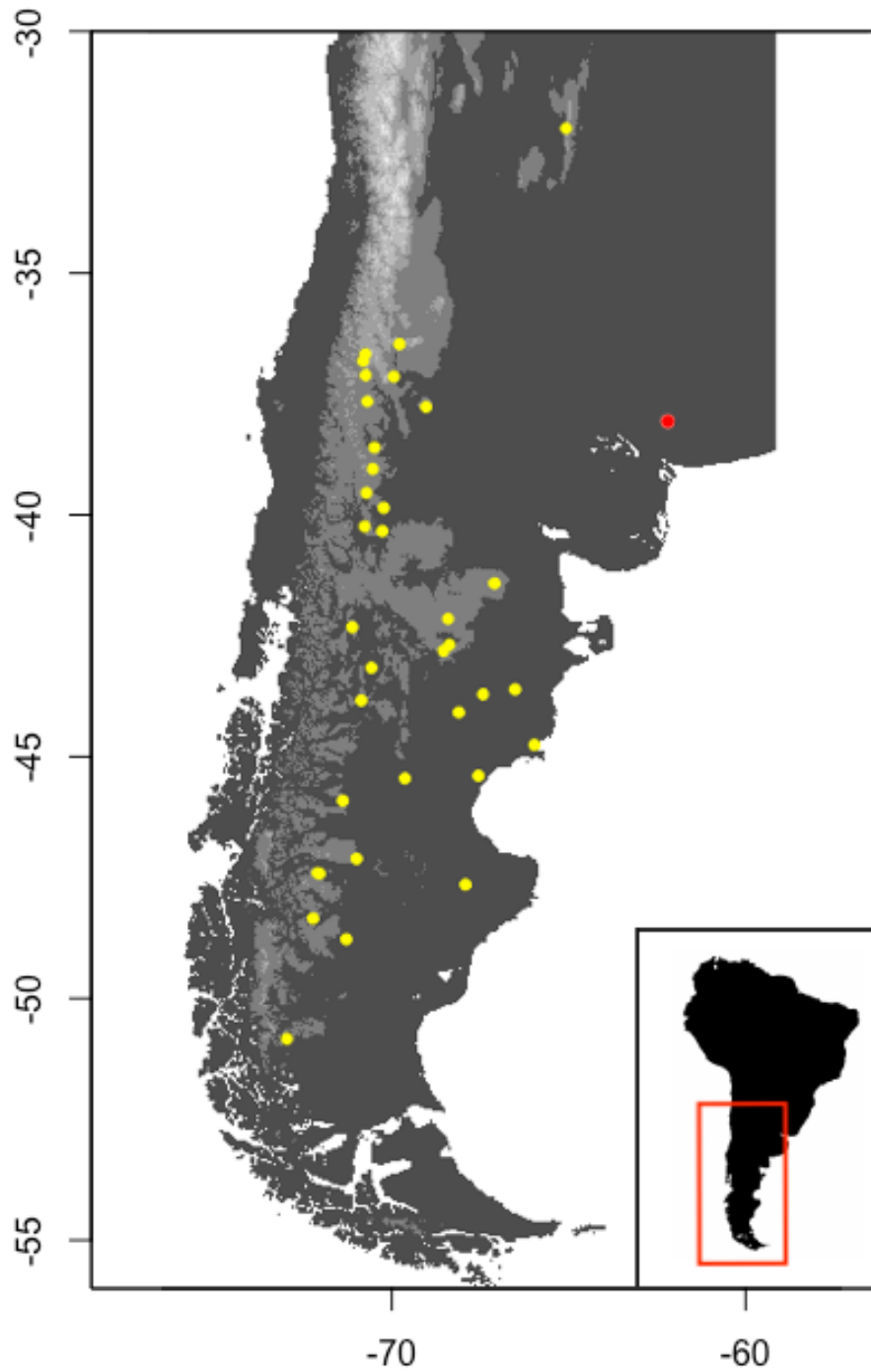


Figure 18. Location of samples obtained, former recognize as *P. xanthopygus* (yellow) and *P. bonariensis* (red), currently known as *P. x. xanthopygus*.

Table 11. List of localities where analyzed tissue samples of *P. x. xanthopygus* were obtained

	Locality	Altitude (m)	Latitude S	Longitude W	Number of specimen s
1	Abra de la Ventana	470	38° 04' 08"	62° 01' 24"	19
2	Cerro Los Linderos	2599	32° 00' 17.8"	64° 56' 0.51"	4
3	Central Chile	1504	33° 51' 32.2"	70° 11' 55.78"	5
4	Los Frisos	1117	36° 28' 20"	69° 38' 54"	10
5	Cañada Molina	1466	37° 07'	70° 36' 14.2"	2
6	Varvarco	1254	36° 49' 27"	70° 40' 26.5"	2
7	El Huecu	1247	37° 39' 38.6"	70° 33' 23.6"	1
8	Piedra del Aguila	687	39° 51' 41"	70° 05' 45.5"	5
9	Auca Mahuida	1606	37° 46' 16.5"	68° 53' 37.4"	10
10	Domuyo	1734	36° 40' 47.3"	70° 36' 30.5"	12
11	Laguna Blanca	1365	39° 03' 13"	70° 24' 6.6"	10
12	Estancia La Porteña	942	38° 36' 39"	70° 21' 4"	4
13	Estancia Corcel Negro	1204	37° 08' 44"	69° 48' 30"	7
14	Estancia Cerro Yuncón	642	40° 20' 42"	70° 07' 52"	6
15	Cerrito Piñon	611	40° 14' 57"	70° 37' 54"	10
16	Las Coloradas	960	39° 33' 21.5"	70° 34' 49"	1
17	Cerro Corona Grande	1406	41° 25' 33"	66° 57' 21.2"	10
18	Arroyo Leleque	615	42° 19' 56"	70° 59' 00"	11
19	Sierra de Talagapa	1495	42° 09' 3"	68° 15' 9"	9
20	Sierra de Tepuel	1294	43° 51' 06"	70° 43' 41"	7
21	Laguna de Aleusco	605	43° 10' 17"	70° 26' 20"	2
22	Estancia La Maroma	1108	42° 41' 48"	68° 14' 10.3"	15
23	Carhué Niyeu	1143	42° 49' 22.3"	68° 23' 52"	10
24	Bajada del Guanaco	510	44° 06'	67° 58' 61.1"	11
25	Las Plumas	167	43° 43' 20"	67° 16' 58"	6
26	Villa Dique Ameghino	81	43° 37' 21"	66° 22' 53"	1
27	Arroyo los Bomberos	69	44° 46' 9.7"	65° 49' 41"	1
28	Pico Salamanca	533	45° 24' 37"	67° 25' 03"	10
29	Establecimiento los Manantiales	650	45° 27' 51"	69° 29' 25.8"	15
30	Lago Blanco	567	45° 55' 33.94"	71° 14' 58.4"	8
31	Río Ecker	710	47° 07' 41.17"	70° 51' 35.96"	10
32	Río de Oro	280	47° 25' 2.6"	71° 57' 5"	1
33	Lago Posadas	155	47° 26' 8.4"	71° 54' 2"	11
34	Estancia La Paloma	122	47° 39' 50"	67° 46' 41"	1
35	Estancia La Ensenada	566	48° 21' 54"	72° 05' 20"	8
36	Lago Cardiel	462	48° 47' 46"	71° 09' 4.8"	8
37	Torres del Paine	543	50° 51' 36.72"	72° 49' 35.98"	1

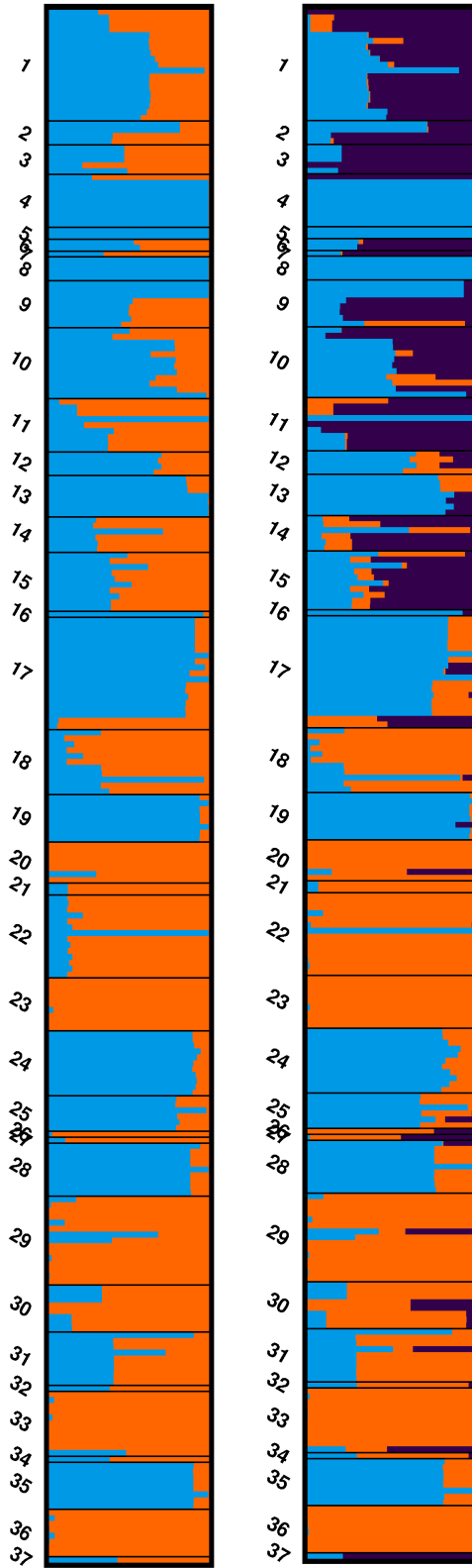


Figure 19. Graphical representation of population structure according to genetic differences, numbers relating to localities described in Table 11. Left K=2, Right K=3.

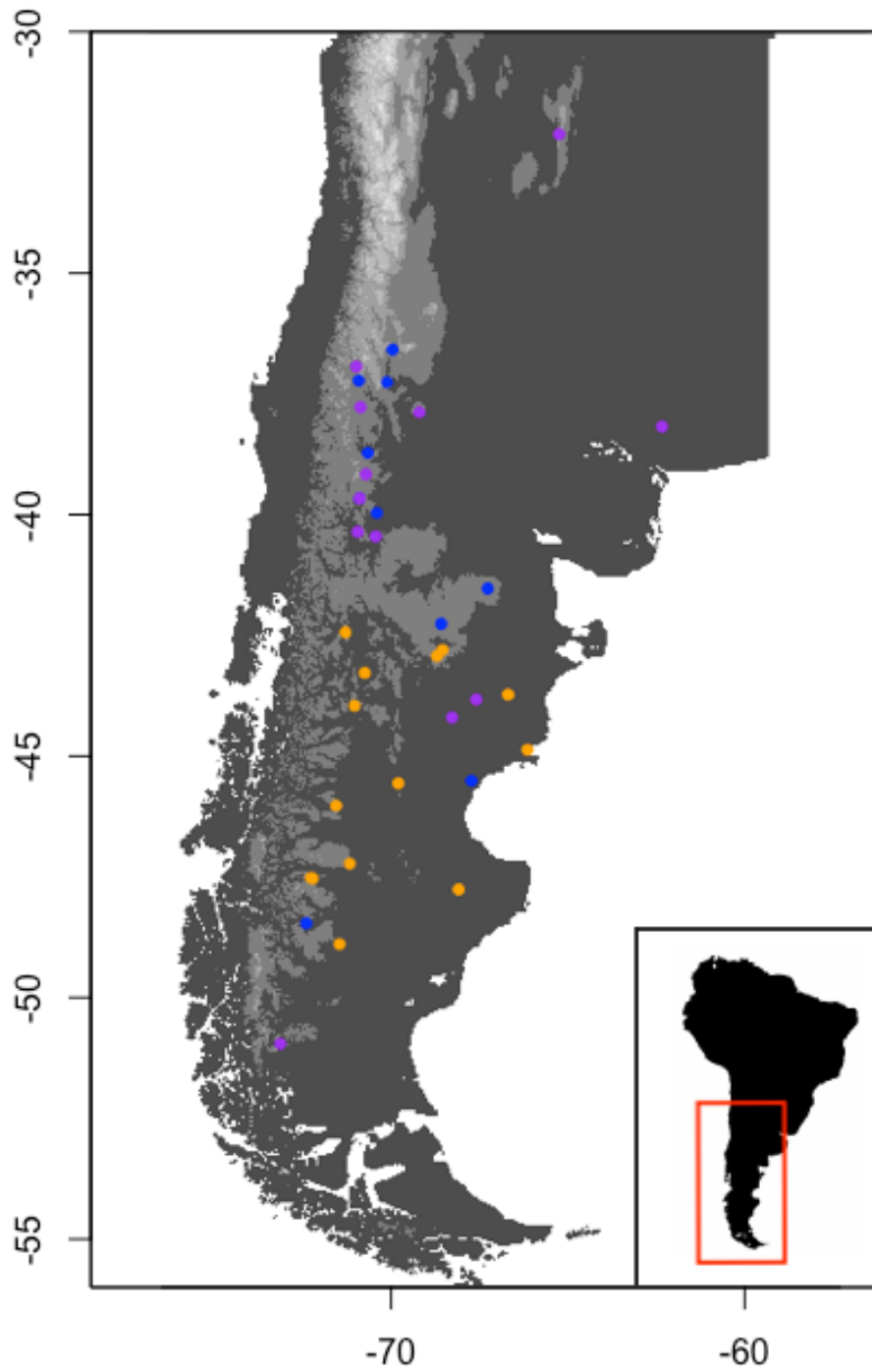


Figure 20. Location of samples obtained according to lineage; purple (high altitude, northern lineage), blue (low altitude northern lineage) and orange (southern lineage)

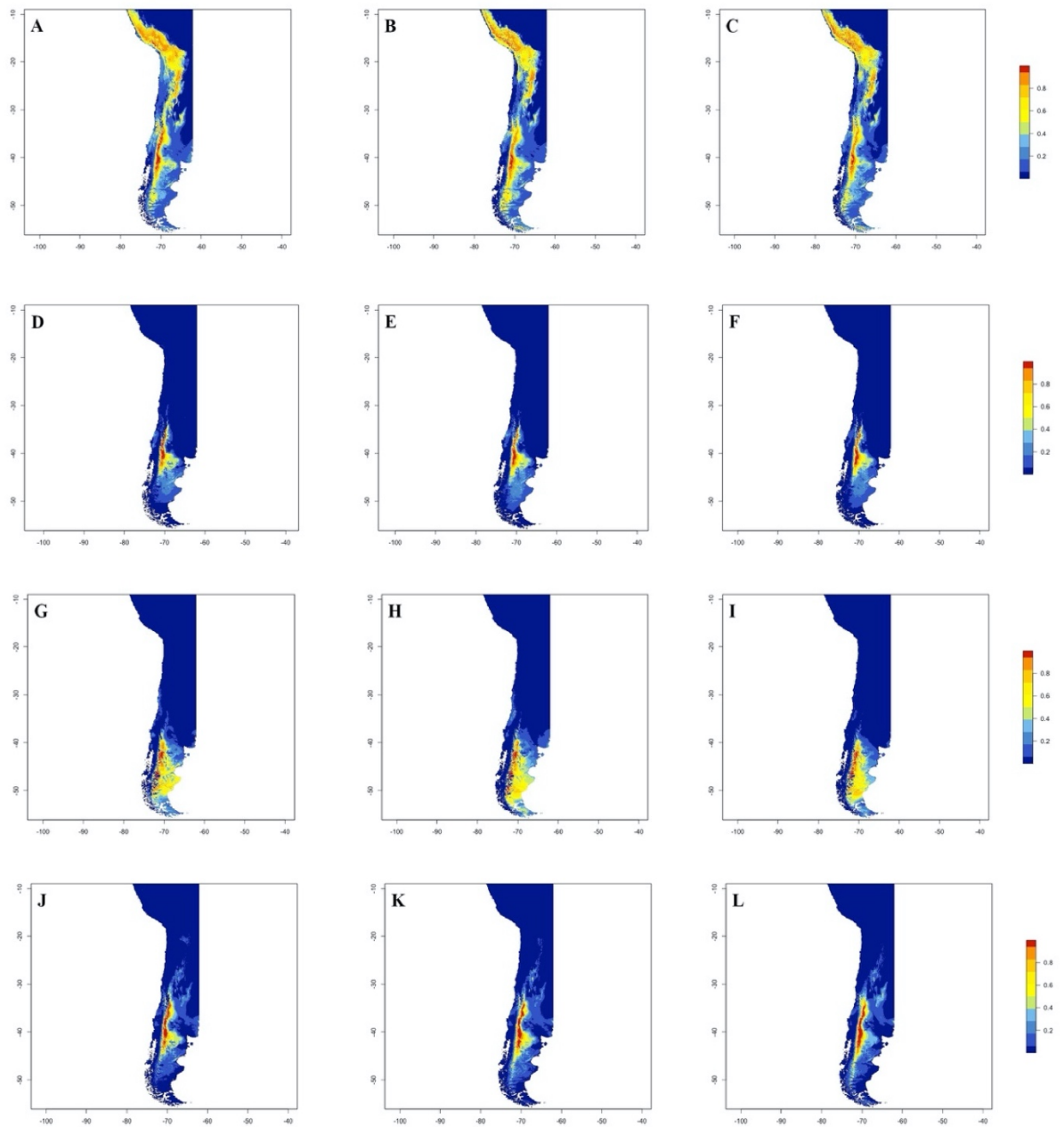
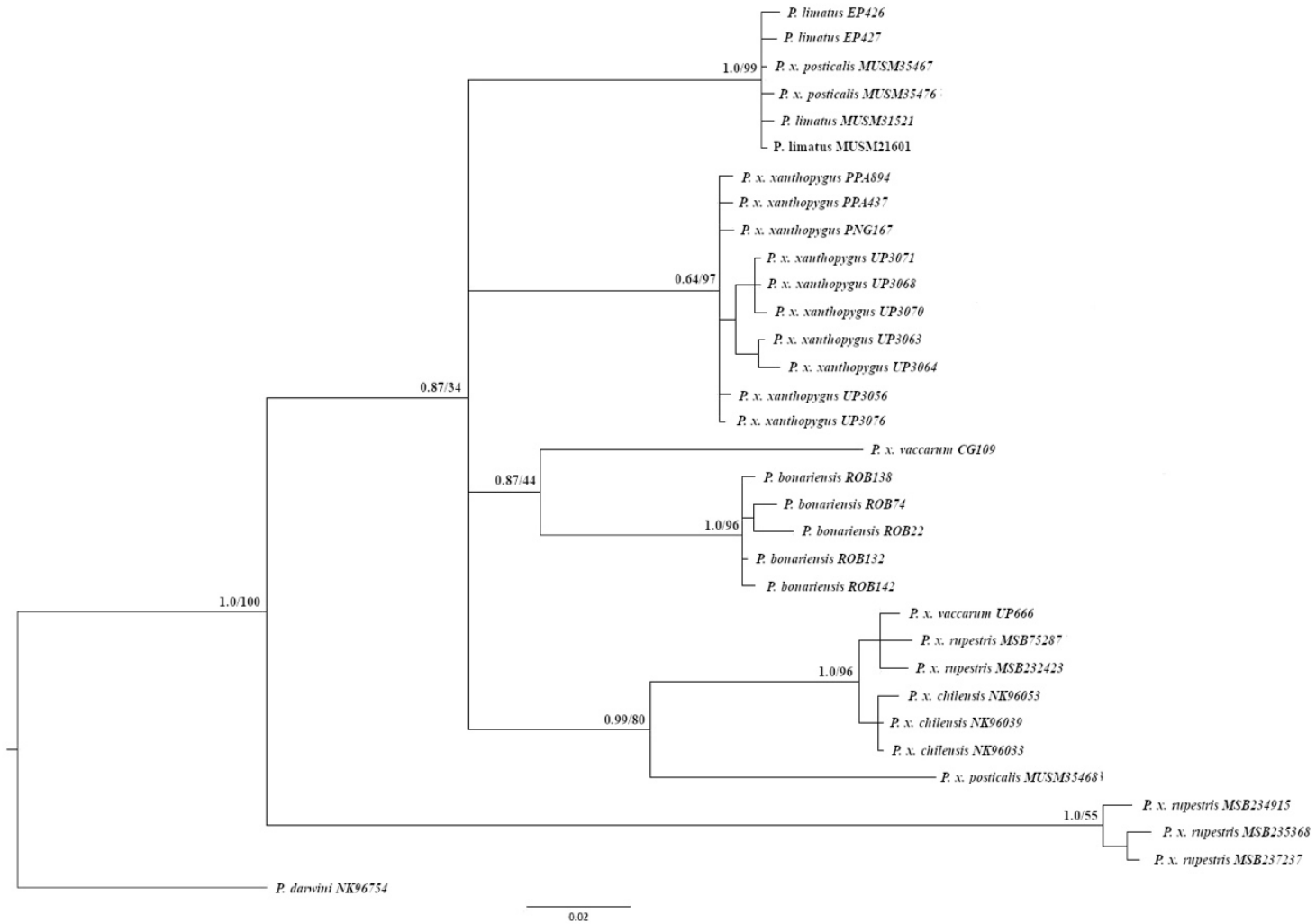


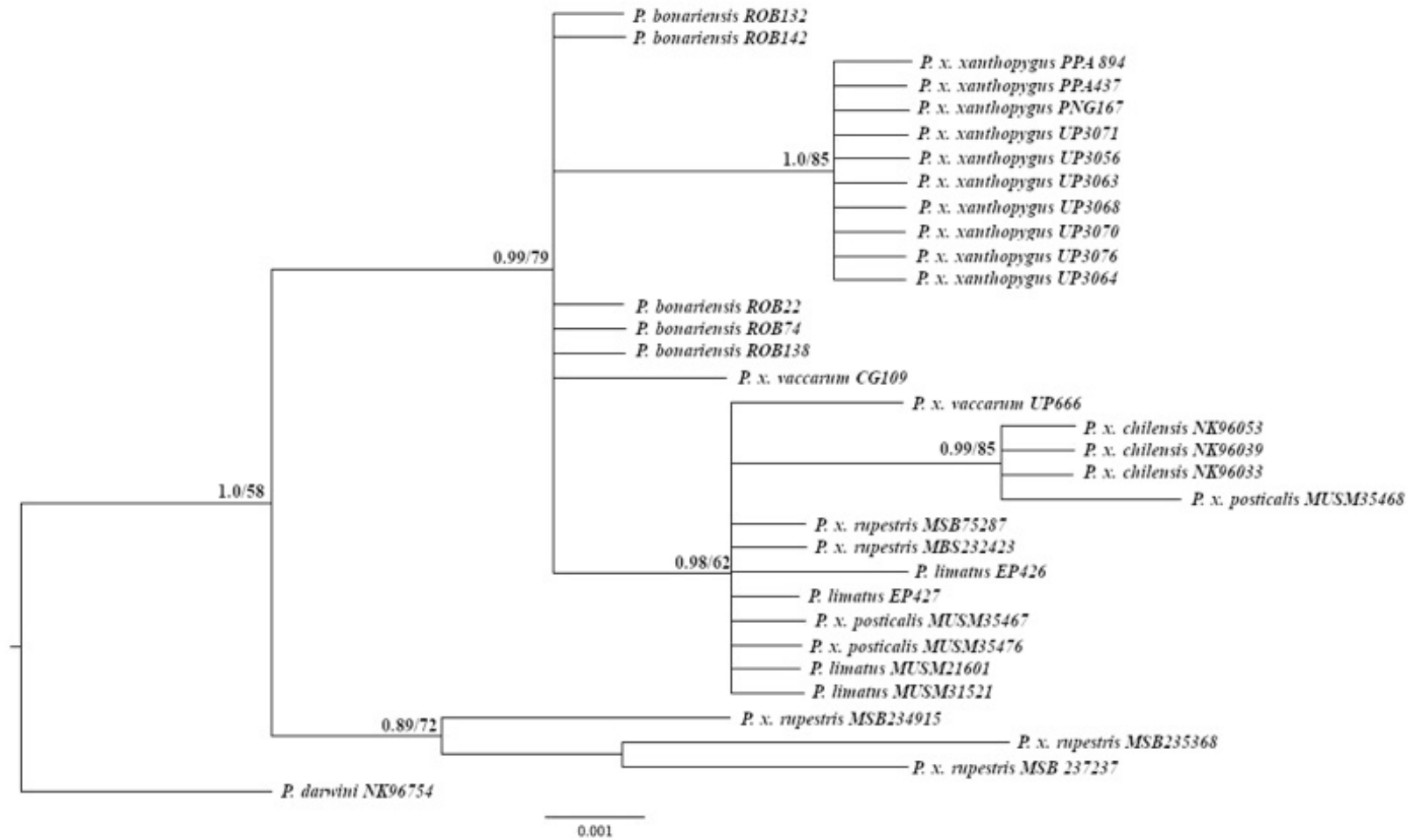
Figure 21. Niche modeling distribution map. (A) 0 Kya Complete Distribution; (B) 12 Kya Complete Distribution; (C) 21 Kya Complete Distribution; (D) 0 Kya Blue Lineage; (E) 12 Kya Blue Lineage; (F) 21 Kya Blue Lineage; (G) 0 Kya Orange Lineage; (H) 12 Kya Orange Lineage; (I) 21 Kya Orange Lineage; (J) 0 Kya Purple Lineage; (K) 12 Kya Purple Lineage; (L) 21 Kya Purple Lineage.

APPENDICES

Appendix A. Maximum Likelihood and Bayesian inference phylogram of Cytochrome B sequences. Number above branches are bootstrap proportions and Bayesian posterior probabilities.



Appendix B. Maximum Likelihood and Bayesian inference phylogram of β Fgb-I7 sequences. Number above branches are bootstrap proportions and Bayesian posterior probabilities.



Appendix C. Description of cranial landmarks

Landmark	Definition
Dorsal view (skull)	<ol style="list-style-type: none">1. Rostral most point of the nasal bones2. Intersection of the rostral curvature of the nasal process of the incisive and the nasal bones in a dorsal projection3. Rostral most point of the zygomatic plate4. Rostral most point of the zygomatic arch5. Caudal most point of the orbit6. Intersection of the parietal-interparietal and interparietal-occipital sutures7. Lattermost point of the occipital8. Caudal end of the curvature of the occipital bone9. Intersection of the sagittal and parietal-interparietal sutures10. Intersection of the coronal and sagittal sutures11. Intersection of the nasofrontal suture in the midline
Ventral view (skull)	<ol style="list-style-type: none">12. Rostral most point of the upper incisors next to the midline13. Lateral most point of the incisive alveolus14. Rostral most point of the rostral palatine fissure15. Rostral most point of the zygomatic plate16. Rostral most point of the orbit17. Rostral most point of the molar row18. Intersection between the first molar and second molar at the midline19. Caudal most point of the molar row20. Caudal most point of the orbit21. Caudal end of the external opening of the bony auditory canal22. Lateral most point of the foramen magnum23. Rostral most point of the foramen magnum

Lateral view (skull)

24. Intersection at the midline between basioccipital and basisphenoid
25. Suture between basisphenoid and basioccipital where it contacts the tympanic bulla
26. Caudal most point of the suture between palatine bones and the rostral border of the mesopterygoid fossa
27. Caudal most point of the palatine fissure
28. Rostral most point of nasal
29. Inner extreme point of incisor at body of premaxillary bone
30. Point at intersection between premaxillary and posterior end of incisive alveolus
31. Rostral most point of molar row on alveolar process of maxilla
32. Intersection between first molar and second molar
33. Caudal most point of molar row on alveolar process of maxilla
34. Rostral most point of the tympanic bulla at the intersection with the squamosal
35. Caudal most point of the tympanic bulla at the intersection with the occipital
36. Caudal most point of the occipital
37. Intersection between occipital and interparietal
38. Intersection between parietal and frontal
39. Rostral most point of the orbit
40. Rostral most point of zygomatic plate
41. Base of the incisor
42. Anterior point of diastema
43. Inferior point of maxillary toothrow
44. Posterior point of diastema

45. Meeting point between 2nd and 3rd molar
 46. Tip of the coronoid process
 47. Medium point of incisura mandibulae
 48. Anterior tip of the condyle
 49. Posterior tip of the condyle
 50. Medium point of the condyle
 51. Medium point of the angular process
 52. Anterior point of the angular process
 53. Inferior medium point of mandible
 54. Posterior point of the symphysis
-

Appendix D. Percentage of variance contributed by each shape component (PC), and cumulative variance for females and males.

Principal Component	Female		Male	
	% Variance	Cumulative %	% Variance	Cumulative %
1	54.889	54.889	52.617	52.617
2	6.170	61.058	7.657	60.275
3	6.048	67.106	6.283	66.558
4	5.678	72.782	5.683	72.241
5	4.526	77.309	4.874	77.115
6	4.390	81.699	4.452	81.567
7	3.608	85.307	4.332	85.899
8	3.050	88.358	3.447	89.346
9	2.535	90.892	2.889	92.245
10	2.165	93.057	1.760	94.005
11	1.982	95.040	1.691	95.696
12	1.562	96.601	1.422	97.117
13	1.068	97.669	1.048	98.166
14	0.874	98.543	0.610	98.776
15	0.751	99.294	0.549	99.325
16	0.524	99.817	0.364	99.688
17	0.183	100.00	0.312	100.00

Appendix E. Percent of variance contributed by each shape component (PC), and cumulative variance obtained after applying Procrustes analysis to the landmark coordinates data.

PC	DORSAL		VENTRAL		LATERAL				MANDIBLE			
	%	Cumulative	%	Cumulative	% Variance		Cumulative %		% Variance		Cumulative %	
	Variance	%	Variance	%	M	F	M	F	M	F	M	F
1	62.357	62.357	28.281	28.281	27.016	32.645	27.016	32.645	15.997	17.329	15.997	17.329
2	13.595	75.952	13.339	41.620	19.551	16.747	46.566	49.392	12.861	13.965	28.858	31.295
3	10.934	86.886	8.034	49.654	9.146	10.254	55.713	59.646	11.220	10.332	40.078	41.627
4	5.718	92.604	7.261	56.915	8.556	8.941	64.269	68.587	10.419	9.951	50.497	51.578
5	4.294	96.898	5.517	62.432	8.184	6.841	72.453	75.434	7.371	7.147	57.868	58.725
6	2.161	99.059	5.213	67.645	6.006	5.045	78.459	80.479	5.569	6.551	63.436	65.276
7	0.941	100.00	4.783	72.427	3.491	3.022	81.950	83.501	5.313	5.298	68.749	70.573
8			3.638	76.080	2.943	2.545	84.893	86.046	4.285	4.090	73.034	74.653
9			2.860	78.940	2.711	2.123	87.604	88.046	3.802	3.690	76.835	78.343
10			2.823	81.765	2.155	1.834	89.759	90.003	3.201	3.245	80.036	81.588
11			2.516	84.281	1.554	1.455	91.313	91.458	3.002	3.014	83.038	84.602
12			2.242	86.523	1.405	1.370	92.718	92.828	2.450	2.331	85.488	86.934
13			1.889	88.411	1.250	1.244	93.969	94.072	2.297	2.009	87.785	88.943
14			1.516	89.927	1.176	1.179	95.145	95.251	2.103	1.838	89.888	90.780
15			1.486	91.413	1.060	1.008	96.204	96.259	1.771	1.657	91.658	92.437
16			1.377	92.790	0.950	0.905	97.154	97.164	1.698	1.393	93.356	93.830
17			1.185	93.975	0.691	0.775	97.845	97.940	1.457	1.167	94.813	94.997
18			1.112	95.078	0.599	0.621	98.444	98.561	1.076	1.111	95.889	96.107
19			0.953	96.040	0.477	0.433	98.921	98.995	0.955	1.035	96.844	97.142

20	0.766	96.806	0.420	0.412	99.341	99.406	0.924	0.876	97.768	98.019
21	0.696	97.501	0.364	0.326	99.705	99.732	0.718	0.591	98.486	98.610
22	0.579	98.080	0.295	0.268	100.00	100.00	0.562	0.534	99.048	99.144
23	0.510	98.590					0.523	0.464	99.571	99.607
24	0.374	98.964					0.429	0.393	100.00	100.00
25	0.344	99.307								
26	0.277	99.585								
27	0.221	99.805								
28	0.195	100.00								

Appendix F. Percent of variance contributed by each shape component (CV), and cumulative variance obtained after applying Procrustes analysis to the landmark coordinates data.

CV	DORSAL		VENTRAL		LATERAL				MANDIBLE			
	%	Cumulative	%	Cumulative	% Variance		Cumulative %		% Variance		Cumulative %	
	Variance	%	Variance	%	M	F	M	F	M	F	M	F
1	62.357	62.357	67.589	67.589	68.604	63.812	68.604	63.812	56.789	56.577	56.789	56.577
2	13.595	75.959	12.024	79.613	12.574	11.903	81.178	75.715	17.648	17.974	74.437	74.551
3	10.934	10.934	9.216	88.828	8.876	9.053	90.054	84.768	9.187	8.812	83.624	83.363
4	5.718	5.718	4.950	93.779	4.863	7.779	94.917	92.547	7.441	6.549	91.065	89.912
5	4.294	4.294	2.857	96.636	2.518	3.584	97.435	96.131	5.463	5.697	96.528	95.609
6	2.161	2.161	2.026	98.662	1.816	2.876	99.251	99.007	2.154	2.226	98.682	97.835
7	0.941	0.941	1.338	100.00	0.749	0.993	100.00	100.00	1.318	2.165	100.00	100.00

Appendix G. Procrustes distances between pairwise groups (upper diagonal) and its respective *p*-values after permutation test with 10,000 permutation rounds (bottom diagonal).

Dorsal View

Group	Bona	Chile	Lima	Posti	Ricar	Rupes	Vacca	Xantho
Bona	-	0.0274	0.0182	0.0193	0.0208	0.0244	0.0156	0.0236
Chile	<.0001*	-	0.0185	0.0152	0.0186	0.0116	0.0256	0.0213
Lima	<.0001*	<.0001*	-	0.0083	0.0128	0.0125	0.0171	0.0159
Posti	0.0003*	<.0001*	0.0019*	-	0.0142	0.0086	0.0194	0.0152
Ricar	0.0280*	0.0122*	0.0731	0.0402*	-	0.0150	0.0144	0.0185
Rupes	<.0001*	<.0001*	<.0001*	0.0008*	0.0197*	-	0.0221	0.0157
Vacca	0.1763	<.0001*	<.0001*	0.0001*	0.5048	<.0001*	-	0.0178
Xantho	<.0001*	<.0001*	<.0001*	<.0001*	0.0166*	<.0001*	0.0016*	-

Ventral View

Group	Bona	Chile	Lima	Posti	Ricar	Rupes	Vacca	Xantho
Bona	-	0.0187	0.0196	0.0185	0.0158	0.0215	0.0115	0.0132
Chile	0.0037*	-	0.0101	0.0107	0.0179	0.0103	0.0172	0.0127
Lima	0.0001*	0.0024*	-	0.0124	0.0159	0.0084	0.0152	0.0124
Posti	0.0007*	0.0013*	<.0001*	-	0.0165	0.0100	0.0163	0.0172
Ricar	0.1857	0.0362*	0.0083*	0.0206*	-	0.0180	0.0128	0.0165
Rupes	<.0001*	0.0006*	0.0017*	0.0002*	0.0031*	-	0.0177	0.0161
Vacca	0.4099	0.0114*	0.0012*	0.0029*	0.4143	<.0001*	-	0.0100
Xantho	0.0807	<.0001*	<.0001*	<.0001*	0.0692	<.0001*	0.2163	-

Lateral Male view

Group	Bona	Chile	Lima	Posti	Ricar	Rupes	Vacca	Xantho
Bona	-	0.0319	0.0289	0.0283	0.0324	0.0329	0.0245	0.0275
Chile	0.0047*	-	0.0218	0.0261	0.0296	0.0179	0.0310	0.0294
Lima	0.0016*	<.0001*	-	0.0208	0.0316	0.0140	0.0322	0.0247
Posti	0.0007*	<.0001*	<.0001*	-	0.0315	0.0167	0.0341	0.0269
Ricar	0.0584*	0.1385	0.0211*	0.0120	-	0.0311	0.0247	0.0280
Rupes	<.0001*	<.0001*	0.0001*	<.0001*	0.0035*	-	0.0345	0.0269
Vacca	0.2951	0.0257*	0.0026*	0.0002*	0.7533	0.0001*	-	0.0205
Xantho	0.0248*	<.0001*	<.0001*	<.0001*	0.1630	<.0001*	0.2902	-

Lateral Female View

Group	Bona	Chile	Lima	Posti	Ricar	Rupes	Vacca	Xantho
Bona	-	0.0386	0.0347	0.0377	0.0358	0.0401	0.0340	0.0328
Chile	0.0013*	-	0.0217	0.0246	0.0231	0.0183	0.0247	0.0256
Lima	<.0001*	0.0006*	-	0.0178	0.0284	0.0155	0.0269	0.0212
Posti	0.0004*	<.0001*	0.0026*	-	0.03122	0.0151	0.0334	0.0245
Ricar	0.0583	0.2820	0.0049*	0.0089*	-	0.0275	0.0320	0.0229
Rupes	<.0001*	0.0060*	0.0129*	0.0120*	0.0149*	-	0.0273	0.0248
Vacca	.0485*	0.0504*	0.0022*	0.0001*	0.0924	0.0013*	-	0.0298
Xantho	0.0072*	<.0001*	0.0007*	<.0001*	0.1716	<.0001*	0.0036	-

Mandible Male View

Group	Bona	Chile	Lima	Posti	Ricar	Rupes	Vacca	Xantho
Bona	-	0.0288	0.0402	0.0294	0.0394	0.0352	0.0361	0.0334
Chile	0.0574	-	0.0333	0.0207	0.0322	0.0262	0.0347	0.0342
Lima	<.0001*	<.0001*	-	0.0250	0.0267	0.0190	0.0369	0.0293
Posti	0.0360*	0.0003*	<.0001*	-	0.0257	0.0189	0.0321	0.0291
Ricar	0.1300	0.2826	0.3921	0.5979	-	0.0255	0.0383	0.0355
Rupes	0.0031*	<.0001*	0.0011*	0.0015*	0.5509	-	0.0271	0.0240
Vacca	0.0933	0.0689	0.0048*	0.1012	0.1096	0.2705	-	0.0233
Xantho	0.0037*	<.0001*	<.0001*	<.0001*	0.0740	<.0001*	0.5034	-

Mandible Female View

Group	Bona	Chile	Lima	Posti	Ricar	Rupes	Vacca	Xantho
Bona	-	0.0325	0.0377	0.0326	0.0357	0.0310	0.0257	0.0238
Chile	0.0399*	-	0.0305	0.0185	0.0298	0.0212	0.0428	0.0322
Lima	0.0035*	<.0001*	-	0.0367	0.0315	0.0289	0.0513	0.0367
Posti	0.0447*	0.0228*	<.0001*	-	0.0407	0.0228	0.0400	0.0320
Ricar	0.4244	0.2995	0.1546	0.0227*	-	0.0356	0.0479	0.0373
Rupes	0.0427*	0.0054*	<.0001*	0.0014*	0.0547	-	0.0405	0.0245
Vacca	0.4420	0.0001*	<.0001*	0.0001*	0.0107*	<.0001*	-	0.0287
Xantho	0.2868	<.0001*	<.0001*	<.0001*	0.0359*	<.0001*	0.0109*	-

REFERENCES

- Albright, JC (2004). Phylogeography of the sigmodontine rodent, *Phyllotis xanthopygus*, and a test of the sensitivity of nested clade analysis to elevation-based alternative distances, doctoral thesis, College of Arts and Sciences: Department of Biological Science, Florida State University (online Proquest).
- Alvarado-Serrano D & Lacey, L (2014). 'Ecological niche models in phylogeographic studies: applications, advances and precautions', *Molecular Ecology Resources*, 14, 233–248.
- Allendorf, FW, Hohenlohe, PA & Luikart, G (2010). 'Genomics and the future of conservation genetics', *Nature Reviews Genetics*, 11(10), 697.
- Andrews, S (2015). FASTQC A Quality control tool for high throughput sequence data, Babraham Institute, Cambridge.
- Arnold, B, Corbett-Detig, RB, Hartl, D & Bomblies, K (2013). 'RADseq underestimates diversity and introduces genealogical biases due to nonrandom haplotype sampling', *Molecular Ecology*, 22(11), 3179-3190.
- Avise, J (2000). *Phylogeography: the history and formation of species VIII*, Harvard University Press, Cambridge.
- Avise, JC, Arnold, J, Ball, RM, Bermingham, E, Lamb, T, Neigel, LE, Reeb, CA & Saunders, NC (1987). 'Intraspecific phylogeography: The mitochondrial DNA bridge between population genetics and systematics', *Annual Review in Ecology and Systematics*, 18(1), 489–522.
- Cabrera, A, (1961). 'Catálogo de los mamíferos de América del Sur. Parte II', *Revista del Museo Argentino de Ciencias Naturales "Bernardino Rivadavia" Ciencias Zoologías*, 4(2), 309–732.
- Cardini, A, Jansson, AU & Elton, S (2007). 'A geometric morphometric approach to the study of ecogeographical and clinal variation in vervet monkeys', *Journal of Biogeography*, 34(10), 1663–1678.
- Catchen, J, Hohenlohe, PA, Bassham, S, Amores, A. & Cresko, WA (2013). 'Stacks: An analysis tool set for population genomics', *Molecular Ecology*, 22(11), 3124-3140
- Crespo, J (1964). 'Descripción de una nueva subespecie de roedor filotino (Mammalia)' *Neotrópica*, 10, 99-101.
- Domínguez–Domínguez, O & Vázquez–Domínguez, E (2009). 'Filogeografía: aplicaciones en taxonomía y conservación', *Animal Biodiversity and Conservation*, 32(1), 59–70.

- Drummond, AJ, Suchard, MA, Xie, D & Rambaut, A (2012). 'Bayesian phylogenetics with BEAUti and the BEAST 1.7', *Molecular Biology and Evolution*, 29(8), 1969-1973.
- Edgar, RC (2004). 'MUSCLE: Multiple sequence alignment with high accuracy and high throughput', *Nucleic Acids Research*, 32(5), 1792-1797.
- Edwards SV (2009). 'Is a new and general theory of molecular systematics emerging?', *Evolution*, 63(1), 1-19.
- Evano G, Regnaut S, Goudet J (2005). 'Detecting the number of clusters of individuals using the software STRUCTURE: a simulation study', *Molecular Ecology*, 14(8), 2611-2620.
- Evin A, Baylac M, Ruedi M, Mucedda M, Pons, CM (2008). 'Taxonomy, skull diversity and evolution in a species complex of *Myotis* (Chiroptera: Vespertilionidae): a geometric morphometric appraisal', *Biological Journal of the Linnean Society*, 95, 529–538.
- Fielding, AH & Bell, JF (1997), 'A review of methods for the assessment of prediction errors in conservation presence/absence models', *Environmental Conservation*, 24(1), 38-49.
- Gaston, K (2009). 'Geographic range limits: achieving synthesis', *Proceedings of the Royal Society V: Biological Sciences*, vol. 276, no. 1661, pp. 1395-1406.
- Gaither, MR, Bernal, MA, Coleman, RR, Bowen, BW, Jones, SA, Simison, WB & Rocha LA (2015), 'Genomic signatures of geographic isolation and natural selection in coral reef fishes', *Molecular Ecology*, 24 (7), 1543-1557.
- Galliari, C, Pardiñas, UF & Goin, FJ (1996), 'Lista comentada de los mamíferos Argéninos', *Mastozoología Neotropical*, 3(1), 39-61.
- Global Biodiversity Information Facility (GBIF) (2019). '*Phyllotis xanthopygus* (Waterhouse, 1837) GBIF Backbone Taxonomy', viewed 21 September 2017, <https://www.gbif.org/species/5219765/>
- Gould, GC (2001). 'The phylogenetic resolving power of discrete dental morphology among extant hedgehogs and the implications for their fossil record', *American Museum Novitates*, 2001(3340), 1–52.
- Graham C, Ron, S, Santos, J, Schneider, C & Mortiz, C (2004). 'Integrating phylogenetics and environmental niche models to explore speciation mechanisms in dendrobatid frogs', *Evolution*, 58(8), 1781-1793.
- Gutiérrez-Tapia P, Palma R (2016). 'Integrating phylogeography and species distribution models: cryptic distributional responses to past climate change in an endemic rodent from the central Chile hotspot', *Diversity and Distributions*, 22 (6), 638-650.

- Hennig, W (1965), 'Phylogenetic systematics', *Annual Review of Entomology*, 10(1), 97-116.
- Hershkovitz, P (1962), *Evolution of neotropical cricetine rodents (Muridae) with special reference to the phyllotine group*, Field Museum of Natural History, Chicago.
- Homburg, K, Dress, C, Gossner, M, Rakosy, L, Vrezec, A & Assmann, T (2013). 'Multiple glacial refugia of the low-dispersal ground beetle *Carabus irregularis* molecular data support predictions of species distribution models', *Plos One*, 8(4), e61185.
- Holmes, MW, Boykins, GK, Bowie, RC, & Lacey, EA (2016). 'Cranial morphological variation in *Peromyscus maniculatus* over nearly a century of environmental change in three areas in California', *Journal of Morphology* 277(1), 96-106.
- Huelsenbeck, JP & Ronquist, F (2001). 'MRBAYES: Bayesian inference of phylogenetic trees', *Bioinformatics*, 17(8), 754-755.
- Hugall, A, Moritz, C, Moussalli, A & Stanisci, J (2002). 'Reconciling paleodistribution models and comparative phylogeography in the wet tropics rainforest land snail *Gnarorosiphia bellendenkerensis* (Brazier 1875)', *Proceedings of the National Academy of Sciences*, 99(9), 6112-6117.
- Irwin, DE (2002). 'Phylogeographic breaks without geographic barriers to gene flow', *Evolution*, 56(12), 2383-2394.
- Jakob, S, Ihlow, A & Blattner, F (2007). 'Combined ecological niche modelling and molecular phylogeography revealed the evolutionary history of *Hodeum maritimum* (Poaceae) – niche differentiation, loss of genetic diversity, and speciation in Mediterranean Quaternary refugia', *Molecular Ecology*, 16(8), 1713-1727.
- Jeffries, DL, Copp, GH, Handley, LL, Olsén, KH, Sayer, CD (2016). 'Comparing RADseq and microsatellites to infer complex phylogeographic patterns, and empirical perspective in the Crucian carp, *Carassius carassius*, L.' *Molecular Ecology*, 25(13), 2997-3018.
- Jojic, V, Nenadovic, J, Blagojevic, J, Paunovic, M, Cvetkovic, D & Vujosevic, M (2012). 'Phenetic relationships among four *Apodemus* species (Rodentia, Muridae) inferred from skull variation', *Zoologischer Anzeiger*, 251, 26-37.
- Jones, B & Sall, J (2011). 'JMP statistical discovery software', *Wiley Interdisciplinary Reviews: Computational Statistics*, 3(3), 188-194.
- Kearse, M, Moir, R, Wilson, A, Stones-Havas, S, Cheung, M, Sturrock, S, Buxton, S, Cooper, A, Markowitz, S, Duran, C & Thierer, T (2012). 'Geneious basic: an integrated and extendable desktop software platform for the organization and analysis of sequence data', *Bioinformatics*, 28(12), 1647-1649.

- Kim, I, Phillips, CJ, Monjeau, JA, Birney, EC, Noack, K, Pumo, DE, Sikes, RS & Dole, JA (1998), 'Habitat islands, genetic diversity, and gene flow in a Patagonian rodent', *Molecular Ecology*, 7(6), 667–678.
- Kirkpatrick M & Barton, N (1997). 'Evolution of a species range', *The American Naturalist*, 150(1), 1–23.
- Klingenberg, CP (2011). 'MorphoJ: An integrated software package for geometric morphometrics', *Molecular Ecology Resources*, 11(2), 353-357.
- Koopman, KF & Hershkovitz, P (1964). 'Evolution of neotropical cricetine rodents (Muridae) with special reference to the phyllotine group', *The American Midland Naturalist*, 71(1), 251-256.
- Kramer KM, Monjeau JA, Birney EC & Sikes, RS (1999), '*Phyllotis xanthopygus*', *Mammalian Species*, 617, 1–7.
- Kuch, M, Rohland, N, Betancourt, J, Latorre, C, Stepan, S & Poinar, H (2002). 'Molecular analysis of a 11700-year-old rodent midden from the Atacama Desert, Chile', *Molecular Ecology*, 11(5), 913-924.
- Lessa, EP, D'Elia, G & Pardiñas, UF (2010). 'Genetic footprints of late Quaternary climate change in the diversity of Patagonian-Fuegian rodents', *Molecular Ecology*, 19(15), 3031-3037.
- Lessa, EP, D'Elia, G, Pardiñas, UF, Patterson, BD & Costa, LP (2012). 'Mammalian biogeography of Patagonia and Tierra del Fuego' in BD. Patterson and LP. Costa(eds.), *Bones, Clones and Biomes: The History and Recent Geography of Neotropical Animals*, University of Chicago Press: Chicago, 379-398.
- Libardi, GS & Percequillo, AR (2016). 'Variation of craniodental traits in russet rats *Euryoryzomys russatus* (Wagner, 1848) (Rodentia: Cricetidae: Sigmodontinae) from Eastern Atlantic Forest', *Zoologischer Anzeiger*, 262, 57-74.
- Lu, X, Ge, D, Xia, L, Huang, C & Yang, Q (2014). 'Geometric morphometric study of the skull shape diversification in Sciuridae (Mammalia, Rodentia)', *Integrative Zoology*, 9, 231-245.
- Macholan, M, Mikula, O & Vohralik, V (2008). 'Geographic phenetic variation of two eastern-Mediterranean non-commensal mouse species, *Mus macedonicus* and *M. cypriacus* (Rodentia: Muridae) based on traditional and geometric approaches to morphometrics', *Zoologischer Anzeiger*, 247, 67-80.
- Mann, G (1978). 'Los pequeños mamíferos de Chile', *Gayana Concepción*, 40, 1-342.

- Matocq, MD, Shurtliff, QR & Feldman, CR (2007). 'Phylogenetics of the woodrat genus *Neotoma* (Rodentia: Muridae): Implications for the evolution of phenotypic variation in male external genitalia', *Molecular Phylogenetics and Evolution*, 42(3), 637–652.
- Mayr, E (1954). 'Change of Genetic and enviromental and evolution', *Evolution as a Process*, 157–180.
- Metcalf, JL, Turney, C, Barnett, R, Martin, F, Bray, SC, Vilstrup, JT, Orlando, L, Salas-Gismondi, R, Loponte, D, Medina, M & De Nigris, M (2016). 'Synergistic roles of climate warming and human occupation in Patagonian megafaunal extinctions during the Last Deglaciation', *Science Advances*, 2(6), e501682.
- Milenkovic, M, Sipetic, JV, Blagojevic, J, Ttovic, S & Vujosevic, M (2010). 'Skull variation in Dinaric-Balkan and Carpathian grey wolf populations revealed by geometric morphometric approaches', *Journal of Mammalogy*, 91, 376 - 386.
- Morando, M, Avila, LJ, Turner, CR & Sites, JW (2007). 'Molecular evidence for a species complex in the patagonian lizard *Liolaemus bibronii* and phylogeography of the closely related *Liolaemus gracilis* (Squamata: Liolaemini)', *Molecular Phylogenetics and Evolution*, 43(3), 952-973.
- Moussalli, A, Moritz, C, Williams, S & Carnaval, A (2009). 'Variable responses of Skinks to a common history of rainforest fluctuation: concordance between phylogeography and palaeo-distribution Models', *Molecular Ecology*. 18(3), 483-499.
- Musser, G & Carleton, M (2005). 'Superfamily Muroidea' in DE Wilson & DM Reeder (eds.), *Mammal Species of the World. A Taxonomic and Geographic Reference* third ed. Johns Hopkins University Press, Baltimore, 894–1531.
- Nabholz, B, Glémin, S & Galtier, N (2009). 'The erratic mitochondrial clock: variations of mutation rate, not population size, affect mtDNA diversity across birds and mammals', *BMC Evolutionary Biology*, 9(54).
- Nespolo, RF, Arim, M & Bozinovic, F (2003). 'Body size as a latent variable in a structural equation model: thermal acclimation and energetics of the leaf-eared mouse', *Journal of Experimental Biology*, 206(13), 2145-2157.
- Osgood, WH (1943). 'The mammals of Chile', *Zoological Series, Field Museum of Natural History*, 30, 1-269.
- Palma, RE, Cancino, RA & Rodríguez-Serrano, E (2010). 'Molecular systematics of *Abrothrix longipilis* (Rodentia: Cricetidae: Sigmodontinae) in Chile', *Journal of Mammalogy*, 91(5), 1102-1111.

- Palma, RE, Boric-Bargetto, D, Torres-Perez, F, Hernandez, CE & Yates, TL (2012) 'Glaciation effects on the phylogeographic structure of *Oligoryzomys longicaudatus* (rodentia: Sigmodontinae) in the southern andes', PLoS ONE, 7(3), e32206.
- Parada, A, Pardiñas, UFJ, Salazar-Bravo, J, D'Elía, G & Palma, RE (2013). 'Dating an impressive Neotropical radiation: Molecular time estimates for the Sigmodontinae (Rodentia) provide insights into its historical biogeography', Molecular Phylogenetics and Evolution, 66(3), 960-968.
- Pardiñas, UFJ, Abba A & Merino, ML (2004). 'Micromamíferos (Didelphimorphia y Rodentia) del sudoeste de la provincia de Buenos Aires (Argentina): taxonomía y distribución'. Mastozoología Neotropical, 11(2), 211-232.
- Pardinas, UF, Teta, P, D'elía, G & Lessa, EP (2011). 'The evolutionary history of sigmodontine rodents in Patagonia and Tierra del Fuego', Biological Journal of the Linnean Society, 103(2), 495-513.
- Patton, JL, Conroy, CJ (2017). 'The conundrum of subspecies: morphological diversity among desert populations of the California vole (*Microtus californicus*, Cricetidae)', Journal of Mammalogy, 98(4), 1010-1026.
- Patton, JL, Pardiñas, UJ & D'Elía, G (eds.) (2015). Mammals of South America, Vol. 2. Rodents, University of Chicago Press, Chicago.
- Pearson, OP & Patton, JL (1976). 'Relationships among South American phyllotine rodents based on chromosome analysis', Journal of Mammalogy, 57(1), 339-350.
- Pearson, OP & Smith, MF (1999). 'Genetic similarity between *Akodon olivaceus* and *Akodon xanthorhinus* (Rodentia: Muridae) in Argentina', Journal of Zoology, 247(1), 43-52.
- Pearson, RG, Raxworthy, CJ, Nakamura, M & Townsend-Peterson, A (2007). 'Predicting species distributions from small numbers of occurrence records: A test case using cryptic geckos in Madagascar', Journal of Biogeography, 34(1), 102-117.
- Peterson, AT, Martinez-Meyer, E & Gonzalez-Salazar, C (2004). 'Reconstructing the Pleistocene geography of the *Aphelocoma jays* (Corvidae)', Diversity and Distributions, 10(4), 237-246.
- Peterson, BK, Weber, JN, Kay, EH, Fisher, HS & Hoekstra, HE (2012). 'Double digest RADseq: an inexpensive method for de novo SNP discovery and genotyping in model and non-model species', PLoS ONE, 7(5), e37135.

- Petit, JR, Jouzel, J, Raynaud, D, Barkov, NI, Barnola, JM, Basile, I, Bender, M, Chappellaz, J, Davis, M, Delaygue, G & Delmotte, M (1999), 'Climate and atmospheric history of the past 420,000 years from the Vostok ice core, Antarctica', *Nature*, 399(6735), 429.
- Plissock, P, Luebert, F, Hilger, HH & Guisan, A (2014). 'Effects of alternative sets of climatic predictors on species distribution models and associated estimates of extinction risk: a test with plants in an arid environment', *Ecological Modelling*, 288, 166-177.
- Pollock, EW & Bush, ABG (2013). 'Atmospheric simulations of southern South America's climate since the Last Glacial Maximum', *Quaternary Science Reviews*, 71, 219-228.
- Pritchard, JK, Stephens, M & Donnelly, P (2000). 'Inference of population structure using multilocus genotype data.', *Genetics*, 155(2), 945–959.
- Prychitko, TM & Moore, WS (2000). 'Comparative Evolution of the Mitochondrial Cytochrome *b* Gene and Nuclear -Fibrinogen Intron 7 in Woodpeckers', *Molecular Biology and Evolution*, 17(7), 1101-1111.
- QGIS Geographic Information System (2006). Version 2.18.9, software, open source geospatial foundation project, <https://www.qgis.org/en/site/>
- R: A Language and Environment for Statistical Computing (2015). Software, The R Project for Statistical Computing, Vienna <http://www.R-project.org/>
- Rabassa, J (2008). 'Late Cenozoic glaciations in Patagonia and Tierra del Fuego', *Developments in Quaternary Science*, 11, 151- 204.
- Rambaut, A & Drummond, A J (2013). 'Tracer', Version 1.6, software, BEAST Software, Auckland <http://tree.bio.ed.ac.uk/software/tracer/>
- Rambaut, A & Drummond, A J (2016). 'Tree Annotator', Verson 1.8.4, software, BEAST Software, Auckland <http://Beast.Bio.Ed.Ac.Uk/>
- Raxworthy, C, Ingram, C, Rabibisoa, N & Pearson, R (2007). 'Applications of ecological niche modeling for species delimitation: a review and empirical evaluation using day geckos (*Phelsuma*) from Madagascar', *System Biology*, 56(6), 907-923.
- Reig, OA (1978). 'Roedores cricétidos del Plioceno superior de la Provincia de Buenos Aires (Argentina)', *Publicaciones del Museo Municipal de Ciencias Naturales de Mar del Plata* "Lorenzo Scaglia, 2(8), 164-190.
- Rissler, LJ & Apodaca, JJ (2007). 'Adding more ecology into species delimitation: ecological niche models and phylogeography help define cryptic species in the black salamander (*Aedeides flavipunctatus*)', *Systematic Biology*, 56(6), 924-942.

- Riverón, S (2011). Estructura Poblacional e Historia Demográfica del “Pericote Patagónico”, *Phyllotis xanthopygus* (Rodentia: Sigmodontinae) en Patagonia Argentina, doctoral thesis, Universidad de la Republica, Uruguay (online Proquest) 100
- Robles, MDR, Cutillas, C, Panei, CJ & Callejón, R (2014). ‘Morphological and molecular characterization of a new trichuris species (*nematoda-Trichuridae*), and phylogenetic relationships of Trichuris species of cricetid rodents from Argentina’, PLoS ONE, 9(11), e112069
- Rohlf, RJ (2008). ‘*TPSDIG*’, Version 2.12, software, Department of Ecology and Evolution, State University of New York, Stony Brook <http://life.bio.sunysb.edu/morph/>
- Sersic, AN, Cosacov, A, Cocucci, AA, Johnson, LA, Pozner, R, Avila, LJ, Sites, JW & Morando, M (2011). ‘Emerging phylogeographical patterns of plants and terrestrial vertebrates from Patagonia’, Biological Journal of the Linnean Society, 103(2), 475-494.
- Soberón, J & Peterson, AT (2005). 'Interpretation of models of fundamental ecological niches and species distributional areas', Biodiversity Informatics, 2, 1-10.
- Spotorno, AE & Walker, LI (1983). 'Análisis electroforético y biométrico de dos especies de *Phyllotis* en Chile Central y sus híbridos experimentales', Revista Chilena de Historia Natural, 56, 51–59.
- Smith, M.F, Thomas, WK & Patton, JL (1992). ‘Mitochondrial DNA-like sequence in the nuclear genome of an akodontine rodent.’, Molecular Biology and Evolution, 9(2), 204-215.
- Steppan, SJ (1993). 'Phylogenetic relationships among the Phyllotini (Rodentia: Sigmodontinae) using morphological characters, Journal of Mammology, 1(3), 187–213.
- Steppan, SJ (1998). 'Phylogenetic relationships and species limits within Phyllotis (Rodentia: Sigmodontinae): concordance between mtDNA sequence and morphology', Journal of Mammology, 79(2), 573–593.
- Steppan, SJ, Ramirez, O, Bandury, J, Huchon, D, Pacheco, V, Walker, L & Spotorno, AE (2007). 'A molecular reappraisal of the systematics of the leaf-eared mice Phyllotis and their relatives' in DA Kelt, EP Lessa, J Salazar-Bravo & JL Patton (eds.), The Quintessential Naturalist: Honoring the Life and Legacy of Oliver P. Pearson. University of California Publications in Zoology, Berkley, 729-826.
- Storz, JF, Quiroga-Carmona, M, Opazo, JC, Bowen, T, Farson, M, Steppan SJ, D’Elía, G (2020). ‘Discovery of the world’s highest-dwelling mammal’, Proceedings of the National Academy of Sciences, 117(31), 18169-18171.

- Tammone, MN, Hajduk, A, Arias, P, Teta, P, Lacey, EA & Pardiñas, UF (2014). 'Last glacial maximum environments in northwestern Patagonia revealed by fossil small mammals', *Quaternary Research*, 82(1), 198-208.
- Teta, P & Pardiñas, UFJ (2014). 'Variación morfológica cualitativa y cuantitativa en *Abrothrix longipilis* (Cricetidae, Sigmodontinae)', *Mastozoología Neotropical*, 21(2), 291-309.
- Teta, PV, Jayat, JP, Lanzone, C, Ojeda, AA, Novillo, A & Ojeda, RA (2018). 'Geographic variation in quantitative skull traits and systematic of southern populations of the leaf-eared mice of the *phyllotis xanthopygus* complex (Cricetidae, Phyllotini) in southern South America', *Zootaxa*, 4446(1), 68–80.
- Thomas, O (1912). 'LII - New bats and Rodents from South America', *Annals and magazine of Natural History*, 10(58), 403-411.
- Thomas, O (1919). 'On small Mammals from "Otro Cerro," North-eastern Rioja, collected by Sr. L. Budin', *Annals and Magazine of Natural History*, 9(3), 489-500.
- Victoriano, PF, Ortiz, JC, Benavides, E, Adams, BJ & Sites JW (2008). 'Comparative phylogeography of codistributed species of Chilean *Liolaemus* (Squamata: Tropiduridae) from the central-southern Andean range' *Molecular Ecology*, 17(10), 2397-2416.
- Viruel, J, Catalan, P & Segarra-Moragues, J (2014). 'Latitudinal environmental niches and riverine barriers shaped the phylogeography of the central Chilean endemic *Dioscorea humilis* (Dioscoreaceae)', *PloS one*, 9(10), e110029.
- Wagner, CE, Keller, I, Wittwer, S, Selz, OM, Mwaiko, S, Greuter, L, Sivasundar, A & Seehausen, O (2013) 'Genome-wide RAD sequence data provide unprecedented resolution of species boundaries and relationships in the Lake Victoria cichlid adaptive radiation', *Molecular Ecology*, 22(3), 787-798.
- Walker, LI, Spotorno, AE & Arrau, J (1984). 'Cytogenetic and reproductive studies of two nominal subspecies of *Phyllotis darwini* and their experimental hybrids', *Journal of Mammalogy*, 65(2), 220–230.
- Walker, LI, Spotorno, AE & Sans, J (1991). 'Genome size variation and its phenotypic consequences in *Phyllotis* rodents', *Hereditas*, 115(2), 99–107.
- Wiens, J (2011). 'The niche, biogeography and species interactions', *Philosophical Transactions of the Royal Society B: Biological Sciences*, 366(1576), 2336-2350.
- Wiens, J, Ackerly, D, Allen, A, Anacker, B, Buckley, L, Cornell, H, Damschen, E, Davies, J, Grytnes, J, Harrison, S, Hawkins, B, Holt, R, McCain, R & Stephens, P (2010). 'Niche

conservatism as an emerging principle in ecology and conservation biology', *Ecology Letters*, 13(10), 1310–1324.

- Wyngaarden, MV, Snelgrove, PV, DiBacco, C, Hamilton, LC, Rodríguez-Ezpeleta, N, Jeffery, NW, Stanley, RR & Bradbury, IR (2017) 'Identifying patterns of dispersal, connectivity and selection in the sea scallop, *Placopecten magellanicus*, using RADseq-derived SNPs', *Evolutionary Applications* 10(1), 102-117.
- Yu, Y, Harris, AJ, Blaire, C & He, X (2015). 'RASP (Reconstruct Ancestral State in Phylogenies): A tool for historical biogeography', *Molecular Phylogenetics and Evolution*, 87, 46-49.
- Zelditch, ML, Swiderski, DL & Sheets, HD (2012). *Geometric morphometrics for biologists: a primer*, Academic Press, Cambridge.
- Zhao, N, Dai, C, Wang, W, Zhang, R, Qu, Y, Song, G, Chen, K, Yang, X, Zou, F & Lei, F (2012). 'Pleistocene climate changes shaped the divergence and demography of asian populations of great tit *Pardus major*: evidence from phylogeographic analysis and ecological niche models', *Journal of Avian Biology*, 43(4), 297-310.
- Zink, R (2015). 'Genetics, morphology, and ecological niche modeling do not support the Subspecies status of the endangered southwestern willow wlycatcher (*Empidonax traillii extimus*)', *The Condor: Ornithological Applications*, 117(1), 76-86.